

Light: A Magical Tool for Controlled Drug Delivery

Yu Tao, Hon Fai Chan, Bingyang Shi,* Mingqiang Li,* and Kam W. Leong*

Light is a particularly appealing tool for on-demand drug delivery due to its noninvasive nature, ease of application, and exquisite temporal and spatial control. Great progress is achieved in the development of novel light-driven drug delivery strategies with both breadth and depth. Light-controlled drug delivery platforms can be generally categorized into three groups: photochemical, photothermal, and photoisomerization-mediated therapies. Various advanced materials, such as metal nanoparticles, metal sulfides and oxides, metal–organic frameworks, carbon nanomaterials, upconversion nanoparticles, semiconductor nanoparticles, stimuli-responsive micelles, polymer- and liposome-based nanoparticles are applied for light-stimulated drug delivery. In view of the increasing interest in on-demand targeted drug delivery, the development of light-responsive systems with a focus on recent advances, key limitations, and future directions is reviewed.

Various nanomaterials, including metal or semiconductor nanoparticles (NPs), magnetic nanoparticles, upconversion nanomaterials, nanocarbons, silicon nanostructures, polymeric nanoparticles, cell- and virus-like nanoparticles, have been introduced for drug delivery.^[3] The incorporation of these powerful nanoplatfoms with target tags emerges as the promising and alternative avenue for the evolvement of controlled and targeted release of therapeutic agents to combat various chronic and acute diseases, including cancers, inflammation, neurological disorders, rheumatoid arthritis, infections, diabetes, and cardiovascular diseases.^[4]

Although impressive progress has been made in the applications of promising

1. Introduction

Nanotechnology development leads to a remarkable advancement in science and medicine,^[1] especially in biotechnology and biomedicine-related fields.^[2] Nanomaterials-based drug delivery has emerged as the predominant branch of nanotechnology, enabling the development of efficient and safe methods for dosage-, temporally- and spatially controllable delivery of drugs at therapeutic levels into targeted organs, tissues, and even cells.

nanomaterials as drug release systems, some key challenges remain to be addressed. For example, a lot of toxic medicines should exhibit “zero-release” property before arriving at the target sites. Consequently, it is greatly desirable to develop smart nanomaterial-based drug-delivery systems with the capability to control the release of therapeutic payloads in response to a given stimulus.^[5] Controlled release approaches offer unique benefits such as improved drug efficacy, minimized toxic side effects, easier control over released drug dosage and drug protection from the harsh environment.^[6] Smart drug delivery systems that can be self-regulated and respond to a number of stimuli (both alone and in combination) arising from either the internal physiological environments (pH variations, enzymatic actions, redox reactions, overexpression of biomarkers, etc.^[7]) or remote/external triggers (temperature changes, competitive binding, ultrasound, light and electrical or magnetic fields,^[3h,8]) have enabled the precisely controlled delivery of preloaded therapeutic agents. Several excellent reviews describing these pharmaceutical delivery systems are available.^[6e,9]


Among external actuation methods mentioned earlier, light is a particularly appealing tool for therapeutic applications due to its noninvasive nature, ease of application, robustness in the biological environment, tuneable intensity, and exquisite temporal and spatial control. Specifically, when compared with other triggers such as temperature and pH, light has the advantages of exerting no adverse effects on biological environments, an important prerequisite for clinical applications, as well as allowing for precisely targeted drug delivery with high spatiotemporal resolution in a noncontact mode, leading to enhanced therapeutic efficacy and patient comfort.^[10] As a result, light has been extensively applied in intelligent targeted delivery platforms for systemic delivery of a variety of therapeutic compounds such as photosensitizers, chemotherapeutic drug molecules, nucleic acids, proteins, and

Prof. Y. Tao, Prof. M. Li
Laboratory of Biomaterials and Translational Medicine
The Third Affiliated Hospital
Sun Yat-sen University
Guangzhou 510630, China
E-mail: limq567@mail.sysu.edu.cn

Prof. H. F. Chan
Institute for Tissue Engineering and Regenerative Medicine
School of Biomedical Science
The Chinese University of Hong Kong
Hong Kong 999077, China

Prof. B. Shi
International Joint Center for Biomedical Innovation
School of Life Sciences
Henan University
Kaifeng, Henan 475004, China
E-mail: bs@henu.edu.cn

Prof. K. W. Leong
Department of Biomedical Engineering
Department of Systems Biology
Columbia University Medical Center
New York, NY 10032, USA
E-mail: kam.leong@columbia.edu

 The ORCID identification number(s) for the author(s) of this article can be found under <https://doi.org/10.1002/adfm.202005029>.

DOI: 10.1002/adfm.202005029

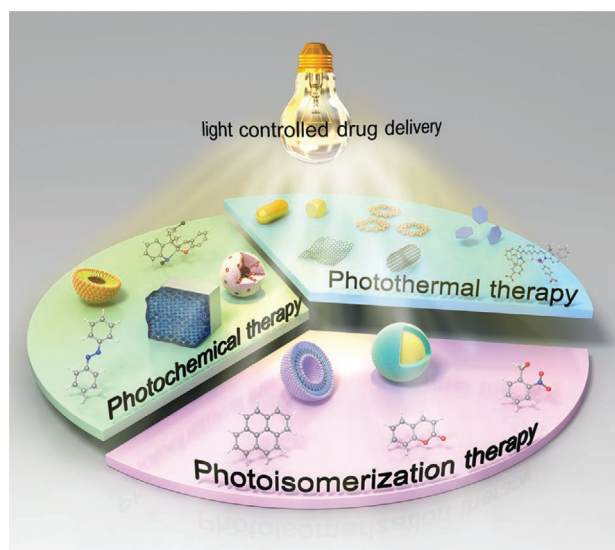


Figure 1. Schematic illustration of light-controlled drug delivery.

enzymes, to disease sites.^[11] Distinct wavelengths, ranging from ultraviolet (UV, 200–400 nm) to visible (400–750 nm) or near-infrared (NIR, 750–2000 nm) light, can be utilized to activate light responsiveness. Among these, UV light is a relatively poor candidate due to its limited tissue penetration capacities and potentially carcinogenic effects under prolonged exposure.^[12] In comparison, NIR light has the advantages of lower phototoxicity, improved penetration depth in biological tissues and reduced background signal, making it more suitable for biological applications.^[6d,13] Whereas, the comprehensive utilization of NIR light is restricted by the limited energy of the NIR photons, which is insufficient to activate a lot of photochemical reactions that require high-energy wavelengths. This problem can be overcome, at least in part, by two-photon absorption or upconversion, which we will discuss in the following section.^[14] Distinct mechanisms have been employed for light-activated delivery systems, such as photodriven isomerization and oxidation–reduction reactions, bond breakage, crosslinking, photo-uncaging, and electrostatic assembly.^[15] The light-based novel delivery platforms can generally be sorted into three broad categories: photochemical-, photothermal-, and photoisomerization-based drug delivery (Figure 1). In this review, we provide an overview of the main recent achievements related to light-responsive systems, focusing on the major advances and applications, key limitations, and potential areas for future study.

2. Photochemically Triggered Drug Delivery

Photochemically triggered drug delivery facilitates the release of encapsulated therapeutic payloads through cleavage of photocleavable covalent bonds present within nanocarriers by light irradiation. The most common compounds applied in photochemical-triggered drug delivery include nitrobenzyl, coumarin, and pyrene derivatives. The nitrobenzyl moiety can be irreversibly cleaved to release a free carboxylic acid and nitrosobenzaldehyde upon UV irradiation.^[16] The ester bonds in coumarin- and pyrene-derivatives can also be cleaved upon

irradiation with UV light.^[17] They can be employed either as a photocage to inhibit bioactivity of therapeutic agents, or as a cleavable linker in the delivery vehicle for smart photocontrolled drug delivery.^[18] Recent advance in nanotechnology has accelerated the development of various types of nanomaterials applied in photochemical-triggered drug delivery.^[19]

2.1. Mesoporous Silica-Based Nanoplatfoms for Photochemically Triggered Small Molecule Drug Delivery

Mesoporous silica nanoparticles (MSNs) have emerged as one type of the most widely used nanomaterials for photochemical-triggered drug release owing to the high biocompatibility, tunable pore size, as well as easy surface modification and functionalization, thanks to the versatility of silane chemistry.^[20] Several excellent reviews on MSN have been published.^[21] Drug cargos can be loaded into the pores of MSN, which are then capped by diverse types of capping agents. Photoirradiation is able to induce the liberation or destruction of the capping agents. Thereafter, the payload drugs can be efficiently released. The first example of MSN-mediated photochemical-triggered drug delivery was reported in 2003 by Fujiwara's group.^[22] Upon irradiation with UV light, the dimerized coumarin on MCM-41 MSN was photocleaved into coumarin monomers, leading to pore opening and subsequent release of guest molecules. In addition, Zhu and co-workers utilized coumarin-modified MSN as a drug delivery vector for anticancer drug release by irradiation with either one- or two-photon excitation.^[14c,23] Coumarin anchored on MSN could effectively act as both the light trigger for uncaging drug delivery and fluorescent tag for imaging application. Similarly, taking advantage of the *o*-nitrobenzyl bromide linkage on MSN, a photoactive delivery system allowing controlled cage and release of drugs or bioactive molecules was demonstrated.^[24] Recently, Liu's group also introduced the cationic poly[2-(*N,N*-dimethylaminoethyl)-methacrylate] anchored on MSN by utilization of a coumarin linker to adsorb P-glycoprotein short-hairpin RNA, while the photosensitive *o*-nitrobenzyl derivative-caged anticancer drug doxorubicin (DOX) was loaded in MSN. The release of short-hairpin RNA and DOX was proved to be individually regulated by UV and visible light excitations both in vitro and in vivo.^[25]

2.2. Gold and Carbon Nanovectors for Photochemically Triggered Small Molecule Drug Delivery

As one type of well-studied nanomaterials, gold nanoparticles (AuNPs) were also used as the nanoscale carrier for light-controlled release of the therapeutic drug fluorouracil via a terminally anchored *o*-nitrobenzyl group. AuNPs served as both the drug carrier and cage for the effective release of the payload upon UV irradiation.^[26] Another typical category of photochemical agents for realizing light-controlled drug release are reactive oxygen species (ROS) photosensitizers. Gao and co-workers reported a photoresponsive nanocomposite, which could produce ROS to effectively cause decomposition after light exposure. The nanocomposite was designed by anchoring graphene oxide on polyamidoamine-pluronic F68 and encapsulating photosensitizer

indocyanine green (ICG) and DOX. The nanocomposite showed a controlled release of DOX in multidrug-resistant cells under photoirradiation. Impressively, the nanocomposite efficiently downregulated P-glycoprotein and ABCB1 gene of MCF-7 cells, showing great cytotoxicity.^[27]

2.3. Organic Nanocarriers for Photochemically Triggered Small Molecule Drug Delivery

In addition to the inorganic nanomaterials, other types of organic nanocarriers, including polymer nanoparticles,^[28] microgels,^[29] liposomes,^[30] micelles,^[31] proteins,^[32] peptides,^[33] and DNA,^[34] have also been applied to demonstrate the photocaging/uncaging behavior.^[35] Different types of cargos, including anticancer drugs/prodrugs (platinum(II) and platinum(IV)-based complexes, DOX, fluorouracil, camptothecin, tamoxifen, dianthracene, and coumarin),^[14c,26,31,36] thiols,^[33] and nitric oxide,^[37] can be carried by the photocaging nanocarriers.

DNA and proteins are the most popular natural organic materials utilized for drug delivery applications owing to the excellent biocompatibility and inherent biodegradability. For example, the amphiphilicity DNA-camptothecin amphiphiles conjugate connecting with photolabile 2-nitrobenzyl ether moiety could be cleaved by UV light, leaving the decapped drug core, which subsequently underwent the spontaneous decomposition process to release camptothecin molecules for cancer therapy.^[38] Liang's group developed human serum albumin nanoparticles decorated with diazirine and encapsulated with tirapazamine and photosensitizer ICG. Under 405 nm light irradiation, the nanoparticles could form crosslinked aggregates and thus realized improved tumor accumulation and retention. Following 808 nm laser irradiation at tumor site generated ROS and local hyperthermia for cytotoxic tirapazamine derivative conversion, leading to effective tumor ablation.^[32] Recently, the self-immolative, light-triggered linker composed of photocaged C4'-oxidized abasic site was also synthesized, which could efficiently conjugate to the target protein or peptide via the alkyl chain and covalently bind amine- or hydroxyl-bearing drugs. Photodecaging led to rapid DOX release via the addition–elimination cascade, enabled targeted, controlled drug delivery.^[39]

Synthetic organic nanocarriers with tunable physical and chemical properties made from biocompatible lipids and polymers were also well-established candidates for the fabrication of photochemical drug release profiles. Liposomes, consisting of single or multiple bilayered membrane structures with amphiphilic lipid molecules, are excellent candidates as drug depots owing to the advantages of prominent biocompatibility, good biodegradability, high drug loading capacity, and facile modification.^[40] Talukdar's group developed the *o*-nitrobenzyl-conjugated indole-2-carboxamide receptor in liposomes as the effective membrane chloride ion carrier. Photoirradiation resulted in the delivery of 90% of the loaded active carrier for efficient cancer killing.^[41] Polymersomes with morphological similarities to liposomes and cellular membranes have also been widely applied in drug carriers.^[42] The NO-releasing polymersomes based on self-assembly of NO-delivering amphiphiles were designed, which were efficiently fabricated by polymerization of photosensitive NO monomers. The NO monomers were

rationally synthesized via the integration of 4-aminobenzyl alcohol derivatives-based self-immolative linkers and photo-cleavable *N*-nitrosoamine moieties, which made it applicable for light-triggered NO release for promising applications in corneal wound healing.^[43]

Other commonly chosen biocompatible polymers, including polyvinyl alcohol (PVA), chitosan, poly(ethylene glycol) (PEG), polyphosphoesters, etc., have also been extensively studied as photochemical therapeutic drug nanocarriers in the past few decades. Gu's group for the first time reported a novel drug delivery platform using a photoactivated hypoxia-triggered modality, which could efficiently generate ROS and deliver DOX in cells through the disassembly of DOX/2-nitroimidazole-grafted PVA nanoparticles.^[28a] The chitosan-based microswimmer that could on-demand release the photocleavable *o*-nitrobenzyl linker conjugated DOX upon an external light stimulus was also proposed. When exposed to 365 nm light, 60% of DOX could be released within 5 min.^[44] Recently, phototriggered photodynamic backbones grafted with PEG and linked with chemodrugs via hypoxia-cleavable linkers were constructed. This nanoprodruge could not only effectively generate ROS upon NIR irradiation but also selectively activate the chemotherapeutic action in hypoxic cancer tissues for synergetic cancer therapy.^[45] As a novel category of biodegradable polyesters, polyphosphoesters were also employed for phototriggered DOX delivery via ROS-labile thioketal linkers. The co-self-assembled photosensitizer chlorin e6 (Ce6) could efficiently induce the cleavage of thioketal linkages and subsequent DOX release and activation for cancer treatment.^[46]

Polymer-based micelles can mimic structures and properties of plasma lipoproteins that form biological carriers, which enables their extensive exploration as drug release vehicles for controlled delivery.^[47] A light-activated platform based on the dual chemotherapeutics-loaded and protoporphyrin-conjugated polymer micelle was constructed. Under red light irradiation, ROS generated through the photoconversion of protoporphyrin efficiently triggered disassociation of micelles codelivering apatinib and DOX to overcome the multidrug resistance of tumors.^[48] For another light-activatable polymer nanomicelles, which were formulated by self-assembly of PEG-stearamine conjugates with ROS-responsive thioketal linkers, the photosensitizer pheophorbide A and DOX could be co-loaded in the nanomicelles for synergistic locoregional photodynamic chemotherapy (Figure 2A).^[49] Recently, the NIR photoactivatable semiconducting polymer nanoblockader that conjugated with a protein biosynthesis blockader through ¹O₂ cleavable linker was also developed. The amphiphilic semiconducting polymer nanoblockader not only enabled the generation of ¹O₂ under NIR photoirradiation for photodynamic therapy, but also permitted photoactivation of blockaders to terminate protein translation, exerting a synergistic action to afford a metastasis-inhibited lung cancer therapy (Figure 2B).^[50]

2.4. Photochemically Triggered Large Molecule Drug Delivery

In addition to small molecule drugs, the photochemically triggered drug delivery platforms could also help shuttle nucleic acid^[51] and protein^[34,52] drugs. An important application

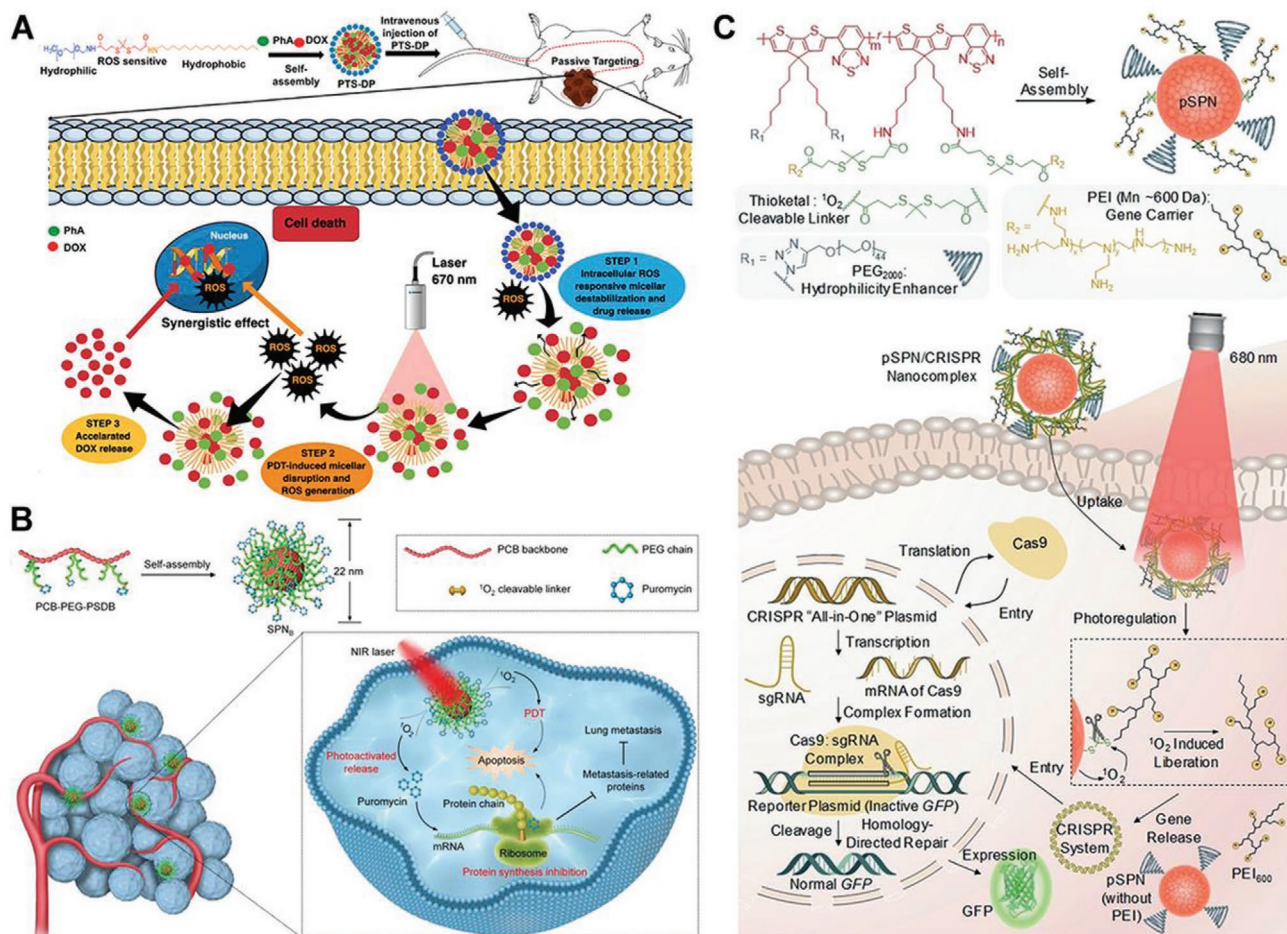


Figure 2. A) Schematic illustration of ROS cascade-responsive drug release of PEG-stearamine conjugate nanomicelles loaded with DOX and phorbide A for enhanced regional chemo-photodynamic therapy. Reproduced with permission.^[49] Copyright 2020, Elsevier. B) Synthesis of NIR photoactivatable semiconducting polymer nanoblockers for metastasis-inhibited cancer therapy. Reproduced with permission.^[50] Copyright 2019, Wiley-VCH. C) Chemical structure and self-assembly of NIR photolabile semiconducting polymer nanotransducer. Schematic of photolabile semiconducting polymer nanotransducer-mediated delivery and photoregulation of CRISPR/Cas9 gene editing under NIR light irradiation. Reproduced with permission.^[53] Copyright 2019, Wiley-VCH.

enabled by photoresponsive nanocarriers for plasmid DNA and protein delivery is gene editing therapy. For instance, ROS-degradable thioketal-crosslinked polyethylenimine (PEI) was synthesized, which could be applied to condense p53 gene and photosensitizer into compact complexes to promote transfection. ROS produced by light irradiation could destroy endosomal membranes and accelerate the escape of p53 gene due to ROS triggered the degradation of thioketal-crosslinked PEI, which jointly accounted for enhanced anticancer gene therapy.^[28b] Similarly, Lyu et al. constructed photoactivatable semiconducting polymer nanoparticles encapsulating CRISPR/Cas9 plasmids for remotely phototriggered gene editing. The photoresponsive Cas9 delivery nanoparticles comprised PEI brushes, $^1\text{O}_2$ -generating backbones and $^1\text{O}_2$ sensitive linkers. NIR irradiation triggered the decomposition of gene vectors and the release of CRISPR/Cas9 plasmids for efficient in vivo gene editing (Figure 2C).^[53] In an effort to optimize the delivery performance, 160 formulations of phototriggerable polymer nanocapsule library composed of a set of amine and bisacrylamide

monomers, which were conjugated with photocleavable linkers based on *o*-nitrobenzyl chemistry, were designed. Among them, six nanoformulations were much more efficient than commercial Lipofectamine through the light-triggered release of siRNA and miRNA, which demonstrated high efficacy in a wound healing animal model.^[54]

Efficient delivery and activation of protein pharmaceuticals, which are extremely valuable for therapeutic use due to the pharmacological selectivity and potency,^[55] could also be triggered by light. Based on the light-induced cleavage of nitrobenzyl carbonate linker between nanocage structures and therapeutic protein cargos, the photolabile DNA nanocages acting as the efficient nanocarrier for triggered release of bioactive protein molecules were synthesized.^[34] In another case, RNase A was first caged with H_2O_2 -cleavable phenylboronic acid, which was then coated with acid degradable and ketal-crosslinked PEI and encapsulated in photosensitizer-modified hyaluronic acid. Upon visible light irradiation, the caged protein prodrug could restore bioactivity of RNase A upon photosensitizer-mediated

ROS production, hence enhancing targeted anticancer capability of the protein drug.^[55a] Similarly, the synthesis of organic semiconducting pro-nanoenzymes with the light-activatable properties for inhibition of lung cancer metastasis were also reported.^[56]

Biomaterials with spatially and temporally regulated presentation of bioactive peptide ligands using external light triggers have also been developed. The 3-(4,5-dimethoxy-2-nitrophenyl)-2-butyl ester caging group modified on the cell-adhesive Arg-Gly-Asp (RGD) peptide could be easily removed with light to render the full active of RGD peptide. The protecting group caged peptide on implanted biomaterials could regulate inflammation, cell adhesion, vascularization, and fibrous encapsulation of the material *in vivo*.^[57] Another typical example is that the proapoptotic peptide brush polymers formed by phototriggered reversible deactivation of radical polymerization of peptide acrylamide monomers, which showed improved cellular uptake, resulting in a significant improvement in cancer cell cytotoxicity.^[58]

2.5. Upconversion Nanoparticles for NIR Triggered Photochemical Drug Delivery

The photocaging approach is ideal for controlled delivery of bioactive agents to target locations at precise times and desired therapeutic doses. However, owing to the fact that UV and visible light of wavelength shorter than 650 nm can hardly penetrate tissues, the biomedical applications of direct UV- or visible light-stimulated delivery *in vivo* are limited. Recently, the NIR window of 650–900 nm has been successfully applied in photochemical drug delivery. Owing to distinct ladder-like energy levels of trivalent lanthanide ions,^[59] upconversion nanoparticles (UCNPs) composed of lanthanides embedded in host lattices of ceramic materials are capable of absorbing and converting NIR into UV/vis lights,^[60] and therefore can be utilized for photochemical-triggered delivery of drugs.^[61] Photolabile 2-nitrobenzylamine groups linked UCNPs could be utilized as the targeted drug delivery platform that successfully delivered DOX upon 980 nm laser excitation.^[36b] Similarly, UCNPs decorated with UV-sensitive *o*-nitrobenzyl groups for DOX and fluorescein molecules delivery were also constructed.^[62] NIR light-triggered drug release of UCNPs could also be realized by incorporation of ROS photosensitizers. UCNPs encapsulating the spectrally matchable photosensitizer (2-(2,6-bis((E)-4-(phenyl(40-(1,2,2-triphenylvinyl)-[1,10-biphenyl]-4-yl)amino)styryl)-4H-pyran-4-ylidene)malononitrile, TTD) of ROS generation characteristics and conjugated with cyclic RGD peptides were designed to efficiently kill triple-negative breast cancer cells during the NIR-regulated photodynamic treatment.^[63]

Recently, more interests are focused on the multifunctional hybrid vesicles containing UCNPs, taking metal–organic frameworks (MOFs) as an example. The superior properties of MOFs, such as well-defined porous structure, tunable composition and porosity, regular size and shape, versatile functionality, and improved biocompatibility, make them promising candidates as drug delivery hosts.^[64] Moreover, the heterodimer composed of UCNPs and the nanophotosensitizer porphyrinic MOFs could also achieve the NIR light-activated photodynamic therapy. For example, Janus nanostructures through the growth

of porphyrinic MOF on Nd³⁺-sensitized UCNPs were successfully developed for mitochondria-targeting, 808 nm NIR light-activated photodynamic therapy.^[65] The core–shell UCNP@porphyrinic MOFs for synergetic photodynamic/immuno-chemotherapy against hypoxic cancer were also rationally designed. The heterostructure enabled NIR light-activated cytotoxic ROS production for photodynamic therapy from MOF shells and hypoxia-activated chemotherapy from the prodrug tirapazamine encapsulated in MOF nanopores. Moreover, the combination of the nanotransducer with antiprogrammed death-ligand 1 therapy completely inhibited untreated distant tumor growth through improved anticancer immunity (**Figure 3A**).^[66]

In addition to small molecule drugs and photosensitizers, UCNPs can also serve as light-triggered scaffolding to help shuttle nucleic acid and protein drugs. Although RNA interference has been widely leveraged as an appealing therapeutic tool for cancer and other diseases, the effective protection of siRNA from leakage and degradation as well as on-demand delivery into target cells remain great challenges. Ju's group designed the photoreleasable tape-wrapped nanocapsules comprising core–shell UCNPs coated with the MSN layer for siRNA targeting polo-like kinase 1 and photosensitizer hypocrellin A loading, and covalently grafting the PEG via the photocleavable linker 2,5-dioxopyrrolidin-1-yl (2-nitro-5-(prop-2-yn-1-yloxy) benzyl) carbonate. After NIR irradiation, UCNPs produced UV emissions could efficiently break photocleavable linker for siRNA release and activate hypocrellin A to generate ROS for tumor suppression (**Figure 3B**).^[67] The similar biofunctional upconversion superballs were assembled by two distinct UCNPs loaded separately with superoxide dismutase-1 siRNA for gene knockdown and the photosensitizer zinc phthalocyanine for photodynamic therapy. The formed superballs could be individually or concomitantly excited by 980/808 nm light for programmed photoactivation of different cancer therapeutics.^[68] NIR light-triggered protein Cas9 delivery was also fulfilled by the integration of UCNPs and UV-sensitive photosensitive molecules. The UCNPs converted NIR into local UV light for efficient cleavage of 4-(hydroxymethyl)-3-nitrobenzoic acid molecules, thereby leading to on-demand CRISPR-Cas9 delivery. Additionally, guided by gRNA against the cancer gene polo-like kinase-1, the nanotransducers successfully inhibited tumor proliferation.^[69]

Moreover, with the help of UCNPs, remote control of enzyme activity was also realized. The NIR light-controlled enzyme activity in living cells was demonstrated based on hollow MSN-encapsulated UCNPs and the photoactivatable caged enzyme inhibitors Ru complexes.^[70] Lee and co-workers demonstrated the NIR light-activatable enzyme nanoplatfrom by utilizing protein kinase A/UCNP complex. The protein kinase A was successfully activated upon NIR irradiation to phosphorylate its substrate, which subsequently induced the downstream response in cells with high precision and spatiotemporal resolution.^[71] Another representative example was applying the UCNP-centered Au nanoparticles tetrahedron for the specific acceleration of the clearance of senescent cells. NIR irradiation induced the disassembly of DNA tetrahedron by breaking the boronic ester linkers. Therefore, granzyme B exposed on the UCNPs efficiently induced senescent cell apoptosis, providing a novel strategy for clinical therapy for aging and age-related diseases (**Figure 3C**).^[72]

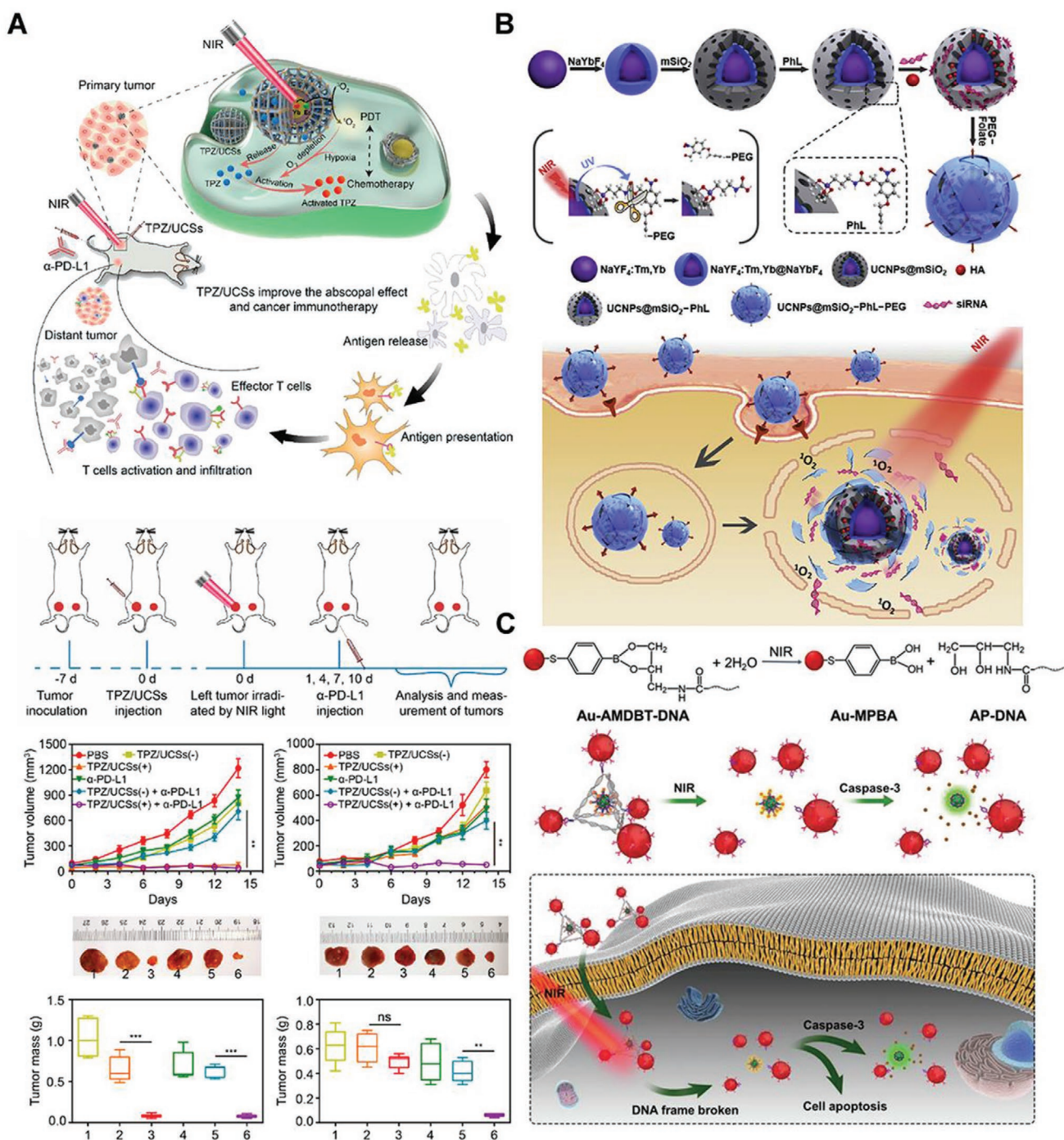


Figure 3. A) Schematic illustration of the structure of tirapazamine/upconversion nanoparticle@porphyrinic MOFs and their application to tumor treatment through a combination of NIR light-triggered photodynamic therapy and hypoxia-activated chemotherapy with immunotherapy. Reproduced with permission.^[66] Copyright 2020, American Chemical Society. B) Schematic illustrations of synthesis of upconversion nanocapsules, and folate receptor-mediated cellular uptake and NIR modulated intracellular siRNA delivery and therapy. Reproduced with permission.^[67] Copyright 2018, Elsevier. C) Schematic illustration of an upconversion-nanoparticle-centered Au nanoparticles tetrahedron used for senescence clearance. Reproduced with permission.^[72] Copyright 2020, Wiley-VCH.

2.6. Chemical Modifications of Nitrobenzyl and Coumarin for NIR Triggered Photochemical Drug Release

Other methods, such as chemical modifications of nitrobenzyl and coumarin compounds can also lead to absorption shifts to

biocompatible longer wavelengths under single-photon excitation or multiphoton absorption, such as the 7-amino coumarin compound modified with vinyl groups,^[19c] nitrobenzyl derivative 2-(2-nitrophenyl)propyloxycarbonyl,^[73] 7-diethylamino-4-thiocoumarinylmethyl protecting group,^[74] modified coumarinylmethyl

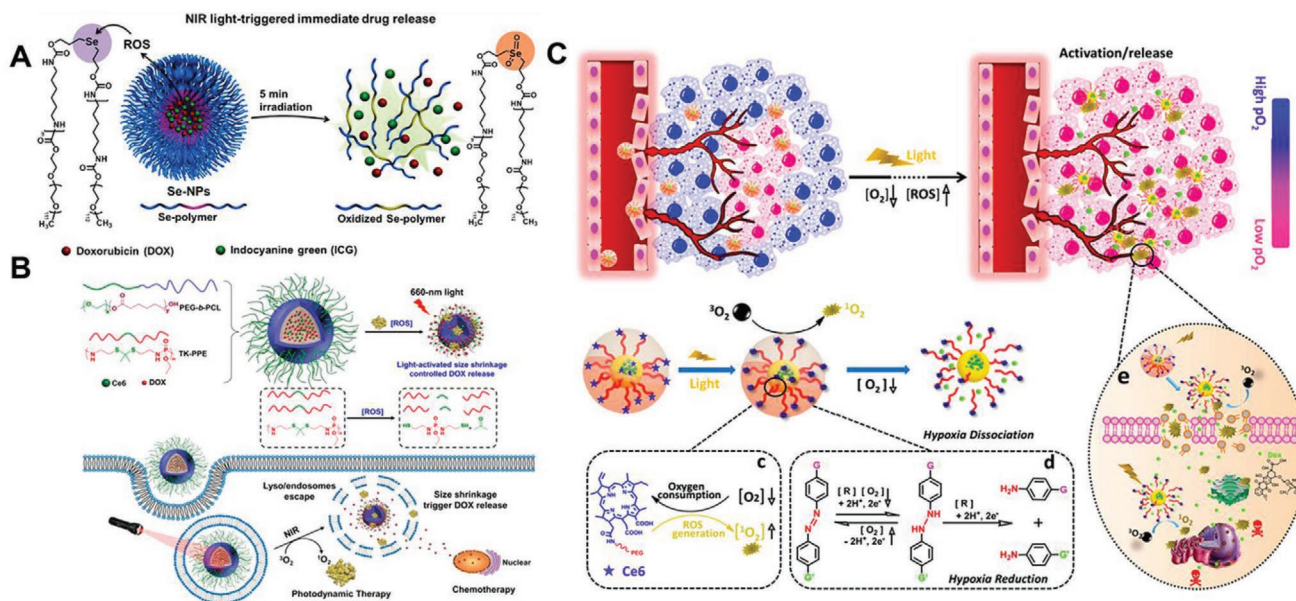


Figure 4. A) Schematic representation of selenium-inserted polymeric nanoparticles with immediate drug release and highly efficient cytoplasmic translocation features upon NIR irradiation for combined chemo-photothermotherapy. Reproduced with permission.^[78] Copyright 2017, American Chemical Society. B) Formation and mechanism of the light-activated shrinkable nanoplast. Reproduced with permission.^[79] Copyright 2018, American Chemical Society. C) Schematic of how the phototriggered nanoplasts worked in combination with hypoxia-triggered and photodynamic therapy strategy. Reproduced with permission.^[81] Copyright 2018, American Chemical Society.

backbone,^[75] etc. For example, Schnermann and co-workers constructed an NIR irradiation-activated uncaging reaction based on C4'-dialkylamine-substituted heptamethine cyanines. The caged phenol-containing small molecules could be efficiently released upon 690 nm light irradiation. The controlled gene expression as well as the reduced cell viability could be realized through the uncaging of estrogen receptor antagonist, 4-hydroxycyclofen.^[76] The coumarin-grafted cyclometalated Ru(II) complexes also exhibited stronger absorption and lower oxidation potential than the coumarin-free counterpart. Coumarin-linked cyclometalated Ru(II) photosensitizer showed a better photodynamic therapy efficacy than a coumarin-free counterpart under both normoxia and hypoxia. Moreover, in vivo experiments demonstrated that the tumor growth in tumor-bearing mice was significantly reduced under photosensitizer-based photodynamic treatment.^[77] These modified nitrobenzyl and coumarin-based materials hold considerable promise for drug delivery in vivo due to the simple implementation of red-shifted absorption and excellent cytocompatibility.

2.7. ROS Triggered Linker Cleavage upon NIR Irradiation for Drug Release

Given the wealth of available NIR-responsive photosensitizers, ROS triggered linker cleavage upon NIR irradiation could also be applied for controlled drug delivery. Various studies employing NIR light-triggered ROS generation for drug release as well as the combination of photodynamic therapy and thermochemotherapy were performed.

An interesting case is presented by Chen and co-workers, in which the NIR light-triggered nanoplast was designed

for highly effective cytoplasmic DOX delivery for synergistic thermochemotherapy (Figure 4A). Under transient NIR laser irradiation, ICG and DOX-loaded selenium-inserted copolymer nanoparticles were quickly dissociated in a few minutes via ROS-induced selenium oxidation, which efficiently promoted continuous drug release.^[78] In a related approach, the ROS-sensitive polymeric nanocarrier to achieve remotely regulated drug delivery by light-triggered size shrinkage was also explored (Figure 4B). Nanocomplex encapsulating DOX and Ce6 was self-assembled from amphiphilic copolymer poly(ethylene glycol)-*b*-poly(ϵ -caprolactone) and ROS-responsive polymer poly(thioetheral phosphoester). Under light exposure, ROS produced by Ce6 was able to cleave thioetheral linkers in situ, which led to quick degradation of the core. Consequently, the nanocarrier shrank and such shrinkage triggered rapid DOX release for cancer therapy both in vitro and in vivo.^[79] A similar theranostic liposome coupling with 2-nitroimidazole linked PEG amphoteric polymer to load hypoxia-activated prodrug tirapazamine, photosensitizer Ce6, and gene probe was described by Zhang's group for synergistically combined photodynamic-chemotherapy. Ce6-mediated photodynamic therapy-induced hypoxia upon irradiation, leading to dissociation of the liposome and activated antitumor efficiency of tirapazamine for enhanced cancer cell eradication.^[80] In another study of the novel delivery system by combining hypoxia-responsive chemotherapy and photodynamic therapy, the nanosystem made up of three primary constituents: the biodegradable poly(ϵ -caprolactone) as the hydrophobic segment, hydrophilic PEG-decorated Ce6 to improve Ce6 loading efficiency, and azobenzene bridges to detect hypoxia microenvironment was developed (Figure 4C). Upon light irradiation, cancer cells could be efficiently killed resulted from ROS generation by Ce6. Moreover, sustained

oxygen consumption could further induce the disassembly of hypoxia-responsive azobenzene to uncage DOX for cancer therapy.^[81] These excellent photochemical nanoplateforms have been successfully applied not only in antitumor chemotherapy, gene therapy, photodynamic therapy, and immunotherapy,^[15b,82] but also in smart carbon monoxide (CO) and nitric oxide (NO) delivery as well as antibacterial applications.^[83]

The photochemical-triggered drug delivery platforms offer advantages such as high cleavage efficiency, precise temporal and spatial control over drug release,^[84] tunable drug delivery rate, avoidance of side effects,^[33] and photosensitive cytotoxicity.^[31] Great progress has been achieved in photochemical-triggered drug delivery since its development. For example, substantial effort has been devoted to the fabrication of delivery vehicles that possess high drug encapsulation levels, minimal leakage in the absence of light and high biocompatibility. Besides, a plethora of work has been done on the design of photolabile groups that can avoid the usage of UV light, such as upconversion nanoparticles and two-photon absorption.^[85] However, some key challenges remain. Though many new photolabile groups have been developed, one major concern lies in the biocompatibility of the by-products of photochemical reactions. For example, the cleavage of *o*-nitrobenzyl groups leads to the generation of highly cytotoxic reactive nitrosobenzaldehyde, which can strongly inhibit enzyme activity,^[86] thus producing undesired side effects *in vivo*.^[16] Several photochemically triggered drug-delivery systems have employed UCNPs to avoid UV exposure. However, the impacts of the UCNPs that convert NIR into UV light on human health are not well established and need further studies.^[87] In addition, the drug delivery platforms that can achieve multiple release cycles have also gained increasing attention and interest. Photochemical activation usually results in an irreversible change in

the carrier. These photochemically triggered drug delivery platforms fail to generate uniform release profiles upon each light activation.^[88] Therefore, photochemically triggered drug-delivery platforms that can realize the stimuli-induced pulsatile release of drugs are still urgently required.

3. Photothermally Controlled Drug Release

Photothermally controlled drug release platforms can efficiently leverage light-to-heat energy transfer to affect thermosensitive components of drug-release vectors to execute drug delivery. So far, various types of nanomaterials possessing photothermal properties have been developed (Figure 5), including gold nanomaterials (gold nanocages, gold nanoshells, gold nanorods, and gold nanostars),^[11c,89] other types of metal nanomaterials (germanium nanocrystals, palladium nanosheets, Au–Cu alloy nanocrystals),^[90] carbon nanomaterials (graphene, carbon nanotubes, mesoporous carbon nanoparticles, fullerenes, graphene quantum dots, and carbon dots),^[89a,91] metal sulfides and oxides (CuS nanoparticles, WS₂, MoS₂ nanosheets, Ag₂S, tungsten oxide nanorods, Fe₂O₃ nanoparticles, molybdenum oxide, and Ti₂O₃ nanoparticles),^[92] heavy-metal and metal-free quantum dots (CdTe, CdSe, black phosphorus quantum dots),^[93] conjugated polymer nanoparticles (polypyrrole, PEDOT:PSS, and peptide–porphyrin nanodots),^[94] NIR organic dye,^[95] MOFs,^[96] etc. These photothermal agents feature good photostability, intense light absorbance, and excellent photothermal conversion efficiency.^[89a,97] Many of these nanomaterials can load and deliver drug alone, whereas other types of nanomaterials can efficiently load the drugs by combining with other nanocarriers or direct conjugating with the thermal-sensitive chemical linker.^[47,98]

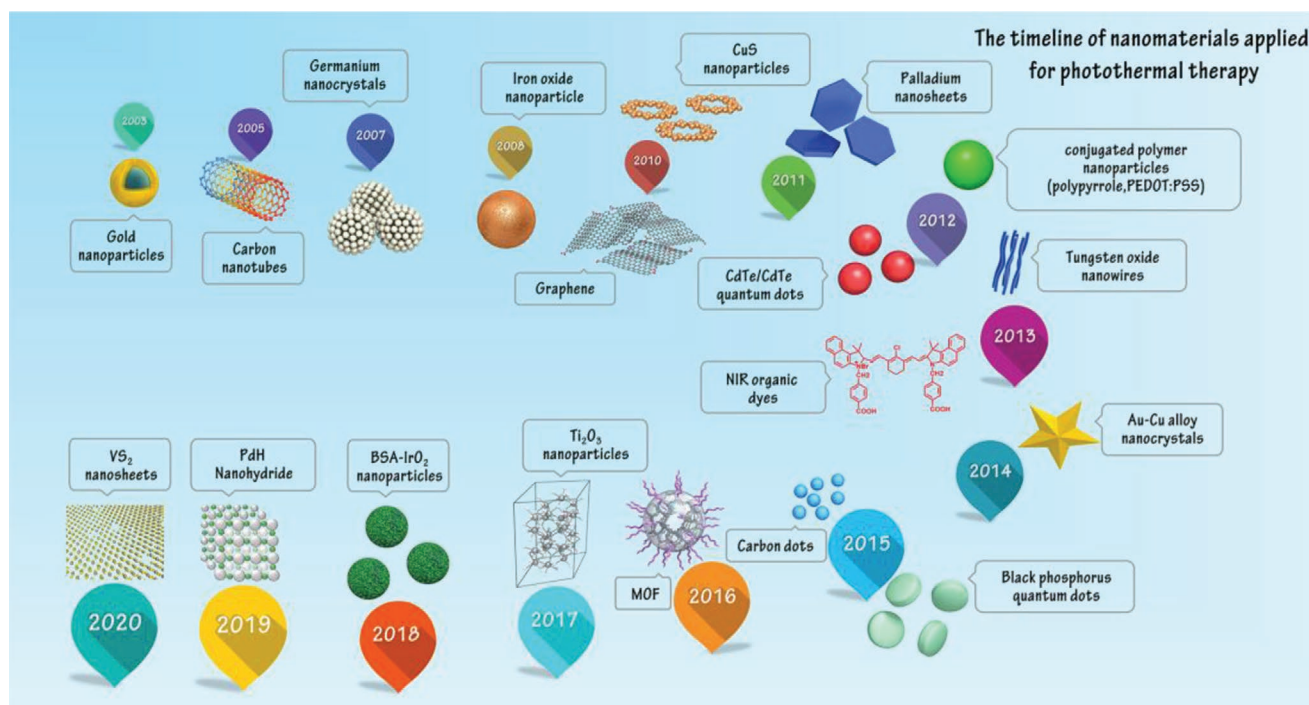


Figure 5. A brief history of the application of nanomaterials for photothermally controlled drug release.

3.1. Gold Nanomaterials for Photothermally Controlled Drug Release

Due to their strong local heating arose from the excitation of surface plasmon vibrations, gold nanomaterials are key agents for photothermally controlled drug release.^[89b] Ali et al. optimized the size, surface modification, concentration of gold nanorods, and the photothermal therapy laser power to induce maximum apoptosis. Mechanism studies indicated that the cell death pathways of photothermal therapy elicited by gold nanorods mainly involved apoptosis and the release of neutrophil extracellular traps. No long-term toxicity of gold nanorods was shown in a 15-month toxicity study in mouse models, demonstrating that the gold nanorods platform was highly safe and efficient for cancer therapy in vivo.^[99] Meanwhile, the gold nanomaterials have also been extensively investigated in the development of combination therapeutic nanoagents. For instance, DNA conjugated gold nanorods, which further encapsulated DOX by intercalating into the major groove of DNA double helix, were developed as the multifunctional nanocarrier for NIR radiation controlled drug delivery in multidrug-resistant breast cancer cell lines.^[100] In another similar study, Tao et al. designed the immunomodulatory CpG DNA-based platform that was linked to DOX and gold nanorods for cancer treatment. Gold nanorods could be utilized as nanovectors

to simultaneously achieve specific functions of chemotherapeutics, hyperthermia, and immunotherapy.^[101] Additionally, biomimetic drug release nanosystems comprised of cancer cell membranes as outer shells and DOX-functionalized gold nanocages as inner cores were developed for the efficient breast cancer targeting chemo-photothermal therapy.^[102] Recently, the novel yolk-shell gold nanostar@ZIF-8 MOF nanocapsule with excellent anticancer drug loading ability and superior 1064 nm NIR-II stimulated photothermal conversion capacity was fabricated. After DOX encapsulation into the cavity, gold nanostar@MOF showed outstanding synergistic chemotherapy and hyperthermia effect for tumor inhibition. At the same time, the infrared/photoacoustic imagings presented great superiority for imaging-guided therapy.^[103]

In addition to DOX, other small molecular drugs could also be loaded on gold nanomaterials via a similar route. In a recent study, the synergistic anticancer nanoplatform that combined photothermal therapy of PEGylated gold nanorods and the following inflammation-mediated active targeting chemotherapy of cytopharmaceuticals was constructed. The photothermal therapy-induced inflammation facilitated cytopharmaceuticals to migrate across tumor sites along chemotactic gradients, which exhibited a promising synergistic strategy for cancer treatment (Figure 6A,B).^[104] In a similar study, gold nanorods were encapsulated into perfluoropentane-filled MSN to form

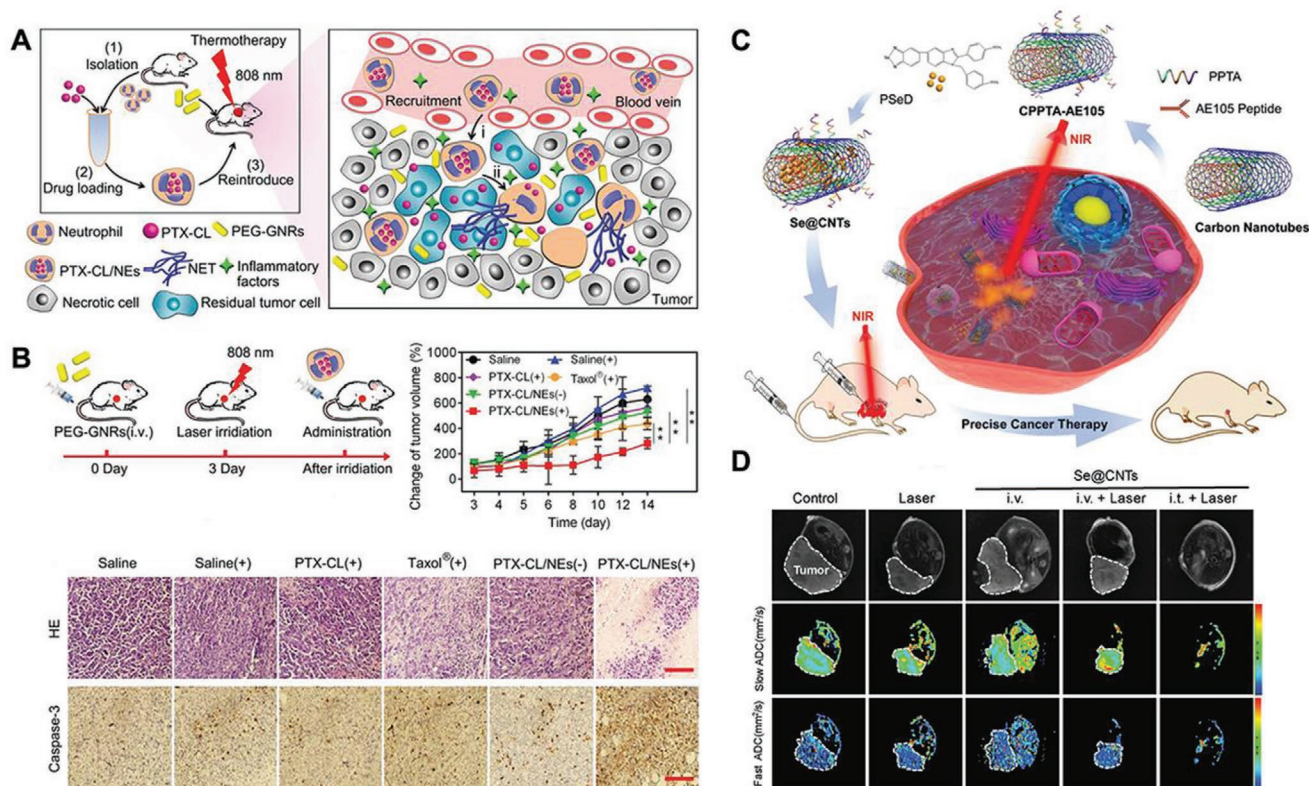


Figure 6. A) Schematic illustration of synergistic anticancer system combining photothermal treatment and inflammation-mediated active targeting chemotherapy. B) The synergistic therapeutic efficiency of photothermal therapy and inflammation-mediated active targeting chemotherapy. The growth profiles of tumors in mice that received different treatments. The HE staining and immunohistochemical staining (caspase-3) of tumor sections after administration of different treatments. Reproduced with permission.^[104] Copyright 2019, Wiley-VCH. C) Rational design and applications of Se@carbon nanotubes in cancer chemo-photothermal therapy. D) T_2 -weighted magnetic resonance images of MDA-MB-231 tumor-bearing mice after various treatments for 14 days. Reproduced with permission.^[116] Copyright 2018, Wiley-VCH.

a biodegradable NIR-responsive nanorattle for photothermal therapy of melanoma cancer. Notably, the heat generated from gold nanorods could induce perfluoropentane undergoing a liquid–gas phase transition to create microbubbles, which would enhance the tumor-targeted ultrasound/photoacoustic imaging signals.^[105]

Besides, the utilization of gold nanorods as the powerful platform for the delivery of large molecular therapeutic cargos has been widely reported. Incorporation of cationic polymer-coated gold nanorods to Cas9 plasmid delivery vehicles allowed the construction of the optogenetically activatable CRISPR-Cas9 systems for programmable genome editing in NIR-II optical window. This modality of optogenetic genome editing and the high transfection activity of nanoCRISPR enabled the successful therapy of deep tumor and rescue of fulminant hepatic failure with minimal off-target effects.^[106] Moreover, by the integration of the highly evolved targeting strategies of bacteriophages with the photothermal properties of gold nanorods, a recent study by Chen and co-workers conjugated the bacteriophages to gold nanorods, which could selectively target and kill specific Gram-negative bacterial cells by using photothermal ablation for antibacterial therapy.^[107]

Thanks to the structure-dependent photothermal performance of gold nanomaterials, the emergence of light-stimulus-responsive self-assembly of AuNPs brings new opportunities for the effective utilization of gold nanomaterials in photothermal-activated drug release for disease therapy as well.^[108] One example of self-assemble AuNPs was laser irradiation-induced covalent cross-linkage of the diazirine terminal groups of PEG ligands on the surface of AuNPs, leading to the generation of crosslinked particle aggregates for enhanced photoacoustic imaging and hyperthermia therapy of malignant tumors.^[109] Gold nanoparticles grafted with complementary DNA strands, tethered with DOX, and coated with polyethylene glycol via a matrix metalloproteinase-cleavable peptide were also developed. The nanoprobe formed aggregates rapidly under matrix metalloproteinase-rich tumor tissues owing to the rapid cleavage of the shielding PEG layer and subsequent exposure of the complementary DNA strands on the nanoparticles, which was beneficial to photoacoustic diagnosis-guided hyperthermia therapy and drug delivery.^[110]

3.2. Carbon Nanosystems for Photothermally Controlled Drug Release

While these gold nanostructures offer great potential for photothermal therapy, several obstacles restrict their practical utilization in clinical applications, such as high cost and easy loss of stable NIR absorbance after laser irradiation. Arising from their excellent thermal conduction characteristics, carbon nanomaterials are superior candidates for achieving effective photothermal actuation.^[111] Therefore, carbon nanosystems were also extensively explored for photothermally controlled drug release owing to the intense light absorption at NIR wavelengths and corresponding high photothermal-conversion efficiency.^[112] To allow photothermal activation of drug release, Mertz's group designed and optimized graphite coated with mesoporous silica shell and systematically studied DOX payload release upon NIR

irradiation.^[113] Subsequently, branched PEI and PEG modified reduced graphene oxide was also constructed as a nanocarrier for photothermally triggered DOX delivery.^[98g] Moreover, the PEI and PEG dual-polymer-functionalized graphene oxide could also be utilized as the nanocarrier for effective delivery of CpG DNA. The immunostimulatory activity of CpG DNA could be efficiently controlled by graphene oxide-PEG-PEI, exhibiting remarkably enhanced immunostimulation responses upon NIR illumination for providing combined immunological and photothermal effects for cancer therapy.^[114]

Apart from graphene materials, other well-studied nanocarbon agents also displayed excellent photothermal efficacy to facilitate photoheating-triggered drug release.^[115] In this regard, Chen's group synthesized organoselenium drug-loaded, urokinase-type plasminogen activator receptors and polypeptides AE105 dual-targeted carbon nanotube-based nanocomposites Se@CNTs for effective combination photothermal chemotherapy of triple-negative breast cancers (Figure 6C,D).^[116] The carbon nanomaterial family has flourished in cancer treatment for decades. Nevertheless, the practical clinical utility of carbon nanomaterials-based therapies is limited by their dilemma of *in vivo* metabolism.^[117] To address this challenge, the carbon–silica nanohybrid was rationally designed and constructed, which could degrade into about 5 nm small nanoparticles after NIR light irradiation for effective *in vivo* elimination. The carbon–silica nanocomposite with excellent photodynamic and photothermal capabilities could also act as inherent immunoadjuvant for synergistic phototherapy and immunotherapy for complete cancer elimination.^[117]

3.3. Metal Nanohybrids for Photothermally Controlled Drug Release

Metal oxides and sulfides, such as CuS NPs were also considered as the optimal candidate for photothermally triggered drug release owing to their outstanding properties, including great photothermal conversion efficiency and excellent NIR absorption.^[118] The photothermal agent CuS could precisely target cancer cells and tumor tissues when modified with different target ligands, such as aptamers, peptides, and antibodies, offering additional merits for cancer therapy.^[119]

With well-established functionalization methods, the CuS NPs could be easily integrated with other functional nanostructures and permit the fabrication of multifunctional nanodevices. As an example, Wei et al. constructed renal-clearable nanomaterials by controlled encapsulating of sub-6 nm CuS nanoclusters on DOX-loaded biodegradable MSN for synergistic chemo-photothermal cancer treatment in two different tumor models *in vivo*.^[98e] In another similar study, membrane materials derived from melanoma cells and red blood cells were encapsulated onto DOX-loaded hollow CuS NPs for combination chemo-photothermal therapy of melanoma (Figure 7A). The cell membranes on hollow CuS NPs endowed the nanoplateform markedly enhanced homogeneous targeting abilities and prolonged circulation lifetime *in vivo*. Thus, the platform exhibited satisfactory combined photothermal/chemotherapy achieving nearly 100% melanoma tumor elimination.^[120] Additionally, a smart nanocarrier system based on

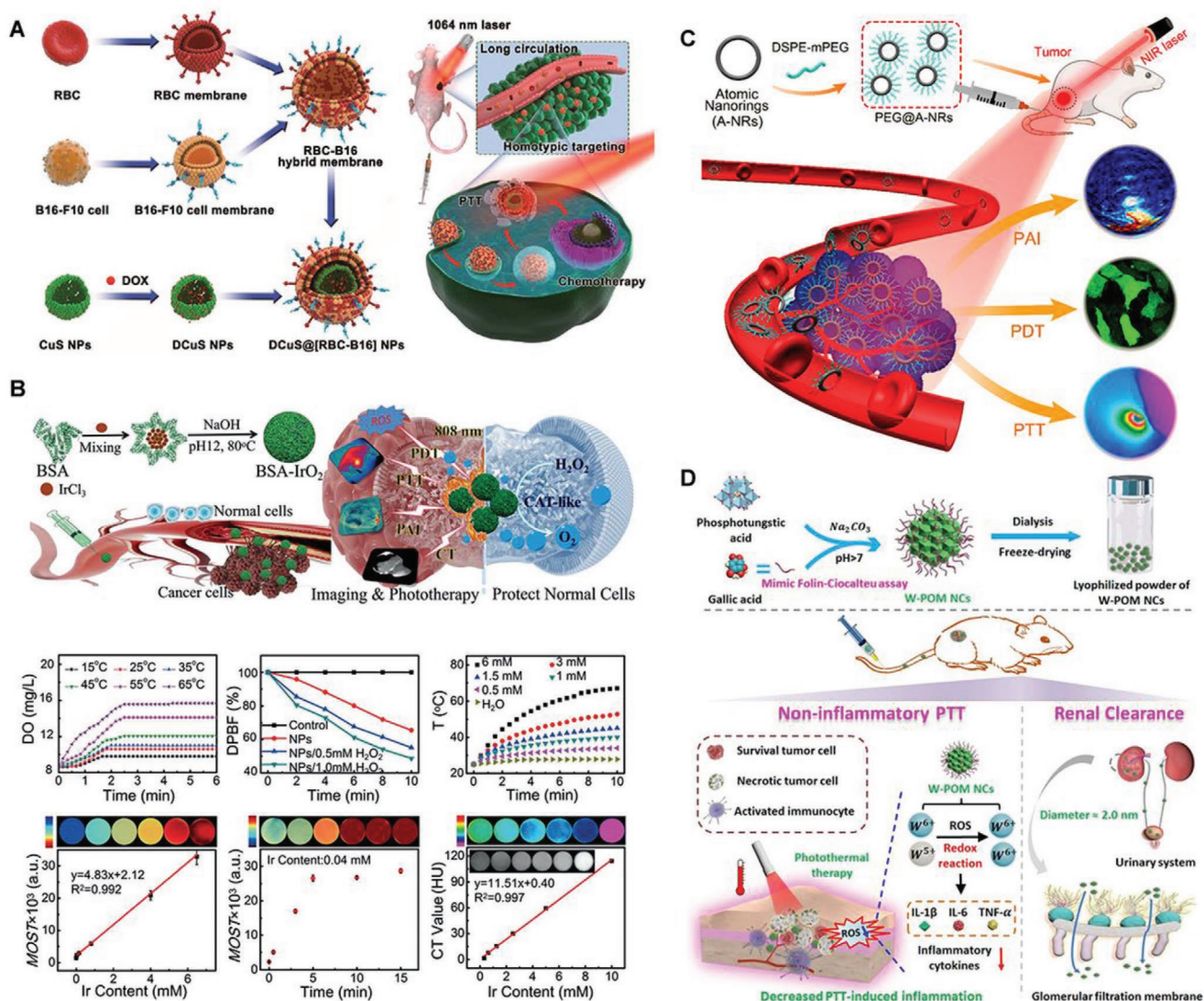


Figure 7. A) Schematic of membrane fusion and coating. Membrane materials are derived from red blood cells and B16-F10 cells and then fused together. The resulting hybrid membrane is used to camouflage DOX-loaded hollow copper sulfide nanoparticles to produce nanoparticles for synergistic photothermal/chemotherapy of melanoma. Reproduced with permission.^[120] Copyright 2018, American Chemical Society. B) Synthetic process and therapeutic mechanism of BSA-IrO₂ NPs. Temperature-dependent H₂O₂-triggered O₂ generation/consumption of 1,3-diphenylisobenzofuran under irradiation/concentration-dependent photothermal curves by BSA-IrO₂ NPs. In vitro photoacoustic images and photoacoustic signals of BSA-IrO₂ NPs at different concentrations of Ir and upon the addition of H₂O₂, as well as CT images and Hounsfield unit values of BSA-IrO₂ NPs solutions. Reproduced with permission.^[124] Copyright 2018, Wiley-VCH. C) Illustration of atomic-level nanorings, a theranostic agent for photoacoustic imaging, photodynamic therapy, and photothermal therapy for cancer. Reproduced with permission.^[128] Copyright 2020, American Chemical Society. D) Schematic illustration for the synthesis and underlying mechanisms of tungsten-based polyoxometalate nanoclusters for noninflammatory photothermal therapy with rapid renal clearance. Reproduced with permission.^[144] Copyright 2020, American Chemical Society.

self-assembly of PEI, double-stranded DNA segments, hydrophobic Cu₉S₅ NPs, and DOX was developed. Upon NIR irradiation, DOX intercalated inside the double-stranded DNA could be efficiently released in the target cancer cells due to photothermal-induced unzipping of the helix.^[121] Incorporation of CuS NPs into MOFs zeolitic imidazolate framework-8 (ZIF-8) also provided an option for NIR light-triggered DOX release for chemo-photothermal therapy since ZIF-8 nanoparticles could be disintegrated under NIR laser irradiation.^[122] Apart from small molecule drug DOX, small drug ions could

also be encapsulated in CuS photothermal platforms, which would open new possibilities for combination therapy. Xu et al. engineered and applied the Ca²⁺ nanogenerator based on the calcium phosphate-doped hollow mesoporous CuS for effective antitumor therapy. Ca²⁺ nanogenerator could generate Ca²⁺ directly and continuously owing to the low pH environment in lysosomes and the NIR acceleration of CuS. Both in vitro and in vivo studies revealed that the nanoplatform displayed high anticancer activity via combined photothermal therapy and imbalance of mitochondrial Ca²⁺ homeostasis.^[123]

In addition to CuS NPs, other types of transition metal oxides and sulfides, such as IrO₂ NPs,^[124] WO_{2.9} nanorods,^[125] ZrO_{2-x} nanosystems,^[126] MoS₂ nanosheets,^[127] sulfur-doped MoO_x nanorings,^[128] Bi_{2.88}Fe₅O₁₂ NPs,^[129] WS₂ nanosheets,^[130] Bi₂S₃ nanorods,^[131] VS₂ nanosheets,^[132] Bi₂O₂Se quantum dots,^[133] etc., were reported to show impressive photothermal effects, which were promising for fabrication of the nanocarriers for photothermally controlled drug delivery. In an interesting study, the BSA-templated IrO₂ nanoparticles were synthesized through one-step biomineralization, which exhibited extraordinary catalase-like photocatalytic activity for normal cells protection and photoacoustic imaging improvement, the large X-ray absorption coefficient for computed tomography imaging, as well as excellent photothermal conversion efficiency for tumor therapy (Figure 7B).^[124] In another example, Sun's group for the first time elaborately designed the oxygen-deficient ZrO_{2-x} nanovector for Ce6 and thiol-PEG-amine conjugation for efficacious fluorescence/photoacoustic bimodal imaging-guided photothermal/photodynamic treatment.^[126] The PEG-coated sulfur-doped MoO_x nanorings-mediated remarkable photothermal performance and ROS generation property were also utilized for photoacoustic-guided synergistic photothermal/photodynamic treatment (Figure 7C).^[128]

Imaging-guided synergistic photothermal therapy provides a novel way to construct precision nanotheranostic agents. A number of multifunctional composite metal nanohybrids have been studied as potential nanoagents for imaging-guided synergistic photothermal therapy with diverse therapeutic and diagnostic payloads, including FePS₃ nanosheets with excellent photothermal conversion activity enabling chemodynamic therapy and hyperthermia effect for cancer therapy,^[134] carbon-encapsulated FeCo nanomaterials as magnetic imaging tracers with magnetothermal and photothermal capabilities,^[135] zirconium-ferriporphyrin MOF nanotransducer complexed with heat shock protein 70 siRNA for computed tomography, photothermal, and photoacoustic trimode imaging modalities-guided combined gene and photothermal-photodynamic therapy for efficient cancer elimination,^[136] FePt/MoS₂ nanomaterials with synergistic photothermal-chemotherapy for improving tumor immunotherapy,^[137] Mo₂C-derived polyoxometalate as a chemodynamic therapy agent,^[138] functionalized MoTe₂ nanosheets with PEG-cyclic RGD and DOX for combined photothermal and chemotherapy,^[139] Cu-based Fenton like agent copper(I) phosphide (Cu₃P) nanocrystal for magnetic resonance imaging-based cancer chemodynamic/photothermal combination therapy,^[140] copper-palladium alloy nanocrystals for multispectral optoacoustic tomography (MSOT) imaging guided photothermal chemotherapy,^[141] PdH nanohydride for combinational hydrogen releasing-triggered hydrogen-photothermal treatment,^[142] polyelectrolyte-multilayer-coated Cs_xWO₃ for computerized tomography (CT)/photoacoustic bimodal imaging-based cancer photodynamic/photothermal therapy,^[143] tungsten-based polyoxometalate nanoclusters for efficient photothermal and anti-inflammatory treatment,^[144] vanadium carbide nanosheets with enhanced NIR photothermal performance,^[145] Bi/phthalocyanine manganese photosensitizer nanocomposites with high magnetic resonance and CT imaging performance for photothermal and photodynamic therapy,^[146] supramolecular photothermal

nanodrugs BSA-pheophorbide a-Mn²⁺ nanoparticle with heating-enhanced photothermal effects,^[147] the MOF Hf-UiO-66 archetype structure incorporated with photoactive tetratopic chlorin ligands for multimodal CT/thermal/photoacoustic imaging-guided photothermal-photodynamic anticancer therapy.^[148] An interesting work presented a core-shell nanotheranostic agents, that is, the FeCo core nanomaterials and bore graphitic carbon shells grafted with PEG, providing not only the high magnetic particle imaging signal intensity and the photoacoustic imaging function, but also photothermal and magnetothermal properties for efficient tumor elimination in mice.^[135] Another successful example comes from the copper-palladium alloy tetrapod nanoparticles with superior NIR photothermal transducing properties for efficient chemophotothermal cancer treatment. Furthermore, NIR-assisted MSOT imaging was utilized to guide light irradiation and achieved accurate cancer eradication with minimum damage to normal cells.^[141] Moreover, ultrasmall tungsten-based polyoxometalate nanoclusters exhibited excellent photothermal conversion efficacy and impressive anti-inflammatory property arising from eliminating inflammation-generated ROS benefiting from the oxidation of tungsten to achieve outstanding therapeutic safety and efficiency (Figure 7D).^[144]

3.4. Black Phosphorus for Photothermally Controlled Drug Release

As mentioned above, a plethora of different inorganic nanomaterials, including gold nanostructures, carbon nanomaterials, and transition-metal dichalcogenides, are the frequently utilized photothermal conversion nanoagents, owing to the excellent NIR light response properties. However, most of them are often limited by nondegradability, metabolizing difficulty, and low biosafety that remain major challenges for clinical applications.^[149] Recently, black phosphorus was also explored as photothermal agents to promote drug delivery. With the superiority of readily degradation in water and air, black phosphorus is promising for in vivo applications.^[150] An interesting work presented the photothermal-responsive nanohydrogel structures, that is, the black phosphorus acting as the photosensitizers were embedded into the hydrogel, thus efficiently generating heat that softened and melted hydrogel for drug delivery upon NIR exposure for efficient cancer therapy.^[149] Black phosphorus quantum dots coated by poly(lactic-co-glycolic acid) (PLGA) were also developed by the emulsion method. Inspired by the good photothermal conversion efficiency of black phosphorus, the biodegradable nanospheres with the tumor-targeting ability showed satisfactory anticancer therapeutic efficacy in both cultured cells and animal models under NIR laser illumination.^[151] The 2D nanosheet formation of the black phosphorus was also constructed, which displayed extremely high DOX loading ability and showed pH/photoresponsive delivery capacity. The acidic tumor microenvironments in cancer cells could accelerate DOX release from the black phosphorus nanosheets, whereas the intrinsic photothermal and photodynamic effects of nanosheets could further promote the drug delivery and simultaneously allow black phosphorus nanosheets to serve

as both efficient photothermal and photodynamic agents to achieve the outstanding in vivo antitumor therapeutic outcome.^[152] Furthermore, to verify the delivery of small drug ions by the photothermal black phosphorus platforms, strontium ion (Sr^{2+}) was utilized as a model small chemical. The SrCl_2 and black phosphorus nanosheets were incorporated into PLGA as the NIR-triggered drug release system for bone regeneration. Due to the presence of black phosphorus nanosheets, the fabricated microspheres showed excellent photothermal effects, which triggered the release of Sr^{2+} by disrupting the PLGA shells. Sr is a trace element associated with promoted osteoblast differentiation and bone formation as well as repressed osteoclastic resorption.^[153] Implantation of microspheres into the rat femoral defect demonstrated favorable tissue compatibility and great bone regeneration ability upon NIR excitation.^[154]

3.5. Organic Nanoparticle for Photothermal Drug Delivery System

Up to now, both light-absorbing organic polymers and small molecules organic dyes have shown great potential in photothermal therapy.^[155] Organic polymers offer a well-documented pharmaceutically relevant platform that has been underexplored for photothermal drug encapsulation and delivery.^[156] To date, different categories photothermal organic nanoparticles for photothermal-triggered drug delivery have been developed, including the amphiphilic polymer nanobioconjugates via coprecipitation of poly(cyclopentadithiophene-*alt*-diketopyrrolopyrrole) and photothermal modulator polystyrene-*b*-poly(acrylic acid) to regulate heat-sensitive Ca^{2+} ion channels in neurons,^[157] semiconducting polymer L1057 nanoparticles fabricated by Pd-catalyzed Stille polymerization of 6,6,12,12-tetrakis(4-hexylphenyl)-*s*-indacenodithieno[3,2-*b*]thiophene-bis(trimethylstannane) and 4,9-dibromo-6,7-bis(4-(hexyloxy)phenyl)[1,2,5]thiadiazolo[3,4-*g*]quinoxaline for NIR-II bioimaging-guided photothermal cancer therapy,^[158] the semiconducting copolymer poly[(diketopyrrolopyrrole-*alt*-cyclopentadithiophene)-*ran*-(diketopyrrolopyrrole-*alt*-thiadiazoloquinoxaline)] for improved anticancer hyperthermia treatment,^[159] NIR-absorbance polymer PDPP3T-O14 composed of poly((2,5-diyl-2,3,5,6-tetrahydro-3,6-dioxo-pyrrolo(3,4-*c*)pyrrole-1,4-diyl)-*alt*-(2,2':5',2''-terthiophene-5,5''-diyl)) as backbone and oligo(ethylene glycol) as side chains for efficient disassembly of amyloid β ($\text{A}\beta$),^[160] cyclo(Arg-Gly-Asp-DPhe-Lys(mpa))-modified donor-acceptor structured conjugated polymer nanoagents polymerized via hydrophobic alkyl chain-appended (4,8-bis((2-octyldecyl)oxy)-benzo[1,2-*b*:4,5-*b'*]dithiophene-2,6-diyl)bis(trimethylstannane)) and 4,8-bis(5-bromo-4-(2-ethylhexyl)thiophen-2-yl)benzo[1,2-*c*:4,5-*c'*]bis[1,2,5]thiadiazole as the electron donor and acceptor for accurate spatiotemporal hyperthermia brain cancer treatment via scalp and skull,^[161] nanodots via peptide-tuned self-assembly of light-activable porphyrins for photoacoustic imaging and efficient cancer treatment,^[94d] porphyrin-based covalent organic framework nanopatform for photoacoustic imaging-guided combined photothermal/photodynamic therapy.^[162] The semiconducting polymer L1057 NPs acting as the theranostic

nanosystems were effectively applied in NIR-II imaging-guided photothermal therapy. Particularly, the outstanding biocompatibility, together with high brightness and excellent stability, allowed for noninvasive real-time visualization of brain vessels and high-resolution detection of tumors and cerebral ischemic stroke (**Figure 8A**).^[158] In addition, photothermal nanomedicines emerged not only as excellent anticancer drug delivery systems, but also as inhibitors for $\text{A}\beta$ aggregation. NIR-absorbance PDPP3T-O14 acted as hyperthermia cores and thermal-stimuli 1,2-dipalmitoyl-*sn*-glycero-3-phosphocholine served as outer NIR-activated gatekeepers. The subsequently curcumin encapsulation and peptides β -sheet breaker peptides LPFFD (Leu-Pro-Phe-Phe-Asp) functionalization could effectively realize high $\text{A}\beta$ -binding affinity, NIR light-triggered drug delivery, as well as photothermal degradation characteristics for complete disassembly of $\text{A}\beta$ (**Figure 8B**).^[160]

Strikingly, polydopamine, as a melanin-like polymer, is also emerging as a competitive photothermal agent for biomedical applications owing to its good biocompatibility, facile synthesis and high NIR photothermal conversion efficiency.^[163] So far, diverse types of polydopamine nanocomposites have been successfully used in a broad class of photothermal therapy applications, like the Fe-alendronate-conjugated, chemodrug SN38-loaded polydopamine nanoparticles for chemo-photothermal treatment of malignant bone tumors,^[164] polydopamine nanoparticles functionalized with adamantane-modified RGD peptides and decorated with β -cyclodextrin substitutions for synergistic targeted cancer photothermal-chemotherapy,^[165] magnetic nanoparticles@gold nanoparticles@polydopamine/doxorubicin/folic acid for tumor chemo-photothermal therapy,^[166] 2D ZIF-8 MOF nanosheets loaded with curcumin and further coated with polydopamine for efficient ablation of tumor in combination of photothermal-chemotherapy,^[167] MnCO-entrapped mesoporous polydopamine nanoparticles of effective CO/Mn²⁺ generation and photothermal transducing capabilities in H_2O_2 -rich and acid tumor microenvironment for photoacoustic/magnetic resonance bimodal imaging-guided tumor treatment,^[163] RGD peptide-functionalized mesoporous polydopamine nanomaterials loading with photosensitizer ICG for biofilms eradication,^[168] L-arginine modified, ICG-loaded mesoporous polydopamine for elimination of the already-formed biofilm by NO-promoted photodynamic/low-temperature photothermal treatment.^[169] All these examples provide valuable insight into the development of polydopamine-based multifunctional and efficient photothermal therapy platforms for further biomedical uses.

Although photothermal organic polymer nanoparticles have shown great potential for photothermal treatment, common polymer nanocomposites show slow metabolism in organisms and are primarily taken up by the reticuloendothelial systems,^[170] which may limit their potential clinical applications. Therefore, a wide spectrum of small-molecule organic dyes, such as IR780,^[171] IR820,^[172] cyanine,^[173] heptamethine cyanine (Cy7),^[174] ICG,^[175] phthalocyanine naphthalocyanine,^[170c] Prussian blue,^[176] BODIPY derivatives,^[177] pigment biliverdin,^[178] methylenabisacrylamide,^[179] etc. have served as attractive candidates for photothermal applications. Since the small organic dye molecules commonly show large molecular sizes and extensive π -conjugated structures with poor water

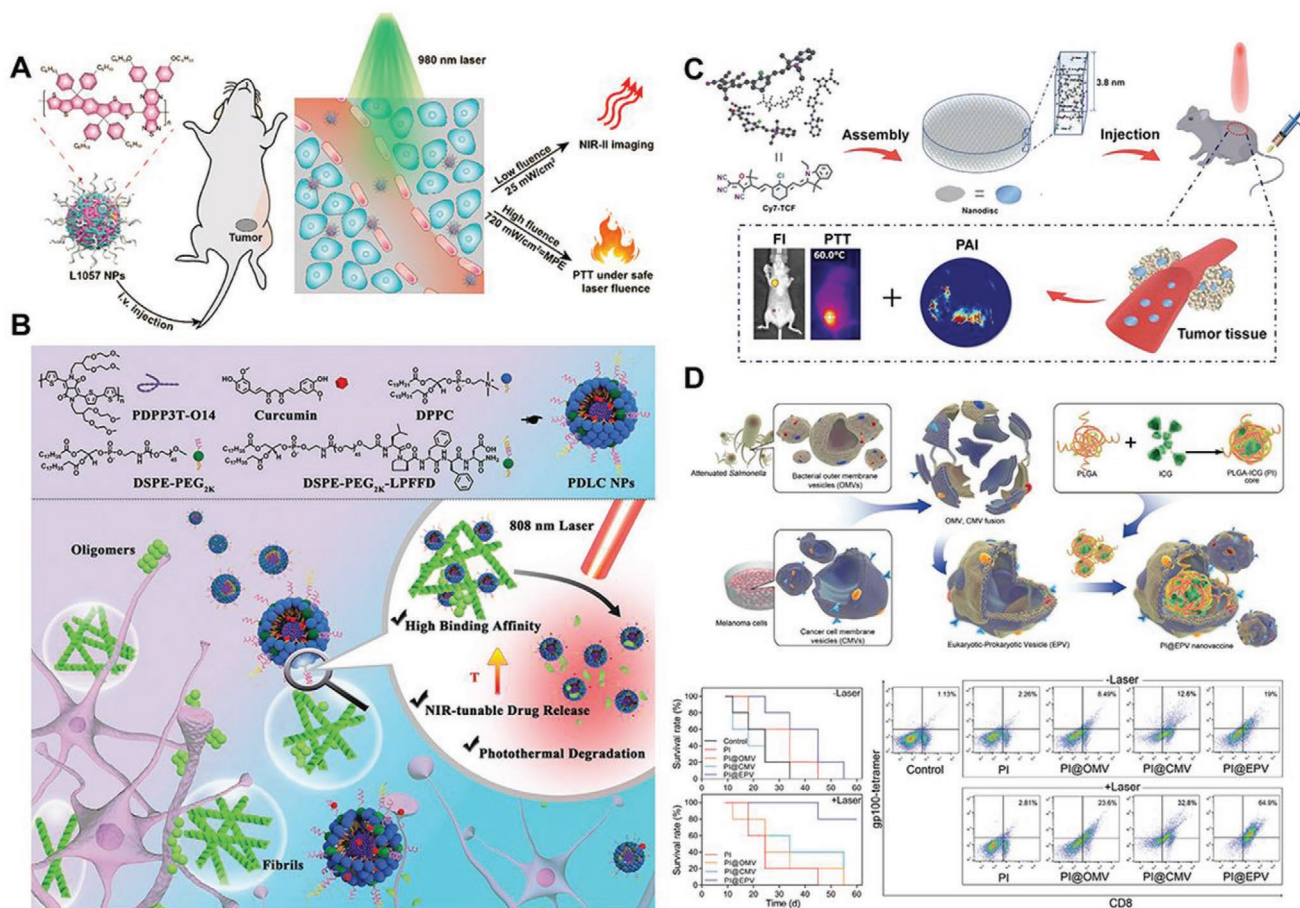


Figure 8. A) Schematic illustration of the preparation of L1057 NPs as a theranostic agent. Reproduced with permission.^[158] Copyright 2020, American Chemical Society. B) Schematic illustration of polymer-dispersed liquid crystal nanoparticles for chemo-photothermal treatment for β aggregation. Reproduced with permission.^[160] Copyright 2020, Wiley-VCH. C) Schematic illustration of Cy7-2-dicyanomethylene-3-cyano-4,5,5-trimethyl-2,5-dihydrofuran self-assembly into a nanodisc to exhibit the phototheranostic functions and accumulation at tumor site, thereby improving the imaging-guided cancer therapeutic efficacy in vivo. Reproduced with permission.^[174] Copyright 2020, Wiley-VCH. D) Schematic illustration of fabrication of eukaryotic-prokaryotic vesicles coated poly(lactic-co-glycolic acid)-indocyanine green moiety-implanted eukaryotic-prokaryotic vesicle nanovaccine. Survival curves of mice after various treatments. Flow cytometric analysis of PE-labeled T-Select MHC Tetramer-positive cells gated CD8⁺ cells expressed in the therapeutic efficacy trial. Reproduced with permission.^[175] Copyright 2020, Wiley-VCH.

dispersibility and photostability, photothermal organic dye delivery systems based on nanocarriers have been developed. A series of unimolecular polymeric micelles with different morphologies including nanoparticles, nanorods, and nanowire were loaded with NIR fluorescence dye IR780 as the photothermal agent. Micelles-IR780 with rodlike structure showed favorable behavior for in vitro cellular uptake and in vivo accumulation for effectively inhibited breast tumor growth.^[171a]

Combined chemo-photothermal therapy could also be realized by the codelivery of photothermal small molecule organic dyes and chemical drugs. For example, IR780 and DOX loaded in polymer micelles and a eutectic mixture of naturally occurring fatty acids were designed and synthesized, which showed light-regulated synergistic, integrated functions of photothermal and chemotherapy.^[171b,c] Similarly, Zhang et al. utilized IR820 to link with cytarabine to form prodrug. This prodrug was then loaded into the ZIF-8 MOFs, which were further encapsulated with hyaluronic acid to produce the active-targeting nanoplatform for fluorescence imaging-guided

photothermal-chemotherapy.^[180] Besides, both programmed-death-ligand 1 antibodies and NIR dye IR820 were loaded into the lipid gel depot. NIR irradiation regulated the delivery of the antibody and increased chemotactic recruitment of tumor-infiltrating lymphocytes, as well as boosted T cell activity against tumors for the efficient photothermal-assisted immunotherapy.^[172]

Cyanine is the NIR fluorescent photosensitizer exhibiting narrow absorbance peaks and high extinction coefficients, which can also generate hyperthermia after NIR irradiation for photothermal therapy.^[173,181] The multicomponent nanocomposites were elaborately fabricated by the coencapsulation of thermosensitive cyanine and DOX into the poly(ether amine) for controllable drug delivery and tunable chemotherapy.^[173] Recently, the Cy7-based 2D phototheranostic nanomedicine was developed by self-assembly of Cy7 to obtain the 2D nanodiscs. The nanodiscs exhibited passive cancer-targeting properties to not only real-time track tumor development by photoacoustic/fluorescence tomography but also realize effective tumor

suppression upon irradiation (Figure 8C).^[174,182] In subsequent work, the PLGA-ICG moiety-implanted eukaryotic–prokaryotic vesicle nanoformulation was also developed, which could not only be applied to trigger the anticancer immune response, but also possessed photothermal modality, allowing for the synergistic photothermal treatment with immunotherapy (Figure 8D).^[175] Furthermore, for a better potential application, Dong's group recently fabricated the nanoscale covalent organic framework nanohybrid by stepwise bonding defect functionalization of porphyrinic photosensitizers and guest encapsulation of photothermal agents naphthalocyanine. The nanohybrid exhibited photothermal transducing capabilities and excellent ¹O₂ generation properties under visible and NIR irradiation, therefore providing the synergistic photothermal/photodynamic therapeutic functions on suppressing breast cancer cell proliferation and invasion.^[170c]

In addition to cyanine dye, considerable endeavors have been devoted to exploring other types of small molecule organic dyes for photothermal therapy. In this regard, a multimodal Prussian blue nanoplatfom was designed and functionalized with therapeutic p53 gene for NIR photoresponsive combined gene therapy/photothermal therapy.^[176] In addition, the photothermal agents based on the BODIPY scaffolds were synthesized with an extremely high photothermal conversion efficiency of 88.3%, which resulted in complete tumor ablation under safe intensity NIR laser irradiation.^[177] Moreover, the utilization of the endogenous NIR absorbing pigment biliverdin, together with short peptides and metal ions, to fabricate photothermal nanoformulations to achieve metabolizable and effective candidates for cancer theranostics, was also demonstrated.^[178] Recently, Chen's group designed lipid nanoagents composed of the stearic acid and lauric acid mixture and coencapsulated with DOX and organic photothermal dye methylenebisacrylamide for quick drug release and excellent cancer-targeting ability in response to NIR irradiation for cancer treatment.^[179]

These photothermal organic polymer nanoparticles and small molecule organic dyes can efficiently convert absorbed light into localized heat. In addition to possessing destructive effect against disease tissues, photothermal organic polymer nanoformulations have been widely applied in controlled release and delivery of drug molecules to targeted areas. Therefore, these multifunctional photochemotherapy systems are promising candidates for disease treatment.

3.6. Imaging-Guided Photothermal-Chemotherapy Nanoplatfoms

Furthermore, given the essential role imagings act in disease diagnosis, developing imaging-guided photothermal-chemotherapy nanoplatfoms has been attracting increasing attention, particularly in the areas of precise and comprehensive evaluations of therapeutic effects, as well as enhancing therapeutic efficiency and reducing side effects. Considerable efforts have been devoted to the creation of imaging-guided photothermal-chemotherapy nanoplatfoms.^[183] Until now, a lot of photothermal nanomaterials with multiple intriguing modal imaging properties, including photoluminescence imaging,^[184] photoacoustic imaging,^[185] X-ray computed tomography imaging,^[186] magnetic

resonance imaging,^[187] surface-enhanced Raman scattering imaging,^[188] ultrasound imaging,^[189] etc. have been developed. As mentioned above, a variety of nanomaterials, including gold nanorod and photocrosslinkable gold nanoparticles for photoacoustic imaging, Mo₂C polyoxometalate for NIR photoacoustic tomography, zirconia nanosystem for fluorescence/photoacoustic bimodal imaging, bismuth (Bi) for CT imaging performance, copper–palladium alloy tetrapod nanoparticles for MSOT images, were well studied to recognize and destroy cancer, showing great properties for biomedical imaging applications, which are particularly promising candidates for early diagnosis of cancer.^[105,109,126,138,141,146a] All these nanomaterials-based imaging techniques show inherent imaging-guided chemo-photothermal therapy advantages, which allow not only the measurement of pharmacokinetics and monitoring of therapeutic outcomes but also the identification of tumor location, type and morphology.^[119d,190] In addition, these nanomaterials could be further functionalized with imaging elements to achieve the desired imaging functions. A successful example comes from liposomes coloaded hollow gold nanospheres, DOX, and perfluorocarbon. By virtue of hyperthermia-triggered gasification of perfluorocarbon, the remarkably improved ultrasound signal could be detected. Therefore, the multifunctional perfluorocarbon liposomes could serve as the efficient nanoagent for ultrasound tomography-guided chemo-photothermal therapy.^[191]

Given the advantages arising from the combination imaging, more work is being conducted by the integration of diverse imaging elements into the nanoformulations to obtain multiple theranostic nanoplatfoms for personalized therapeutic interventions, such as iridium oxide nanoparticles for simultaneous computed tomography and photoacoustic/thermal imaging, Cs_xWO₃ for X-ray computed and photoacoustic tomography dual imaging, Cu₃P nanocrystal for thermal imaging and photoacoustic imaging agent and in situ self-generation magnetic resonance imaging, MnCO-entrapped mesoporous polydopamine nanoparticles for magnetic resonance/photoacoustic bimodal imaging, zirconium-ferriporphyrin MOF nanoshuttles for photothermal/photoacoustic/computed tomography trimodal imagings.^[124,136,140,143,163]

Although great progress has been made in this field, photothermally controlled drug release systems are still being tested in animal studies. For successful photothermally triggered drug-delivery, the photothermal conversion materials need to realize efficient light-to-heat energy transfer and the photolabile moieties should achieve effective drug delivery. Gold nanomaterials remain the popular choice of thermally responsive materials. However, the long-term in vivo effects of gold nanomaterials are still unknown.^[192] Additionally, most of the photothermal nanomaterials are constructed with nondegradable inorganic nanomaterials, which may hamper their clinical applications because of their potential long-term toxicity. Some thermosensitive polymer materials, such as poly(*N*-isopropylacrylamide), are well tolerated, but their monomers are cytotoxic.^[193] In order to overcome these limitations, the development of new, biocompatible, biodegradable photothermal nanomaterials with favorable thermodynamic properties and efficient therapeutic performance is underway. The NIR light absorbers usually require high power and long exposure time to realize light-to-heat energy transfer. Thus, the heat generated

from the photothermal systems may damage surrounding tissues. This highlights the requirement for either the design of platforms with high NIR absorbance and efficient photothermal conversion, thereby reducing the amount of the light exposure time and the risk of raising the nearby tissue temperature, or illumination equipment that can target the delivery vehicles precisely. In addition, the construction of photothermally controlled drug release systems with targeting and imaging functionalities is still a hot topic for photothermal theranostic applications. The targeting, imaging, and therapeutic multifunctionalities of these platforms are all extraordinarily important for conducting cancer diagnosis and therapy, especially for early tumor theranostics.

4. Photoisomerization-Based Drug Release

Photoisomerization-based drug release refers to conformational changes of molecules to trigger gate-opening for drug escape upon light energy absorption. Light irradiation can cause reversible photoisomerization reactions of selected organic compounds, including spiropyrans and azobenzenes, without byproduct generation. Spiropyrans undergo reversible structural conversion from neutral spiropyran isomer to the zwitterionic, positively charged merocyanine upon irradiation with UV light, while after visible light illumination converts opened merocyanine back to closed spiropyran conformation.^[194] Azobenzenes can be reversibly isomerized from *trans* orientation to *cis* form by the irradiation of UV light and from *cis*-to-*trans* conversion under visible light.^[9b,195] A significant advantage of photoisomerization-based drug release systems is that the photoisomerization compounds can efficiently control the “on/off” drug release with excellent temporal resolution.^[196] Stimuli-induced pulsatile release of drugs may also be realized, thereby avoiding the multiple drug administrations. More details about light-activated molecular switches have been summarized elsewhere.^[15a,197] Up to now, a series of nanomaterials have been applied in production of photoisomerization-based drug delivery nanoplateforms.

4.1. Mesoporous Silica Nanoparticles for Photoisomerization Drug Delivery

MSNs are popular candidates for photoisomerization-based drug delivery. Recently, a photon-manipulated mesoporous delivery platform was fabricated based on azobenzene-tethered DNA. The azobenzene photoisomerization caused the dehybridization of complementary DNA, resulting in the uncaging of pore gates of MSN and DOX release for cancer therapy.^[198] Similar systems were applied to deliver cholesterol and DNA.^[198,199] When covalently attaching spiropyran on MSNs, the photoresponsive release nanosystem was achieved by modulating wetting states of mesoporous silica surfaces. The mesoporous silica surface-functionalized with an optimized ratio of fluorinated silane to spiropyran could be protected from being wet, effectively suppressing the delivery of anti-cancer drug camptothecin. Under UV light exposure, the conformation of spiropyran changed from the “closed” to “open” configuration resulted in surface wetting, giving rise to drug

uncaging to enhance cytotoxicity for cancer cells.^[200] Light-triggered nanoplateforms grounded on hollow MSNs conjugated with spiropyran-containing copolymer were also fabricated. The light-responsive spiropyran motifs were linked to pore outlets of the mesoporous silica nanocarriers, and the fluorescent dye molecules were loaded in pore voids for gate monitoring intentions. Afterward, the molecular-gate effect could be initiated by encapsulation of generation 1.5 poly(amidoamine) dendrimers, acting as nanoscopic molecular movable gates.^[201] Moreover, the direct chemical modification of photoisomeric moieties onto the rotaxane offers an alternative strategy in construction of photoisomerization drug delivery systems. It has been reported that the photothermal-triggered rotaxane-modified MSN for remote-regulated drug delivery was developed, which was based on dynamic back and forth motions of cyclohexaamylose rings driven by the photothermal-activated *trans*-*cis* isomerization of azobenzene. The synthesized nanocarrier was adopted for in vivo delivery of curcumin into five-day-old zebrafish embryos for successful therapy of heart failure.^[202]

4.2. MOF for Photoisomerization Drug Delivery Systems

By virtue of the noninvasive, directional, and rapid characteristics of photoresponsive supramolecular nanosystems, considerable research effort has been made to introduce new ways to transport drug molecules, including MOFs. Brown and co-workers described the construction of azobenzene-functionalized isoreticular MOF and demonstrated the capability to controllably deliver the guest propidium iodide dyes from its pores upon 408 nm light irradiation. This phototriggered cargo delivery could be switched on and off by regulating the azobenzene configuration using the light of appropriate wavelength.^[203] In another case, the novel class of light-activatable cytotoxic molecules were developed. The platinum(II) complexes were linked to the light-switchable 1,2-dithienylethene-containing ligands, which showed interchangeable photoisomeric structures with different DNA-interacting characteristics. Two isomers exhibited distinct cytotoxic properties, the closed forms being much more cytotoxic than the open ones against many types of cancer cells. These phenomena might open up opportunities toward the development of new avenues for photoactivated therapy.^[204] In addition, the photoactivatable azobenzene-modified covalent organic frameworks containing pendant azobenzene groups in the pore channels were also fabricated to form photoisomeric nanocarriers. The synthesized covalent organic framework could be effectively utilized for rhodamine B storage and on-demand release (Figure 9A).^[205]

4.3. Liposomes and Micelles for Photoisomerization Drug Delivery

The photoisomerization reaction has been widely employed to destabilize liposomes and micelles by inducing conformational changes of the amphiphilic components for drug release.^[18,206] In this case, the liposome, composed of palmitic acid and azobenzene modified cholesterol sulfate, exhibited triggered release of a model drug sulforhodamine B upon UV irradiation.

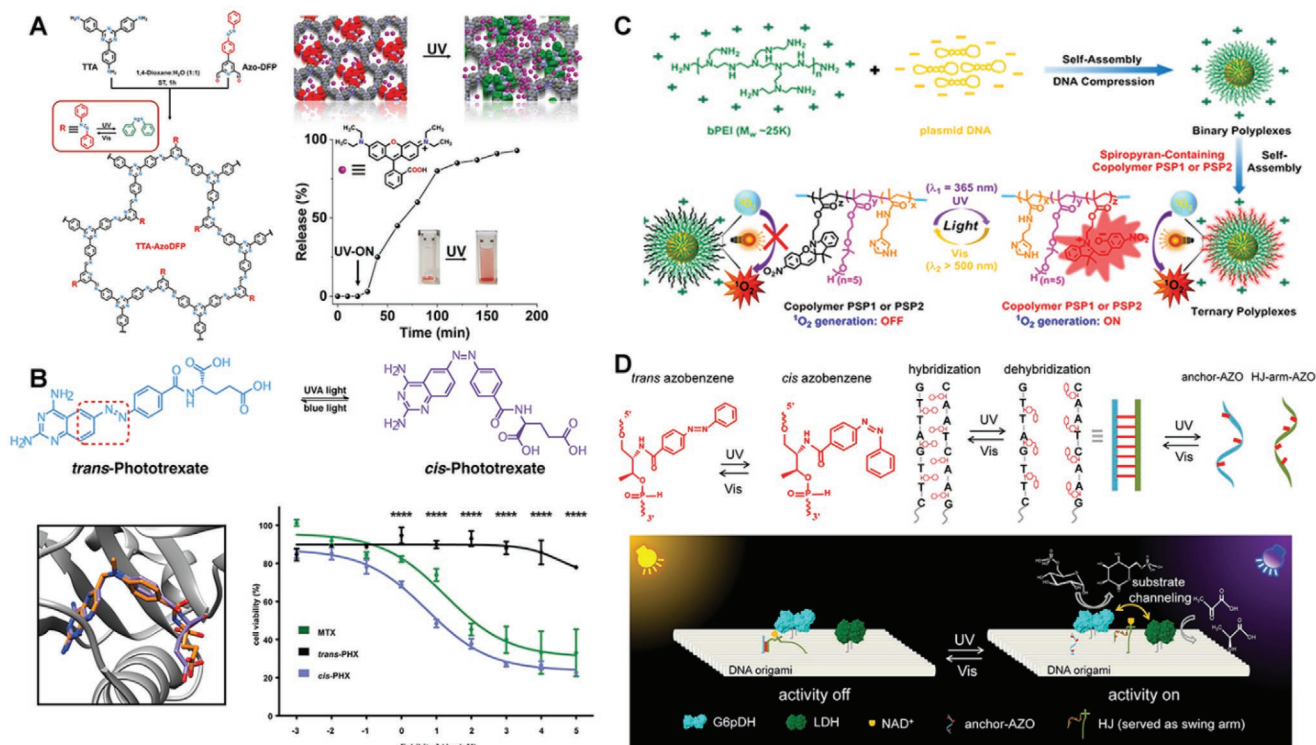


Figure 9. A) Synthesis of light-responsive azobenzene-functionalized covalent organic framework (TTA-AzoDFP) obtained under solvothermal conditions. Schematic representation of the release of Rhodamine B from the pores of TTA-AzoDFP after UV irradiation, UV-vis generated release profile of Rhodamine B-loaded TTA-AzoDFP upon UV irradiation. Reproduced with permission.^[205] Copyright 2019, American Chemical Society. B) Chemical structures of phototrexate in the *trans* and *cis* configurations. Zoomed views of *cis* (in purple) phototrexate superimposed on the crystallographic structure of methotrexate (in orange) in the active site of the human dihydrofolate reductase. HeLa cell viability assay at different concentrations of methotrexate, *cis*-phototrexate and *trans*-phototrexate. Reproduced with permission.^[222] Copyright 2018, American Chemical Society. C) Schematic presentations of sequential self-assembly preparation of photosensitizer-containing copolymer ternary polyplexes, and light-induced reversible ¹O₂ generation. Reproduced with permission.^[225] Copyright 2019, American Chemical Society. D) Schematic illustration of synthetic light-driven substrate channeling for precise regulation of enzyme cascade activity on DNA origami with different wavelength of light. Reproduced with permission.^[227] Copyright 2018, American Chemical Society.

The drug release could be efficiently ceased when the liposome was exposed to blue light.^[207] Similar concept was adopted to develop an on-demand adjustable local anesthesia.^[6b] Moreover, for a better potential application, Hindley et al. reported a nanosystem comprised of nested vesicles. Upon UV irradiation, inner compartments of nested vesicles acting as the phototransducers could polymerize diacetylene chains to induce the pore formation and subsequent the enzymatic reaction activation. The adjustable delivery and hydrolysis of the beta-galactosidase substrate were proved, and the reaction rate was able to be regulated by varying light exposure time. This microreactor could be utilized in various fields such as drug release and biocatalysis.^[208] Light-responsive micelles using spiropyran as the smart photoswitch were also developed as drug nanocarriers. The disassembly of micelles could be controlled by the UV source due to the reversible photochemical isomerization of spiropyran, which subsequently accelerated the release of DOX.^[209] The photoresponsive moieties could either be incorporated into the lipid bilayer or be modified into the phospholipid's hydrophobic tails to disrupt the conformations of the liposomes and micelles for drug delivery.^[210] Furthermore, an impressive advance in photoisomeric liposomes is the incorporation of the azobenzene derivatives conjugated

DNA-backbones with lipid to enable controlled drug delivery of drug after UV exposure. In this regard, the lipid-mediated self-assembled DNA nanostructure was used to construct the drug delivery platform targeting hepatocyte growth factor receptor. The DNA nanostructure consisted of both the lipidated GC-rich DNA intercalated with DOX and the separate lipidated cMet-binding aptamer. The 2',6'-dimethyl azobenzene compounds were incorporated into DOX-binding GC-rich DNA structure to realize photoisomerization-triggered drug delivery for chemotherapy. The combined features of the DNA nanostructure increased serum stability, favored cell internalization and enabled light-regulated delivery of the chemotherapeutic into H1838 tumor cells to enhance cell mortality.^[211]

4.4. Polymer Nanoparticles for Photoisomerization Drug Delivery Systems

Polymer nanoparticles, such as spiropyran-indoline-PEG nanoparticles, were also employed in chemotherapeutic docetaxel delivery.^[212] UV irradiation induced the shrinkage of the nanoparticles from 103 to 49 nm, which enhanced tissue penetration, drug release and cancer therapy efficiency in nude mice.^[213] In

a more recent study, the photoswitchable photochromic polymersomes from hydrophilic diblock copolymer poly(ethylene oxide)-*b*-PSPA were also fabricated, where SPA was carbamate linker conjugated spiropyran monomer. After self-assembly, spiropyran moieties underwent reversible light-activated isomerization between zwitterionic merocyanine and hydrophobic spiropyran states, thereby enabling on-demand and switchable delivery of 4',6-diamidino-2-phenylindole within living HeLa cells upon varied UV–vis light irradiation.^[214] Next, the spiropyran-incorporated copolymer could shift from hydrophobic to hydrophilic under UV exposure, which facilitated the uncaging and delivery of the encapsulated drug.^[215] Furthermore, the photodynamic nanoplatfoms incorporating spiropyran into highly biocompatible cationic copolymers were also developed, and spiropyran acted in nanomedicines as the photosensitizer for photoactivatable generating ROS in living cells.^[216]

On the other hand, the PEG-POSS-(Azo)₇ polymer with tadpole shape could self-assemble into the large vesicle. Under alternated UV and dark conditions, the azobenzene in the polymer underwent reversible *trans*–*cis* isomerization, which resulted in the smooth-curling transformation and quick delivery of the preloaded drug.^[217] The other example is related to the target-directed photoisomerization in vivo by designing the target-stimulated initiation and improvement of chemiluminescence strategy for disease-specific chemotherapy. The chemiluminescence fluorophore anticancer camptothecin and substrate were coloaded in the nanocarriers consisting of azobenzene and cyclodextrin. H₂O₂ in tumor microenvironment triggered chemiluminescence isomerized azobenzene, activating the dissociation of nanocarriers and camptothecin delivery with high tumor-inhibition-rate.^[218] More recently, new research findings have confirmed that the atomic/molecular layer deposition technique could be applied to synthesize crystalline iron–azobenzene thin films using azobenzene-4,4'-dicarboxylic acid and gaseous FeCl₃ precursors. These thin films exhibited reversible water capture and release performances that could be activated via *trans*–*cis* photoisomerization of azobenzene in the structure, which opened up new prospects for on-demand controlled cargo release and gas storage.^[219]

Benefiting from photoisomerization-controlled precise drug chemotherapy, other types of isomerization structures have also been applied in polymer nanoparticles for photoisomerization-triggered drug delivery. The charge-tunable supramolecular nanocarrier was developed for NO combined photodynamic elimination of bacteria biofilms with minimal collateral damage to surrounding healthy tissues upon light irradiation. The nanocarrier was prepared by loading Ce6 prodrugs and GSH-sensitive α -cyclodextrin linked NO prodrugs into pH-responsive PEG block polypeptide copolymers through host–guest chemistry. The nanocarrier showed negatively charged surfaces at pH 7.4 and reversibly positive charged surfaces at pH 5.5, enhancing effective infiltration into biofilm, which subsequently exhibited fast NO release and GSH reduction to promote photodynamic biofilm killing.^[220] Another example of this regard comes from the establishment of the ATP delivery nanosystem combined of DNA nanomachines coupled with light-activated nanoactuation with ATP aptamer into conical polyimide nanochannels. The transport line could efficiently shepherd ATP across the polymer membrane upon alternant light exposure.^[221] Recently, the

utilization of phototrexate as the first photoswitchable inhibitor of human dihydrofolate reductases was also explored. Studies of the light-controlled human dihydrofolate reductase enzymatic action, cell proliferation, as well as the in vivo effects in zebrafish showed that photoactivated *cis* phototrexate behaved as the potent antifolate while the *trans* configuration was inactive, opening up new avenues for light-manipulated chemotherapies with negligible side effects (Figure 9B).^[222]

More gratifyingly, considerable research effort has been devoted to the design and fabrication of photoisomeric polymers for allowing large molecule drug (proteins and DNA) delivery and enzyme activity regulation. In this case, Ravoo and co-workers developed the self-assembled ternary complexes composed of the target biomolecules the amphiphilic cyclodextrin, as well as linker molecules with a charged functionality and an azobenzene unit for in vitro photoresponsive capture and delivery of proteins and DNA.^[223] An azobenzene-containing cyclic dipeptide PAP-DKP-Lys was also applied as the photoresponsive hydrogelator. The self-healing gels formed in the presence of light could encapsulate and release dsDNA or DOX in a light-dependent manner.^[224] Similarly, the photo-regulated gene nanocarrier was also fabricated by grafting the PEI/DNA nanocomplex with spiropyran-modified cationic copolymers. The nanocarrier featured reversible singlet oxygen formation induced by spiropyran and aggregation-prompted improved photosensitization, allowing for greatly enhanced transgene expression (Figure 9C).^[225]

In a recent study, the amphiphilic block copolymers consisting of poly(pentafluorophenyl methacrylate) were developed and functionalized with donor–acceptor Stenhouse adducts, leading to visible-light-induced enhanced permeable effect of polymersome membranes owing to switchable polarity from the nonpolar triene–enol conformation to the highly polarizable cyclopentenone configuration. The nanoreactors could provide general strategies to photoregulate reactions on and off in enzyme activity regulation or drug delivery.^[226] It was also demonstrated that the light-activated nanosystem on DNA origami could be utilized to tune enzymatic cascade reactions. Azobenzene grafted on DNA strands enabled reversible switching of substrate positions to switchable inhibit or activate enzymatic cascade reactions. DNA origami allowed accurate regulation of interenzyme distance to optimize the photoregulation efficacy (Figure 9D).^[227] In addition, the novel photoresponsive nanoassemblies with switchable dimensions and enzymatic properties from the combination of spiropyran and lysozyme were also constructed.^[228] Moreover, in efforts to develop photo-switchable antibiotics, Feringa and co-workers introduced antibacterial nanoagents whose activity could be efficiently regulated under visible light exposure. Light-activated core nanostructures based on diaminopyrimidines with excellent antibacterial characteristics were produced and further modified with azobenzene for tunable antibacterial activities in both directions.^[229]

4.5. NIR Light-Triggered Photoisomerization Drug Delivery Systems

Due to the potential toxicity and shallow tissue penetration ability of UV light, different strategies have been employed to

replace UV with NIR light in the photoisomerization-based drug release systems, including applying NIR two-photon absorption and using NIR photosensitizers, as well as incorporating upconversion nanoparticles.^[230] For instance, an NIR-responsive drug release platform was fabricated by capping photocontrollable azobenzene-linked rotaxane onto gold nanorod-MSN core-shell nanohybrids. The drug delivery efficacy of the nanoplatform was demonstrated in the live zebrafish embryo models under NIR laser stimulation, showing significant drug infiltration into adjacent tissues.^[231] In another case, the MSN nanovalve arising from the conjugated azobenzene and two-photon fluorophore was developed. When cultured with target cancer cells and exposure to high power laser for a short period of time, the nanovalves showed efficient two-photon activated drug delivery and killing of cancer cells.^[230a] Similarly, the MSN modified with azobenzene and the original two-photon fluorophore moieties was also designed. NIR prompted the two-photon excitation and appreciable Förster resonance energy transfer to the azobenzene, subsequently triggering the release of camptothecin and induced cancer cell death in vitro.^[230b] Another active area of research is to develop modified azobenzene-based photoswitches with responsiveness to visible or NIR light.^[232] The redshifted photoswitchable control could be obtained through the incorporation of an azobenzene photoswitch in the fatty acid chains and modification of tetra-ortho-chlorination to the fatty acid azobenzene.^[233] NIR-absorbing azobenzene compounds offered great potentials in the development of NIR-modulated accurate drug delivery in vivo.^[232a,234] Red-light-activated supramolecular valves fabricated by β -cyclodextrin and tetra-ortho-methoxy-substituted azobenzene were applied to regulate DOX delivery from MSN.^[235]

Another strategy to apply NIR light for photoisomerization drug delivery is to incorporate UCNPs.^[236] Considerable effort on designing NIR responsive UCNPs integrated with photolabile azobenzene to deliver various drug payloads has been made. Idris et al. were among the first groups to utilize MSN-coated UCNPs as the nanotransducer to shift NIR light with the deep tissue penetration ability to visible wavelengths, as well as the nanocarrier for photosensitizer delivery. The multiwavelength-emission ability of UCNPs by using a single excitation source enabled synchronous stimulation of two photosensitizers for improved photodynamic therapy for non-invasive deep-cancer therapy.^[237] By encapsulating UCNPs with azobenzene-functionalized MSN using NIR light, a novel paradigm for accurate in vitro regulation of drug amount by applying NIR light was demonstrated. The dosage of delivered drug could be precisely regulated by changing the time duration or power of NIR irradiation.^[238] The liposomes containing azobenzene derivatives and the phospholipid modified UCNPs were also developed for remote accurate regulation of drug delivery to overcome multidrug-resistant in cancer therapy upon 980 nm NIR irradiation.^[236b] More recently, by grafting of hyaluronic acid and HIV-1 TAT peptide with DNA-azobenzene-UCNPs nanodevices, Ju and co-workers successfully developed the nanopump for targeted photoactivable DOX delivery. Upon NIR irradiation, UCNPs emitted visible and UV lights to fuel continuous azobenzene photoisomerization to activate switchable DNA hybridization and dehybridization for 86.7% DOX delivery for efficient

anticancer therapy (Figure 10A).^[239] Similar to the operating mode of the UCNPs mentioned above, the nanocapsules based on up/downconversion nanoparticles and layer-by-layer self-assembly of azobenzene conjugated polymers were also fabricated (Figure 10B). Under NIR irradiation, the nanocapsules were able to decompose into small up/downconversion nanoparticles from original large-sized framework through triggering azobenzene photoisomerizations of moieties in nanocapsules. The original nanocapsules (180 nm) were able to achieve prolonged blood circulation and high tumor accumulation. After NIR light exposure, the small 20 nm nanoparticles could be eliminated from cancer tissue within an hour and deliver the encapsulated anticancer drug for chemotherapy.^[240] In addition, the transplatinum(IV) prodrug could be efficiently switched to cytotoxic platinum(II) through the NIR-to-UV method based on a multifunctional upconversion drug delivery platform.^[241] Moreover, nanosystems to realize NIR-triggered reversible bacterial clustering were also synthesized. The nanosystems composed of photoisomeric azobenzene glycoconjugates and β -cyclodextrin functionalized UCNPs. Under NIR irradiation, UCNPs activated the azobenzene isomerization, resulting in nanosystem dissociation and bacterial cluster dispersion, opening up new perspectives for technological breakthroughs of antivirulence therapeutics (Figure 10C).^[242]

Similarly, UCNP nanocomposites combined with photoactive spiropyran have also been developed to release different cargos from small molecular drugs (antitumor prodrugs/drugs) to therapeutic macromolecules (DNA, RNA, proteins, and enzymes). Qu's group for the first time developed a facile DNA-mediated solvothermal strategy for the construction of hollow UCNPs that could be used to achieve NIR light-regulated noninvasive protein delivery. After conjugated with photosensitive spiropyran dye, NIR triggered release was performed in living cells. Importantly, intracellular NIR activated delivery of enzyme in a high spatial and temporal accuracy was realized and the uncaged enzyme also retained its bioactivity.^[243] In a follow-up study, they also designed the NIR-activated cage mimicking the nanosystem by anchoring spiropyran on MSN coated UCNPs. Hydrophobic anticancer payloads could be concealed in nanosystems and released via NIR light-activated photoisomerism of spiropyran. Furthermore, the UV and visible light emissions from UCNPs could trigger ROS generation by curcumin after NIR irradiation, further enhancing the antitumor efficacy (Figure 10D).^[244] In addition, precise photodynamic therapy could also be achieved by constructing the nanoarchitecture of MSN-encapsulated UCNPs containing porphyrin photosensitizers embedded in silica walls and photochromic diarylethene loaded in MSN pores. NIR irradiation resulted in the photoisomerization of diarylethene from close to open conformation, enabling complete recovery of $^1\text{O}_2$ generation ability for switchable photodynamic cancer therapy.^[245]

Although reversible photoisomerization provides an opportunity to develop cyclic on and off multipulse delivery platforms for drug delivery in vivo, there are some limitations that may hinder its use in practice. One concern of the photoisomerizable molecules is its potential toxicity in vivo. For example, some azobenzene molecules can be irreversibly degraded with

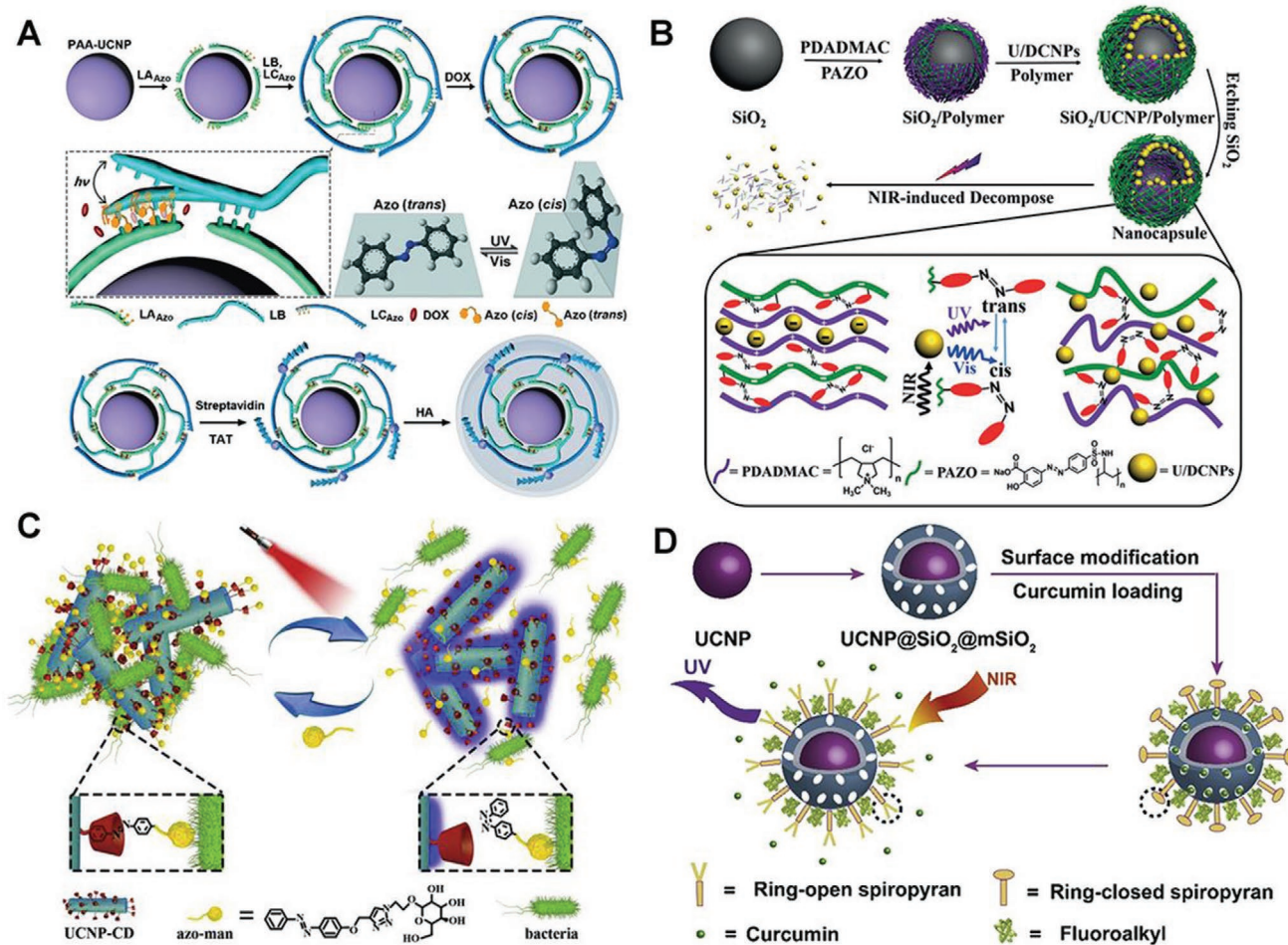


Figure 10. A) Schematic illustration of UCNPs-DNA_{Azo}/DOX assembly and UCNPs-DNA_{Azo}/DOX-TAT-hyaluronic acid synthesis. Reproduced with permission.^[239] Copyright 2019, Wiley-VCH. B) Illustration of the fabrication of the up/downconversion nanoparticle functionalized hollow polymer nanocapsules and the NIR light induced decomposing process from 180 nm nanocapsules to scattered polymers and 20 nm up/downconversion nanoparticles. Reproduced with permission.^[240] Copyright 2018, Wiley-VCH. C) Schematic illustration of NIR-driven reversible bacteria clustering. Reproduced with permission.^[242] Copyright 2019, Elsevier. D) Schematic illustration of NIR-controlled cage mimicking system for Curcumin delivery through spiropyran modified on mesoporous silica coated upconversion nanoparticles. The Curcumin release by taking advantage of the upconversion capability of UCNP and the conformational transformation of spiropyran molecules immobilized on mesoporous silica. Reproduced with permission.^[244] Copyright 2017, Elsevier.

light irradiation or by azoreductase,^[246] which is an enzyme generated by bacteria in the gastrointestinal tract.^[247] Unfortunately, several degradation products such as nitrobenzene, are considered toxic by the US Food and Drug Administration.^[248] Design and development of photoisomerization delivery vehicles with additional functionalities is another important issue that needs to be addressed in future studies. For instance, the photoisomerization induced size change of the nanoplatform may be advantageous for cancer therapeutic applications, where the tissue microenvironment can facilitate drug targeting. Up to now, there have already been some approaches to improve the photoisomerizable on-demand drug release systems, such as designing new photoisomerizable groups that respond to visible or NIR light. These photoisomerizable groups have already been incorporated into delivery vehicles.^[232a] In vivo researches are underway to further investigate the safety and efficacy of these systems.

5. Outlook

The application of light for therapeutic purposes can be traced back several thousand years. Light is a clean and effective external stimulus that does not require physical contact. Consequently, light has drawn great attention in the past decade and has been widely applied in stimuli-triggered drug release systems.^[60b,249] Up to now, the light-controlled drug delivery has been successfully utilized in chemotherapy,^[250] small molecular gas delivery,^[83c,251] gene therapy,^[51a,252] photodynamic therapy,^[253] anesthetic,^[88] antibacterial,^[83b,254] immunotherapy,^[101,255] stem cell differentiation,^[60b] photocaged cell adhesion,^[256] etc. (Figure 11). UV light is the most common wavelength to be used since most photoactivatable molecules respond to UV light irradiation. Unfortunately, the clinical application of UV light is restricted by its low tissue penetration ability and cytotoxic effects on biological molecules. NIR

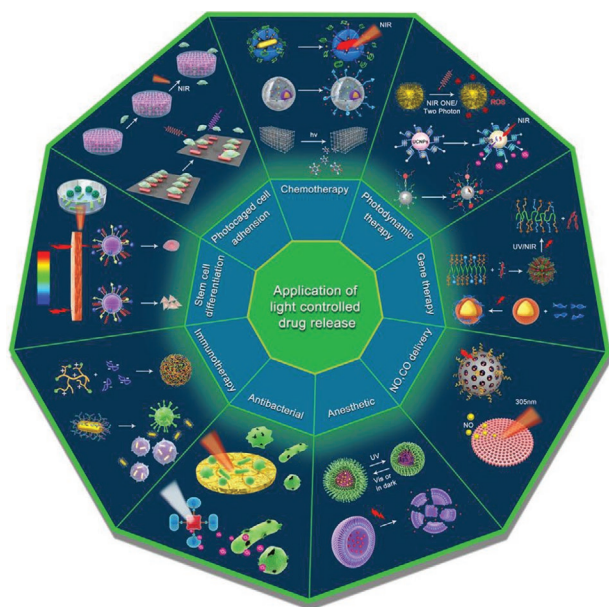


Figure 11. Applications of light-controlled drug delivery.

light with safer characteristics and deeper tissue penetration has attracted significant attention for utilization in medicine and smart photoresponsive drug delivery systems. The photoresponsive reactive components should not only respond to low-energy and long-wavelength lights, but also remain photochemically inert and stable under physiological and dark conditions. These photoresponsive reactive species with tuneable absorbance properties may propel the existing promising light-controlled drug delivery platforms for clinical application. In addition, the biocompatibility of these light-responsive drug-delivery systems remains an important consideration for researchers. Up to date, a wide spectrum of biomaterials has been applied for phototriggered drug delivery, ranging from inorganic nanocarriers including silica nanoparticles, metallic nanocomposites, carbon nanomaterials, and upconversion nanoparticles, to organic nanocarriers such as liposomes, micelles, and polymer nanoparticles. Inorganic nanocarriers with high porosity or large surface areas usually permit high drug loading efficiency and multiple functionalities including targetability. In addition, many of these inorganic nanocarriers possess unique shape and size-dependent optical, magnetic, and electronic properties, which create a great promise for their imaging-guided therapy applications. However, due to the long-term accumulation in certain tissues after administration, the in vivo toxicity and difficult degradation properties of such inorganic nanocarriers may pose risks or potential side effects to the body. Compared with inorganic biomaterials, many organic nanocarriers have equipped with unique characteristics including good biocompatibility and easy biodegradability. However, some of them are unstable during delivery and thus more prone to causing undesired side effects owing to the drug loss. Therefore, investigations of hybrid biomaterials combining particular features of organic and inorganic nanocarriers are still needed in developing potentially clinically relevant phototherapy. Moreover, the phototriggered

drug delivery systems may result in the generation of new photolabile groups that may produce toxicity. As a result, most of these systems are limited to in vitro applications owing to biocompatibility issues. Therefore, the development of highly biocompatible nanoparticles even after light irradiation is urgently needed. Furthermore, although some in vivo studies have been performed, they are restricted to small animals. Their translational potential remains uncertain, awaiting further research.

Second, the majority of the light-controlled drug delivery systems are irreversible. Light often induces an irreversible change of the drug carrier, limiting the control of drug delivery profile. The establishment of reversible light-controlled drug delivery systems with cytocompatible wavelengths remains of great importance to adjust therapeutic effects in vivo. Incorporation of photoswitchable molecules, such as spiropyrans and azobenzenes, has succeeded in creating reversible constructs.^[257] In the future, the exploration of other biocompatible photoisomerization agents, such as light-responsive proteins, which undergo conformational changes or reversible dimerization, may pave the way to wider applications for light-controlled drug delivery systems.

The independent construction of different photoreactions within the same individual is also appealing for the clinical trial arena of the phototriggered drug delivery systems. The application of two independent photomodulation drug delivery systems in one individual therapy remains challenging, because the unexpected coexcitation of the photoactive species usually occurs due to the overlap of their excitation spectra. Continued effort must concentrate on designing photoactive components that possess well-separated maximum absorbance peaks and narrow absorption bandwidths to confirm the independent activation.^[258] Thereafter, the combinational light-activated on-demand drug delivery platforms that can independently release distinct therapeutics can be achieved, which would be useful to investigate the biological importance of different physiochemical cues. Furthermore, more attention should be given to designing delivery vehicles with additional functionalities besides the light-triggered release of drugs.

6. Conclusion

External control of drug delivery by light allows accurate spatial resolution and temporal regulation over the release of a broad range of therapeutic compounds, including but not limited to small molecule drugs, proteins, and genes. These light-actuated on-demand drug-release platforms have been designed to combat diseases ranging from cardiovascular disorders to chemotherapy, infection, and inflammation control. In this review, we provide a comprehensive summary on light-controlled drug delivery systems, including recent progress, key limitations and challenges, and future directions. Future research should aim to translate light-responsive system-based therapy. Moving at a fast pace fuelled by ongoing breakthroughs in nanomaterials and nano-optics, this exciting field may impact controlled drug delivery and healthcare with significant societal benefit.

Acknowledgements

This work was supported by the National Key R&D Program of China (2019YFA0111300), the National Natural Science Foundation of China (21907113 and 51903256), the Guangdong Province Science and Technology Innovation Special Fund (International Scientific Cooperation, 2018A050506035), and the National Institutes of Health (UH3TR002151, UG3NS115598, and RO1AR073935).

Conflict of Interest

The authors declare no conflict of interest.

Keywords

drug delivery, light, photochemical, photoisomerization, photothermal

Received: June 14, 2020

Revised: July 7, 2020

Published online: September 9, 2020

- [1] R. Paull, J. Wolfe, P. Hébert, M. Sinkula, *Nat. Biotechnol.* **2003**, *21*, 1144.
- [2] a) M. C. Roco, *Curr. Opin. Biotechnol.* **2003**, *14*, 337; b) S. K. Sahoo, S. Parveen, J. J. Panda, *Nanomed.: Nanotechnol., Biol. Med.* **2007**, *3*, 20.
- [3] a) M. Karimi, S. Bahrami, S. B. Ravari, P. S. Zangabad, H. Mirshekari, M. Bozorgomid, S. Shahreza, M. Sori, M. R. Hamblin, *Expert Opin. Drug Delivery* **2016**, *13*, 1609; b) H. Wang, F. Ke, A. Mararenko, Z. Wei, P. Banerjee, S. Zhou, *Nanoscale* **2014**, *6*, 7443; c) J. T. Robinson, S. M. Tabakman, Y. Liang, H. Wang, H. Sanchez Casalongue, D. Vinh, H. Dai, *J. Am. Chem. Soc.* **2011**, *133*, 6825; d) M. Karimi, N. Solati, M. Amiri, H. Mirshekari, E. Mohamed, M. Taheri, M. Hashemkhani, A. Saeidi, M. A. Estiar, P. Kiani, A. Ghasemi, S. M. M. Basri, A. R. Aref, M. R. Hamblin, *Expert Opin. Drug Delivery* **2015**, *12*, 1071; e) J. L. Liu, A. B. Dixit, K. L. Robertson, E. Qiao, L. W. Black, *Proc. Natl. Acad. Sci. USA* **2014**, *111*, 13319; f) Z. Hosseini-doust, B. Mostaghaci, O. Yasa, B.-W. Park, A. V. Singh, M. Sitti, *Adv. Drug Delivery Rev.* **2016**, *106*, 27; g) M. Karimi, M. Eslami, P. Sahandi-Zangabad, F. Mirab, N. Farajisafilo, Z. Shafaei, D. Ghosh, M. Bozorgomid, F. Dashkhaneh, M. R. Hamblin, *Wiley Interdiscip. Rev.: Nanomed. Nanobiotechnol.* **2016**, *8*, 696; h) M. Karimi, P. Sahandi Zangabad, A. Ghasemi, M. Amiri, M. Bahrami, H. Malekzad, H. Ghahramanzadeh Asl, Z. Mahdieh, M. Bozorgomid, A. Ghasemi, M. R. Rahmani Taji Boyuk, M. R. Hamblin, *ACS Appl. Mater. Interfaces* **2016**, *8*, 21107; i) L. Wang, Y. Yuan, S. Lin, J. Huang, J. Dai, Q. Jiang, D. Cheng, X. Shuai, *Biomaterials* **2016**, *78*, 40; j) S. Huang, J. Liu, Q. He, H. Chen, J. Cui, S. Xu, Y. Zhao, C. Chen, L. Wang, *Nano Res.* **2015**, *8*, 4038.
- [4] a) D. N. Heo, W. K. Ko, H. J. Moon, H. J. Kim, S. J. Lee, J. B. Lee, M. S. Bae, J. K. Yi, Y. S. Hwang, J. B. Bang, E. C. Kim, S. H. Do, I. K. Kwon, *ACS Nano* **2014**, *8*, 12049; b) M. Bensellam, D. R. Laybutt, J.-C. Jonas, *Mol. Cell. Endocrinol.* **2012**, *364*, 1; c) M. Karimi, H. Zare, A. Bakhshian Nik, N. Yazdani, M. Hamrang, E. Mohamed, P. Sahandi Zangabad, S. M. Moosavi Basri, L. Bakhtiari, M. R. Hamblin, *Nanomedicine* **2016**, *11*, 513; d) E. Carrasco, M. I. Calvo, A. Blázquez-Castro, D. Vecchio, A. Zamarrón, I. J. D. de Almeida, J. C. Stockert, M. R. Hamblin, Á. Juarranz, J. Espada, *J. Invest. Dermatol.* **2015**, *135*, 2611; e) H. Abrahamse, M. R. Hamblin, *Biochem. J.* **2016**, *473*, 347; f) C. Yu, P. Avci, T. Canteenwala, L. Y. Chiang, B. J. Chen, M. R. Hamblin, *J. Nanosci. Nanotechnol.* **2016**, *16*, 171.
- [5] Y. Wang, B. Li, L. Zhang, H. Song, L. Zhang, *ACS Appl. Mater. Interfaces* **2013**, *5*, 11.
- [6] a) K. Malachowski, J. Breger, H. R. Kwag, M. O. Wang, J. P. Fisher, F. M. Selaru, D. H. Gracias, *Angew. Chem., Int. Ed.* **2014**, *53*, 8045; b) A. Y. Rwei, J.-J. Lee, C. Zhan, Q. Liu, M. T. Ok, S. A. Shankarappa, R. Langer, D. S. Kohane, *Proc. Natl. Acad. Sci. USA* **2015**, *112*, 15719; c) D. Luo, N. Li, K. A. Carter, C. Lin, J. Geng, S. Shao, W.-c. Huang, Y. Qin, G. E. Atilla-Gokcumen, J. F. Lovell, *Small* **2016**, *12*, 3039; d) A. Bagheri, H. Arandiyani, C. Boyer, M. Lim, *Adv. Sci.* **2016**, *3*, 1500437; e) S. Mura, J. Nicolas, P. Couvreur, *Nat. Mater.* **2013**, *12*, 991; f) T. M. Allen, P. R. Cullis, *Science* **2004**, *303*, 1818.
- [7] M. Karimi, *Smart Internal Stimulus-Responsive Nanocarriers for Drug and Gene Delivery*, IOP Concise Physics, Bristol, UK **2015**.
- [8] M. Karimi, A. Ghasemi, P. Sahandi Zangabad, R. Rahighi, S. M. Moosavi Basri, H. Mirshekari, M. Amiri, Z. Shafaei Pishabad, A. Aslani, M. Bozorgomid, D. Ghosh, A. Beyzavi, A. Vaseghi, A. R. Aref, L. Haghani, S. Bahrami, M. R. Hamblin, *Chem. Soc. Rev.* **2016**, *45*, 1457.
- [9] a) C. Alvarez-Lorenzo, A. Concheiro, *Chem. Commun.* **2014**, *50*, 7743; b) B. P. Timko, T. Dvir, D. S. Kohane, *Adv. Mater.* **2010**, *22*, 4925; c) M. Abbas, Q. Zou, S. Li, X. Yan, *Adv. Mater.* **2017**, *29*, 1605021; d) J. Li, H. Duan, K. Pu, *Adv. Mater.* **2019**, *31*, 1901607.
- [10] a) R. Bouchaala, N. Anton, H. Anton, T. Vandamme, J. Vermot, D. Smail, Y. Mély, A. S. Klymchenko, *Colloids Surf., B* **2017**, *156*, 414; b) G. Lan, K. Ni, W. Lin, *Coord. Chem. Rev.* **2019**, *379*, 65; c) J. Son, G. Yi, J. Yoo, C. Park, H. Koo, H. S. Choi, *Adv. Drug Delivery Rev.* **2019**, *138*, 133; d) B. Liu, C. Li, P. Yang, Z. Hou, J. Lin, *Adv. Mater.* **2017**, *29*, 1605434; e) S. Shabahang, S. Kim, S.-H. Yun, *Adv. Funct. Mater.* **2018**, *28*, 1706635; f) L. Xu, F. Mou, H. Gong, M. Luo, J. Guan, *Chem. Soc. Rev.* **2017**, *46*, 6905.
- [11] a) A. Bansal, Y. Zhang, *Acc. Chem. Res.* **2014**, *47*, 3052; b) G. Chen, H. Qiu, P. N. Prasad, X. Chen, *Chem. Rev.* **2014**, *114*, 5161; c) J. Liu, C. Detrembleur, S. Mornet, C. Jerome, E. Duguet, *J. Mater. Chem. B* **2015**, *3*, 6117; d) E. S. Shibu, M. Hamada, N. Murase, V. Biju, *J. Photochem. Photobiol., C* **2013**, *15*, 53; e) S. Gai, G. Yang, P. Yang, F. He, J. Lin, D. Jin, B. Xing, *Nano Today* **2018**, *19*, 146; f) D. C. Thang, Z. Wang, X. Lu, B. Xing, *Theranostics* **2019**, *9*, 3308; g) Z. Gu, M. Yan, B. Hu, K.-I. Joo, A. Biswas, Y. Huang, Y. Lu, P. Wang, Y. Tang, *Nano Lett.* **2009**, *9*, 4533; h) Y. Lu, Y. Lin, Z. Chen, Q. Hu, Y. Liu, S. Yu, W. Gao, M. D. Dickey, Z. Gu, *Nano Lett.* **2017**, *17*, 2138.
- [12] a) Y. Min, J. Li, F. Liu, E. K. L. Yeow, B. Xing, *Angew. Chem., Int. Ed.* **2014**, *53*, 1012; b) L. Cheng, K. Yang, Y. Li, J. Chen, C. Wang, M. Shao, S.-T. Lee, Z. Liu, *Angew. Chem., Int. Ed.* **2011**, *50*, 7385.
- [13] M. Karimi, P. Sahandi Zangabad, S. Baghaee-Ravari, M. Ghazadeh, H. Mirshekari, M. R. Hamblin, *J. Am. Chem. Soc.* **2017**, *139*, 4584.
- [14] a) Q. Liu, Y. Sun, T. Yang, W. Feng, C. Li, F. Li, *J. Am. Chem. Soc.* **2011**, *133*, 17122; b) X. Xie, N. Gao, R. Deng, Q. Sun, Q.-H. Xu, X. Liu, *J. Am. Chem. Soc.* **2013**, *135*, 12608; c) Q. Lin, Q. Huang, C. Li, C. Bao, Z. Liu, F. Li, L. Zhu, *J. Am. Chem. Soc.* **2010**, *132*, 10645.
- [15] a) C. S. Linsley, B. M. Wu, *Ther. Delivery* **2017**, *8*, 89; b) N. Fomina, J. Sankaranarayanan, A. Almutairi, *Adv. Drug Delivery Rev.* **2012**, *64*, 1005.
- [16] H. Zhao, E. S. Sterner, E. B. Coughlin, P. Theato, *Macromolecules* **2012**, *45*, 1723.
- [17] a) A. P. Pelliccioli, J. Wirz, *Photochem. Photobiol. Sci.* **2002**, *1*, 441; b) H. Wang, W. Zhang, C. Gao, *Biomacromolecules* **2015**, *16*, 2276.
- [18] E. R. Ruskowitz, C. A. DeForest, *Nat. Rev. Mater.* **2018**, *3*, 17087.

- [19] a) Y. Zhang, C. Y. Ang, M. Li, S. Y. Tan, Q. Qu, Z. Luo, Y. Zhao, *ACS Appl. Mater. Interfaces* **2015**, *7*, 18179; b) Q. Jin, F. Mitschang, S. Agarwal, *Biomacromolecules* **2011**, *12*, 3684; c) Q. Huang, C. Bao, W. Ji, Q. Wang, L. Zhu, *J. Mater. Chem.* **2012**, *22*, 18275.
- [20] a) X. Huang, X. Teng, D. Chen, F. Tang, J. He, *Biomaterials* **2010**, *31*, 438; b) J. G. Croissant, Y. Fatieiev, N. M. Khashab, *Adv. Mater.* **2017**, *29*, 1604634; c) J.-J. Hu, D. Xiao, X.-Z. Zhang, *Small* **2016**, *12*, 3344.
- [21] a) V. Mamaeva, C. Sahlgren, M. Lindén, *Adv. Drug Delivery Rev.* **2013**, *65*, 689; b) J. Wen, K. Yang, F. Liu, H. Li, Y. Xu, S. Sun, *Chem. Soc. Rev.* **2017**, *46*, 6024; c) J. Liang, Z. Liang, R. Zou, Y. Zhao, *Adv. Mater.* **2017**, *29*, 1701139; d) H. Mekaru, J. Lu, F. Tamanoi, *Adv. Drug Delivery Rev.* **2015**, *95*, 40; e) Y. Wang, H. Gu, *Adv. Mater.* **2015**, *27*, 576; f) C.-A. Cheng, T. Deng, F.-C. Lin, Y. Cai, J. I. Zink, *Theranostics* **2019**, *9*, 3341.
- [22] N. K. Mal, M. Fujiwara, Y. Tanaka, T. Taguchi, M. Matsukata, *Chem. Mater.* **2003**, *15*, 3385.
- [23] W. Ji, N. Li, D. Chen, X. Qi, W. Sha, Y. Jiao, Q. Xu, J. Lu, *J. Mater. Chem. B* **2013**, *1*, 5942.
- [24] C. Wu, C. Chen, J. Lai, J. Chen, X. Mu, J. Zheng, Y. Zhao, *Chem. Commun.* **2008**, *23*, 2662.
- [25] M. Wu, X. Lin, X. Tan, J. Li, Z. Wei, D. Zhang, Y. Zheng, A.-x. Zheng, B. Zhao, Y. Zeng, X. Liu, J. Liu, *ACS Appl. Mater. Interfaces* **2018**, *10*, 19416.
- [26] S. S. Agasti, A. Chompoosor, C.-C. You, P. Ghosh, C. K. Kim, V. M. Rotello, *J. Am. Chem. Soc.* **2009**, *131*, 5728.
- [27] M. Wang, J. Wu, Y. Li, F. Li, X. Hu, G. Wang, M. Han, D. Ling, J. Gao, *J. Controlled Release* **2018**, *288*, 34.
- [28] a) C. Qian, J. Yu, Y. Chen, Q. Hu, X. Xiao, W. Sun, C. Wang, P. Feng, Q.-D. Shen, Z. Gu, *Adv. Mater.* **2016**, *28*, 3313; b) J. Wang, H. He, X. Xu, X. Wang, Y. Chen, L. Yin, *Biomaterials* **2018**, *171*, 72; c) L. Yang, H. Sun, Y. Liu, W. Hou, Y. Yang, R. Cai, C. Cui, P. Zhang, X. Pan, X. Li, L. Li, B. S. Sumerlin, W. Tan, *Angew. Chem., Int. Ed.* **2018**, *57*, 17048.
- [29] C. T. Huynh, M. K. Nguyen, G. Y. Tonga, L. Longé, V. M. Rotello, E. Alsberg, *Adv. Healthcare Mater.* **2016**, *5*, 305.
- [30] a) X. Xie, Y. Yang, Y. Yang, H. Zhang, Y. Li, X. Mei, *Drug Delivery* **2016**, *23*, 2756; b) S. Ghosh, K. A. Carter, J. F. Lovell, *Biomaterials* **2019**, *218*, 119341.
- [31] X. Hu, J. Tian, T. Liu, G. Zhang, S. Liu, *Macromolecules* **2013**, *46*, 6243.
- [32] J. Chen, L. Liu, S. M. Motevalli, X. Wu, X.-H. Yang, X. Li, L. Han, A. Magrini, W. Guo, J. Chang, M. Bottini, X.-J. Liang, *Adv. Funct. Mater.* **2018**, *28*, 1707291.
- [33] M. M. Mahmoodi, D. Abate-Pella, T. J. Pundsack, C. C. Palsuledesai, P. C. Goff, D. A. Blank, M. D. Distefano, *J. Am. Chem. Soc.* **2016**, *138*, 5848.
- [34] R. E. Kohman, S. S. Cha, H.-Y. Man, X. Han, *Nano Lett.* **2016**, *16*, 2781.
- [35] W. Lee, D. Kim, S. Lee, J. Park, S. Oh, G. Kim, J. Lim, J. Kim, *Nano Today* **2018**, *23*, 97.
- [36] a) N. Guo, Y. Song, H. You, G. Jia, M. Yang, K. Liu, Y. Zheng, Y. Huang, H. Zhang, *Eur. J. Inorg. Chem.* **2010**, *2010*, 4636; b) Y.-H. Chien, Y.-L. Chou, S.-W. Wang, S.-T. Hung, M.-C. Liao, Y.-J. Chao, C.-H. Su, C.-S. Yeh, *ACS Nano* **2013**, *7*, 8516; c) T. A. Theodossiou, A. R. Gonçalves, K. Yannakopoulou, E. Skarpen, K. Berg, *Angew. Chem., Int. Ed.* **2015**, *54*, 4885; d) G. Collet, T. Lathion, C. Besnard, C. Piguët, S. Petoud, *J. Am. Chem. Soc.* **2018**, *140*, 10820; e) P. Samanta, K. Kapat, S. Maiti, G. Biswas, S. Dhara, D. Dhara, *J. Colloid Interface Sci.* **2019**, *555*, 132.
- [37] a) W. Fan, W. Bu, Z. Zhang, B. Shen, H. Zhang, Q. He, D. Ni, Z. Cui, K. Zhao, J. Bu, J. Du, J. Liu, J. Shi, *Angew. Chem.* **2015**, *127*, 14232; b) A. Paul, A. Jana, S. Karthik, M. Bera, Y. Zhao, N. D. P. Singh, *J. Mater. Chem. B* **2016**, *4*, 521.
- [38] X. Tan, B. B. Li, X. Lu, F. Jia, C. Santori, P. Menon, H. Li, B. Zhang, J. J. Zhao, K. Zhang, *J. Am. Chem. Soc.* **2015**, *137*, 6112.
- [39] C. Zang, H. Wang, T. Li, Y. Zhang, J. Li, M. Shang, J. Du, Z. Xi, C. Zhou, *Chem. Sci.* **2019**, *10*, 8973.
- [40] Y. Tao, M. Li, B. Kim, D. T. Auguste, *Theranostics* **2017**, *7*, 899.
- [41] S. B. Salunke, J. A. Malla, P. Talukdar, *Angew. Chem., Int. Ed.* **2019**, *58*, 5354.
- [42] E. Rideau, R. Dimova, P. Schwille, F. R. Wurm, K. Landfester, *Chem. Soc. Rev.* **2018**, *47*, 8572.
- [43] Y. Duan, Y. Wang, X. Li, G. Zhang, G. Zhang, J. Hu, *Chem. Sci.* **2020**, *11*, 186.
- [44] U. Bozuyuk, O. Yasa, I. C. Yasa, H. Ceylan, S. Kizilel, M. Sitti, *ACS Nano* **2018**, *12*, 9617.
- [45] D. Cui, J. Huang, X. Zhen, J. Li, Y. Jiang, K. Pu, *Angew. Chem., Int. Ed.* **2019**, *58*, 5920.
- [46] a) P. Pei, C. Sun, W. Tao, J. Li, X. Yang, J. Wang, *Biomaterials* **2019**, *188*, 74; b) H. Cheng, X.-Y. Jiang, R.-R. Zheng, S.-J. Zuo, L.-P. Zhao, G.-L. Fan, B.-R. Xie, X.-Y. Yu, S.-Y. Li, X.-Z. Zhang, *Biomaterials* **2019**, *195*, 75.
- [47] Y. Dai, H. Sun, S. Pal, Y. Zhang, S. Park, C. P. Kabb, W. D. Wei, B. S. Sumerlin, *Chem. Sci.* **2017**, *8*, 1815.
- [48] X. Wei, L. Liu, X. Guo, Y. Wang, J. Zhao, S. Zhou, *ACS Appl. Mater. Interfaces* **2018**, *10*, 17672.
- [49] S. Uthaman, S. Pillarisetti, A. P. Mathew, Y. Kim, W. K. Bae, K. M. Huh, I.-K. Park, *Biomaterials* **2020**, *232*, 119702.
- [50] J. Li, D. Cui, Y. Jiang, J. Huang, P. Cheng, K. Pu, *Adv. Mater.* **2019**, *31*, 1905091.
- [51] a) I. A. Shestopalov, S. Sinha, J. K. Chen, *Nat. Chem. Biol.* **2007**, *3*, 650; b) L. Li, R. Tong, H. Chu, W. Wang, R. Langer, D. S. Kohane, *Proc. Natl. Acad. Sci. USA* **2014**, *111*, 17099.
- [52] a) E. Cabane, V. Malinova, S. Menon, C. G. Palivan, W. Meier, *Soft Matter* **2011**, *7*, 9167; b) S. G. Yüz, J. Ricken, S. V. Wegner, *Adv. Sci.* **2018**, *5*, 1800446.
- [53] Y. Lyu, S. He, J. Li, Y. Jiang, H. Sun, Y. Miao, K. Pu, *Angew. Chem., Int. Ed.* **2019**, *58*, 18197.
- [54] J. Bleresch, V. Francisco, C. Rebelo, A. Jiménez-Balsa, H. Antunes, C. Gonzato, S. Pinto, S. Simões, K. Liedl, K. Haupt, L. Ferreira, *Angew. Chem., Int. Ed.* **2020**, *59*, 1985.
- [55] a) H. He, Y. Chen, Y. Li, Z. Song, Y. Zhong, R. Zhu, J. Cheng, L. Yin, *Adv. Funct. Mater.* **2018**, *28*, 1706710; b) K. Dutta, D. Hu, B. Zhao, A. E. Ribbe, J. Zhuang, S. Thayumanavan, *J. Am. Chem. Soc.* **2017**, *139*, 5676.
- [56] J. Li, J. Huang, Y. Lyu, J. Huang, Y. Jiang, C. Xie, K. Pu, *J. Am. Chem. Soc.* **2019**, *141*, 4073.
- [57] T. T. Lee, J. R. García, J. I. Paez, A. Singh, E. A. Phelps, S. Weis, Z. Shafiq, A. Shekaran, A. del Campo, A. J. García, *Nat. Mater.* **2015**, *14*, 352.
- [58] H. Sun, W. Choi, N. Zang, C. Battistella, M. P. Thompson, W. Cao, X. Zhou, C. Forman, N. C. Gianneschi, *Angew. Chem., Int. Ed.* **2019**, *58*, 17359.
- [59] F. Wang, R. Deng, J. Wang, Q. Wang, Y. Han, H. Zhu, X. Chen, X. Liu, *Nat. Mater.* **2011**, *10*, 968.
- [60] a) M. Haase, H. Schäfer, *Angew. Chem., Int. Ed.* **2011**, *50*, 5808; b) J. Li, W. Y.-W. Lee, T. Wu, J. Xu, K. Zhang, D. S. Hong Wong, R. Li, G. Li, L. Bian, *Biomaterials* **2016**, *110*, 1; c) Y. Zhang, W. Zhang, K. Zeng, Y. Ao, M. Wang, Z. Yu, F. Qi, W. Yu, H. Mao, L. Tao, C. Zhang, T. T. Y. Tan, X. Yang, K. Pu, S. Gao, *Small* **2020**, *16*, 1906797; d) Z. Yan, H. Qin, J. Ren, X. Qu, *Angew. Chem., Int. Ed.* **2018**, *57*, 11182.
- [61] a) B. Yan, J. C. Boyer, D. Habault, N. R. Branda, Y. Zhao, *J. Am. Chem. Soc.* **2012**, *134*, 16558; b) W. Wang, Q. Liu, C. Zhan, A. Barhoumi, T. Yang, R. G. Wylie, P. A. Armstrong, D. S. Kohane, *Nano Lett.* **2015**, *15*, 6332; c) Y. Yang, F. Liu, X. Liu, B. Xing,

- Nanoscale* **2013**, *5*, 231; d) G. Chen, H. Ågren, T. Y. Ohulchanskyy, P. N. Prasad, *Chem. Soc. Rev.* **2015**, *44*, 1680.
- [62] a) J. Xiang, X. Tong, F. Shi, Q. Yan, B. Yu, Y. Zhao, *J. Mater. Chem. B* **2018**, *6*, 3531; b) X.-l. Tang, J. Wu, B.-l. Lin, S. Cui, H.-m. Liu, R.-t. Yu, X.-d. Shen, T.-w. Wang, W. Xia, *Acta Biomater.* **2018**, *74*, 360; c) J. Xiang, F. Ge, B. Yu, Q. Yan, F. Shi, Y. Zhao, *ACS Appl. Mater. Interfaces* **2018**, *10*, 20790.
- [63] G. Jin, R. He, Q. Liu, M. Lin, Y. Dong, K. Li, B. Z. Tang, B. Liu, F. Xu, *Theranostics* **2019**, *9*, 246.
- [64] a) G. Lan, K. Ni, Z. Xu, S. S. Veroneau, Y. Song, W. Lin, *J. Am. Chem. Soc.* **2018**, *140*, 5670; b) R. Haldar, L. Heinke, C. Wöll, *Adv. Mater.* **2020**, *32*, 1905227; c) Y. Wang, J. Yan, N. Wen, H. Xiong, S. Cai, Q. He, Y. Hu, D. Peng, Z. Liu, Y. Liu, *Biomaterials* **2020**, *230*, 119619.
- [65] C. Liu, B. Liu, J. Zhao, Z. Di, D. Chen, Z. Gu, L. Li, Y. Zhao, *Angew. Chem., Int. Ed.* **2020**, *59*, 2634.
- [66] Y. Shao, B. Liu, Z. Di, G. Zhang, L.-D. Sun, L. Li, C.-H. Yan, *J. Am. Chem. Soc.* **2020**, *142*, 3939.
- [67] Y. Zhang, K. Ren, X. Zhang, Z. Chao, Y. Yang, D. Ye, Z. Dai, Y. Liu, H. Ju, *Biomaterials* **2018**, *163*, 55.
- [68] Z. Zhang, M. K. G. Jayakumar, X. Zheng, S. Shikha, Y. Zhang, A. Bansal, D. J. J. Poon, P. L. Chu, E. L. L. Yeo, M. L. K. Chua, S. K. Chee, Y. Zhang, *Nat. Commun.* **2019**, *10*, 4586.
- [69] Y. Pan, J. Yang, X. Luan, X. Liu, X. Li, J. Yang, T. Huang, L. Sun, Y. Wang, Y. Lin, Y. Song, *Sci. Adv.* **2019**, *5*, eaav7199.
- [70] Z. Chen, R. Thiramanas, M. Schwendy, C. Xie, S. H. Parekh, V. Mailänder, S. Wu, *Small* **2017**, *13*, 1700997.
- [71] H.-D. Gao, P. Thanasekaran, C.-W. Chiang, J.-L. Hong, Y.-C. Liu, Y.-H. Chang, H.-M. Lee, *ACS Nano* **2015**, *9*, 7041.
- [72] A. Qu, X. Wu, S. Li, M. Sun, L. Xu, H. Kuang, C. Xu, *Adv. Mater.* **2020**, *32*, 2000184.
- [73] a) L. Donato, A. Mourrot, C. M. Davenport, C. Herbivo, D. Warther, J. Léonard, F. Bolze, J.-F. Nicoud, R. H. Kramer, M. Goeldner, A. Specht, *Angew. Chem., Int. Ed.* **2012**, *51*, 1840; b) J. Olejniczak, J. Sankaranarayanan, M. L. Viger, A. Almutairi, *ACS Macro Lett.* **2013**, *2*, 683; c) C.-J. Carling, J. Olejniczak, A. Foucault-Collet, G. Collet, M. L. Viger, V. A. Nguyen Huu, B. M. Duggan, A. Almutairi, *Chem. Sci.* **2016**, *7*, 2392.
- [74] L. Fournier, C. Gauron, L. Xu, I. Aujard, T. Le Saux, N. Gagey-Eilstein, S. Maurin, S. Dubruille, J.-B. Baudin, D. Bensimon, M. Volovitch, S. Vriz, L. Jullien, *ACS Chem. Biol.* **2013**, *8*, 1528.
- [75] a) L. Fournier, I. Aujard, T. Le Saux, S. Maurin, S. Beaupierre, J.-B. Baudin, L. Jullien, *Chem. - Eur. J.* **2013**, *19*, 17494; b) J. Babin, M. Pelletier, M. Lepage, J.-F. Allard, D. Morris, Y. Zhao, *Angew. Chem.* **2009**, *121*, 3379.
- [76] A. P. Gorka, R. R. Nani, J. Zhu, S. Mackem, M. J. Schnermann, *J. Am. Chem. Soc.* **2014**, *136*, 14153.
- [77] Z. Lv, H. Wei, Q. Li, X. Su, S. Liu, K. Y. Zhang, W. Lv, Q. Zhao, X. Li, W. Huang, *Chem. Sci.* **2018**, *9*, 502.
- [78] Y. Wang, Y. Deng, H. Luo, A. Zhu, H. Ke, H. Yang, H. Chen, *ACS Nano* **2017**, *11*, 12134.
- [79] Z. Cao, Y. Ma, C. Sun, Z. Lu, Z. Yao, J. Wang, D. Li, Y. Yuan, X. Yang, *Chem. Mater.* **2018**, *30*, 517.
- [80] K. Zhang, Y. Zhang, X. Meng, H. Lu, H. Chang, H. Dong, X. Zhang, *Biomaterials* **2018**, *185*, 301.
- [81] W. Wang, L. Lin, X. Ma, B. Wang, S. Liu, X. Yan, S. Li, H. Tian, X. Yu, *ACS Appl. Mater. Interfaces* **2018**, *10*, 19398.
- [82] A. Y. Rwei, W. Wang, D. S. Kohane, *Nano Today* **2015**, *10*, 451.
- [83] a) K. Liu, Y. Liu, Y. Yao, H. Yuan, S. Wang, Z. Wang, X. Zhang, *Angew. Chem., Int. Ed.* **2013**, *52*, 8285; b) J. Xu, X. Zhou, Z. Gao, Y.-Y. Song, P. Schmuki, *Angew. Chem., Int. Ed.* **2016**, *55*, 593; c) H. W. Choi, J. Kim, J. Kim, Y. Kim, H. B. Song, J. H. Kim, K. Kim, W. J. Kim, *ACS Nano* **2016**, *10*, 4199.
- [84] E. Palao, T. Slanina, L. Muchová, T. Šolomek, L. Vitek, P. Klán, *J. Am. Chem. Soc.* **2016**, *138*, 126.
- [85] A. Barhoumi, Q. Liu, D. S. Kohane, *J. Controlled Release* **2015**, *219*, 31.
- [86] J. H. Kaplan, B. Forbush, J. F. Hoffman, *Biochemistry* **1978**, *17*, 1929.
- [87] A. Gnach, T. Lipinski, A. Bednarkiewicz, J. Rybka, J. A. Capobianco, *Chem. Soc. Rev.* **2015**, *44*, 1561.
- [88] C. Zhan, W. Wang, J. B. McAlvin, S. Guo, B. P. Timko, C. Santamaria, D. S. Kohane, *Nano Lett.* **2016**, *16*, 177.
- [89] a) Q. Chen, J. Wen, H. Li, Y. Xu, F. Liu, S. Sun, *Biomaterials* **2016**, *106*, 144; b) S. Hwang, J. Nam, S. Jung, J. Song, H. Doh, S. Kim, *Nanomedicine* **2014**, *9*, 2003; c) R. S. Riley, E. S. Day, *Wiley Interdiscip. Rev.: Nanomed. Nanobiotechnol.* **2017**, *9*, e1449; d) M. Aioub, M. A. El-Sayed, *J. Am. Chem. Soc.* **2016**, *138*, 1258.
- [90] a) W. Sun, G. Zhong, C. Kübel, A. A. Jelle, C. Qian, L. Wang, M. Ebrahimi, L. M. Reyes, A. S. Helmy, G. A. Ozin, *Angew. Chem.* **2017**, *129*, 6426; b) T. N. Lambert, N. L. Andrews, H. Gerung, T. J. Boyle, J. M. Oliver, B. S. Wilson, S. M. Han, *Small* **2007**, *3*, 691; c) A. J. McGrath, Y. H. Chien, S. Cheong, D. A. Herman, J. Watt, A. M. Henning, L. Gloag, C. S. Yeh, R. D. Tilley, *ACS Nano* **2015**, *9*, 12283; d) R. He, Y.-C. Wang, X. Wang, Z. Wang, G. Liu, W. Zhou, L. Wen, Q. Li, X. Wang, X. Chen, J. Zeng, J. G. Hou, *Nat. Commun.* **2014**, *5*, 4327.
- [91] a) Y. Chen, L. Wang, J. Shi, *Nano Today* **2016**, *11*, 292; b) C. Chung, Y.-K. Kim, D. Shin, S.-R. Ryoo, B. H. Hong, D.-H. Min, *Acc. Chem. Res.* **2013**, *46*, 2211; c) M. Hashemi, M. Omid, B. Muralidharan, H. Smyth, M. A. Mohagheghi, J. Mohammadi, T. E. Milner, *ACS Appl. Mater. Interfaces* **2017**, *9*, 32607; d) Y. Chen, P. Xu, M. Wu, Q. Meng, H. Chen, Z. Shu, J. Wang, L. Zhang, Y. Li, J. Shi, *Adv. Mater.* **2014**, *26*, 4294; e) S. Wang, Q. Lin, J. Chen, H. Gao, D. Fu, S. Shen, *Carbon* **2017**, *112*, 53; f) Q. Kong, L. Zhang, J. Liu, M. Wu, Y. Chen, J. Feng, J. Shi, *Chem. Commun.* **2014**, *50*, 15772; g) D. Chen, C. A. Dougherty, K. Zhu, H. Hong, *J. Controlled Release* **2015**, *210*, 230; h) M. Thakur, M. K. Kumawat, R. Srivastava, *RSC Adv.* **2017**, *7*, 5251; i) M. Lan, S. Zhao, Z. Zhang, L. Yan, L. Guo, G. Niu, J. Zhang, J. Zhao, H. Zhang, P. Wang, G. Zhu, C.-S. Lee, W. Zhang, *Nano Res.* **2017**, *10*, 3113; j) M. Zheng, Y. Li, S. Liu, W. Wang, Z. Xie, X. Jing, *ACS Appl. Mater. Interfaces* **2016**, *8*, 23533.
- [92] a) M. Zhou, R. Zhang, M. Huang, W. Lu, S. Song, M. P. Melancon, M. Tian, D. Liang, C. Li, *J. Am. Chem. Soc.* **2010**, *132*, 15351; b) C. M. Hessel, V. P. Pattani, M. Rasch, M. G. Panthani, B. Koo, J. W. Tunnell, B. A. Korgel, *Nano Lett.* **2011**, *11*, 2560; c) Z. Chen, Q. Wang, H. Wang, L. Zhang, G. Song, L. Song, J. Hu, H. Wang, J. Liu, M. Zhu, D. Zhao, *Adv. Mater.* **2013**, *25*, 2095; d) W. Yin, L. Yan, J. Yu, G. Tian, L. Zhou, X. Zheng, X. Zhang, Y. Yong, J. Li, Z. Gu, Y. Zhao, *ACS Nano* **2014**, *8*, 6922; e) S. S. Chou, B. Kaehr, J. Kim, B. M. Foley, M. De, P. E. Hopkins, J. Huang, C. J. Brinker, V. P. Dravid, *Angew. Chem., Int. Ed.* **2013**, *52*, 4160; f) T. Yang, Y. a. Tang, L. Liu, X. Lv, Q. Wang, H. Ke, Y. Deng, H. Yang, X. Yang, G. Liu, Y. Zhao, H. Chen, *ACS Nano* **2017**, *11*, 1848; g) Q. Jiang, W. Zeng, C. Zhang, Z. Meng, J. Wu, Q. Zhu, D. Wu, H. Zhu, *Sci. Rep.* **2017**, *7*, 17782; h) G. K. Larsen, W. Farr, S. E. Hunyadi Murph, *J. Phys. Chem. C* **2016**, *120*, 15162; i) Y. Yong, X. Cheng, T. Bao, M. Zu, L. Yan, W. Yin, C. Ge, D. Wang, Z. Gu, Y. Zhao, *ACS Nano* **2015**, *9*, 12451; j) J. Gao, C. Wu, D. Deng, P. Wu, C. Cai, *Adv. Healthcare Mater.* **2016**, *5*, 2437.
- [93] a) M. Chu, X. Pan, D. Zhang, Q. Wu, J. Peng, W. Hai, *Biomaterials* **2012**, *33*, 7071; b) Z. Sun, H. Xie, S. Tang, X.-F. Yu, Z. Guo, J. Shao, H. Zhang, H. Huang, H. Wang, P. K. Chu, *Angew. Chem.* **2015**, *127*, 11688.
- [94] a) X. Liang, Y. Li, X. Li, L. Jing, Z. Deng, X. Yue, C. Li, Z. Dai, *Adv. Funct. Mater.* **2015**, *25*, 1451; b) X. Song, C. Liang, H. Gong, Q. Chen, C. Wang, Z. Liu, *Small* **2015**, *11*, 3932; c) L. Cheng, K. Yang, Q. Chen, Z. Liu, *ACS Nano* **2012**, *6*, 5605; d) Q. Zou, M. Abbas, L. Zhao, S. Li, G. Shen, X. Yan, *J. Am. Chem. Soc.* **2017**, *139*, 1921.
- [95] a) B. Zhou, Y. Li, G. Niu, M. Lan, Q. Jia, Q. Liang, *ACS Appl. Mater. Interfaces* **2016**, *8*, 29899; b) L. Cheng, W. He, H. Gong,

- C. Wang, Q. Chen, Z. Cheng, Z. Liu, *Adv. Funct. Mater.* **2013**, *23*, 5893.
- [96] W. Wang, L. Wang, Y. Li, S. Liu, Z. Xie, X. Jing, *Adv. Mater.* **2016**, *28*, 9320.
- [97] a) Y.-W. Chen, Y.-L. Su, S.-H. Hu, S.-Y. Chen, *Adv. Drug Delivery Rev.* **2016**, *105*, 190; b) P. C. Ray, S. A. Khan, A. K. Singh, D. Senapati, Z. Fan, *Chem. Soc. Rev.* **2012**, *41*, 3193.
- [98] a) F. Teodorescu, Y. Oz, G. Quéniat, A. Abderrahmani, C. Foulon, M. Lecoeur, R. Sanyal, A. Sanyal, R. Boukherroub, S. Szunerits, *J. Controlled Release* **2017**, *246*, 164; b) H. Choi, G.-H. Lee, K. S. Kim, S. K. Hahn, *ACS Appl. Mater. Interfaces* **2018**, *10*, 2338; c) J. Liu, C. Wang, X. Wang, X. Wang, L. Cheng, Y. Li, Z. Liu, *Adv. Funct. Mater.* **2015**, *25*, 384; d) K. Mebrouk, M. Ciancone, T. Vives, S. Cammas-Marion, T. Benvegnu, C. Le Goff-Gaillard, Y. Arlot-Bonnemains, M. Fourmigué, F. Camerel, *ChemMedChem* **2017**, *12*, 1753; e) Q. L. Wei, Y. Chen, X. B. Ma, J. F. Ji, Y. Qiao, B. Zhou, F. Ma, D. S. Ling, H. Zhang, M. Tian, J. Tian, M. Zhou, *Adv. Funct. Mater.* **2018**, *28*, 1704634; f) T. Yin, J. Liu, Z. Zhao, Y. Zhao, L. Dong, M. Yang, J. Zhou, M. Huo, *Adv. Funct. Mater.* **2017**, *27*, 1604620; g) H. Kim, D. Lee, J. Kim, T. I. Kim, W. J. Kim, *ACS Nano* **2013**, *7*, 6735; h) C. Wang, H. Xu, C. Liang, Y. Liu, Z. Li, G. Yang, L. Cheng, Y. Li, Z. Liu, *ACS Nano* **2013**, *7*, 6782.
- [99] M. R. K. Ali, M. A. Rahman, Y. Wu, T. Han, X. Peng, M. A. Mackey, D. Wang, H. J. Shin, Z. G. Chen, H. Xiao, R. Wu, Y. Tang, D. M. Shin, M. A. El-Sayed, *Proc. Natl. Acad. Sci. USA* **2017**, *114*, E3110.
- [100] W. Zhang, F. Wang, Y. Wang, J. Wang, Y. Yu, S. Guo, R. Chen, D. Zhou, *J. Controlled Release* **2016**, *232*, 9.
- [101] Y. Tao, E. Ju, Z. Liu, K. Dong, J. Ren, X. Qu, *Biomaterials* **2014**, *35*, 6646.
- [102] H. Sun, J. Su, Q. Meng, Q. Yin, L. Chen, W. Gu, Z. Zhang, H. Yu, P. Zhang, S. Wang, Y. Li, *Adv. Funct. Mater.* **2017**, *27*, 1604300.
- [103] X. Deng, S. Liang, X. Cai, S. Huang, Z. Cheng, Y. Shi, M. Pang, P. a. Ma, J. Lin, *Nano Lett.* **2019**, *19*, 6772.
- [104] L. Zhang, Y. Zhang, Y. Xue, Y. Wu, Q. Wang, L. Xue, Z. Su, C. Zhang, *Adv. Mater.* **2019**, *31*, 1805936.
- [105] C. Li, Y. Zhang, Z. Li, E. Mei, J. Lin, F. Li, C. Chen, X. Qing, L. Hou, L. Xiong, H. Hao, Y. Yang, P. Huang, *Adv. Mater.* **2018**, *30*, 1706150.
- [106] X. Chen, Y. Chen, H. Xin, T. Wan, Y. Ping, *Proc. Natl. Acad. Sci. USA* **2020**, *117*, 2395.
- [107] H. Peng, R. E. Borg, L. P. Dow, B. L. Pruitt, I. A. Chen, *Proc. Natl. Acad. Sci. USA* **2020**, *117*, 1951.
- [108] a) R. Xing, K. Liu, T. Jiao, N. Zhang, K. Ma, R. Zhang, Q. Zou, G. Ma, X. Yan, *Adv. Mater.* **2016**, *28*, 3669; b) S. Huo, N. Gong, Y. Jiang, F. Chen, H. Guo, Y. Gan, Z. Wang, A. Herrmann, X.-J. Liang, *Sci. Adv.* **2019**, *5*, 6264.
- [109] X. Cheng, R. Sun, L. Yin, Z. Chai, H. Shi, M. Gao, *Adv. Mater.* **2017**, *29*, 1604894.
- [110] K. Yang, Y. Liu, Y. Wang, Q. Ren, H. Guo, J. B. Matson, X. Chen, Z. Nie, *Biomaterials* **2019**, *223*, 119460.
- [111] B. Han, Y.-L. Zhang, Q.-D. Chen, H.-B. Sun, *Adv. Funct. Mater.* **2018**, *28*, 1802235.
- [112] G. Hong, S. Diao, A. L. Antaris, H. Dai, *Chem. Rev.* **2015**, *115*, 10816.
- [113] C. Wells, O. Vollin-Bringel, V. Fiegel, S. Harlepp, B. Van der Schueren, S. Bégin-Colin, D. Bégin, D. Mertz, *Adv. Funct. Mater.* **2018**, *28*, 1706996.
- [114] Y. Tao, E. Ju, J. Ren, X. Qu, *Biomaterials* **2014**, *35*, 9963.
- [115] X. Zhu, W. Feng, J. Chang, Y.-W. Tan, J. Li, M. Chen, Y. Sun, F. Li, *Nat. Commun.* **2016**, *7*, 10437.
- [116] C. Mei, N. Wang, X. Zhu, K.-H. Wong, T. Chen, *Adv. Funct. Mater.* **2018**, *28*, 1805225.
- [117] H. Wang, X. Pan, X. Wang, W. Wang, Z. Huang, K. Gu, S. Liu, F. Zhang, H. Shen, Q. Yuan, J. Ma, W. Yuan, H. Liu, *ACS Nano* **2020**, *14*, 2847.
- [118] S. Goel, F. Chen, W. Cai, *Small* **2014**, *10*, 631.
- [119] a) S. Liu, J. Pan, J. Liu, Y. Ma, F. Qiu, L. Mei, X. Zeng, G. Pan, *Small* **2018**, *14*, 1703968; b) X. Deng, K. Li, X. Cai, B. Liu, Y. Wei, K. Deng, Z. Xie, Z. Wu, P. a. Ma, Z. Hou, Z. Cheng, J. Lin, *Adv. Mater.* **2017**, *29*, 1701266; c) L. Du, H. Qin, T. Ma, T. Zhang, D. Xing, *ACS Nano* **2017**, *11*, 8930; d) X. Zhao, C.-X. Yang, L.-G. Chen, X.-P. Yan, *Nat. Commun.* **2017**, *8*, 14998; e) N. Li, Q. Sun, Z. Yu, X. Gao, W. Pan, X. Wan, B. Tang, *ACS Nano* **2018**, *12*, 5197; f) Q. Xiao, X. Zheng, W. Bu, W. Ge, S. Zhang, F. Chen, H. Xing, Q. Ren, W. Fan, K. Zhao, Y. Hua, J. Shi, *J. Am. Chem. Soc.* **2013**, *135*, 13041.
- [120] D. Wang, H. Dong, M. Li, Y. Cao, F. Yang, K. Zhang, W. Dai, C. Wang, X. Zhang, *ACS Nano* **2018**, *12*, 5241.
- [121] S. Liang, Z. Xie, Y. Wei, Z. Cheng, Y. Han, J. Lin, *Dalton Trans.* **2018**, *47*, 7916.
- [122] Z. Wang, X. Tang, X. Wang, D. Yang, C. Yang, Y. Lou, J. Chen, N. He, *Chem. Commun.* **2016**, *52*, 12210.
- [123] L. Xu, G. Tong, Q. Song, C. Zhu, H. Zhang, J. Shi, Z. Zhang, *ACS Nano* **2018**, *12*, 6806.
- [124] W. Zhen, Y. Liu, L. Lin, J. Bai, X. Jia, H. Tian, X. Jiang, *Angew. Chem., Int. Ed.* **2018**, *57*, 10309.
- [125] L. Sun, Z. Li, R. Su, Y. Wang, Z. Li, B. Du, Y. Sun, P. Guan, F. Besenbacher, M. Yu, *Angew. Chem., Int. Ed.* **2018**, *57*, 10666.
- [126] L. Sun, X. Jiao, W. Liu, Y. Wang, Y. Cao, S.-J. Bao, Z. Xu, Y. Kang, P. Xue, *ACS Appl. Mater. Interfaces* **2019**, *11*, 41127.
- [127] a) T. Liu, C. Wang, X. Gu, H. Gong, L. Cheng, X. Shi, L. Feng, B. Sun, Z. Liu, *Adv. Mater.* **2014**, *26*, 3433; b) T. Liu, S. Shi, C. Liang, S. Shen, L. Cheng, C. Wang, X. Song, S. Goel, T. E. Barnhart, W. Cai, Z. Liu, *ACS Nano* **2015**, *9*, 950.
- [128] Y. Wang, N. Gong, Y. Li, Q. Lu, X. Wang, J. Li, *J. Am. Chem. Soc.* **2020**, *142*, 1735.
- [129] C. Yang, Y. Chen, W. Guo, Y. Gao, C. Song, Q. Zhang, N. Zheng, X. Han, C. Guo, *Adv. Funct. Mater.* **2018**, *28*, 1706827.
- [130] a) L. Cheng, J. Liu, X. Gu, H. Gong, X. Shi, T. Liu, C. Wang, X. Wang, G. Liu, H. Xing, W. Bu, B. Sun, Z. Liu, *Adv. Mater.* **2014**, *26*, 1886; b) L. Cheng, C. Yuan, S. Shen, X. Yi, H. Gong, K. Yang, Z. Liu, *ACS Nano* **2015**, *9*, 11090.
- [131] C. Zhang, D. Li, P. Pei, W. Wang, B. Chen, Z. Chu, Z. Zha, X. Yang, J. Wang, H. Qian, *Biomaterials* **2020**, *237*, 119835.
- [132] Y. Zhou, Q. Xu, T. Ge, X. Zheng, L. Zhang, P. Yan, *Angew. Chem.* **2020**, *132*, 3348.
- [133] H. Xie, M. Liu, B. You, G. Luo, Y. Chen, B. Liu, Z. Jiang, P. K. Chu, J. Shao, X.-F. Yu, *Small* **2020**, *16*, 1905208.
- [134] Q. Zhang, Q. Guo, Q. Chen, X. Zhao, S. J. Pennycook, H. Chen, *Adv. Sci.* **2020**, *7*, 1902576.
- [135] G. Song, M. Kenney, Y.-S. Chen, X. Zheng, Y. Deng, Z. Chen, S. X. Wang, S. S. Gambhir, H. Dai, J. Rao, *Nat. Biomed. Eng.* **2020**, *4*, 325.
- [136] K. Zhang, X. Meng, Y. Cao, Z. Yang, H. Dong, Y. Zhang, H. Lu, Z. Shi, X. Zhang, *Adv. Funct. Mater.* **2018**, *28*, 1804634.
- [137] D. Zhang, P. Cui, Z. Dai, B. Yang, X. Yao, Q. Liu, Z. Hu, X. Zheng, *Nanoscale* **2019**, *11*, 19912.
- [138] G. Liu, J. Zhu, H. Guo, A. Sun, P. Chen, L. Xi, W. Huang, X. Song, X. Dong, *Angew. Chem., Int. Ed.* **2019**, *58*, 18641.
- [139] N. Ma, M.-K. Zhang, X.-S. Wang, L. Zhang, J. Feng, X.-Z. Zhang, *Adv. Funct. Mater.* **2018**, *28*, 1801139.
- [140] Y. Liu, J. Wu, Y. Jin, W. Zhen, Y. Wang, J. Liu, L. Jin, S. Zhang, Y. Zhao, S. Song, Y. Yang, H. Zhang, *Adv. Funct. Mater.* **2019**, *29*, 1904678.
- [141] Y. Zhang, R. Sha, L. Zhang, W. Zhang, P. Jin, W. Xu, J. Ding, J. Lin, J. Qian, G. Yao, R. Zhang, F. Luo, J. Zeng, J. Cao, L.-p. Wen, *Nat. Commun.* **2018**, *9*, 4236.
- [142] S. Yu, G. Li, P. Zhao, Q. Cheng, Q. He, D. Ma, W. Xue, *Adv. Funct. Mater.* **2019**, *29*, 1905697.
- [143] W. Guo, C. Guo, N. Zheng, T. Sun, S. Liu, *Adv. Mater.* **2017**, *29*, 1604157.

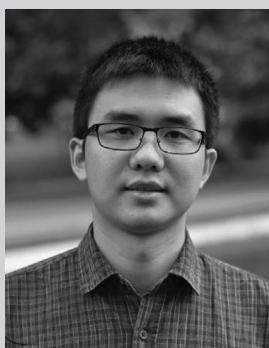
- [144] J. Zhou, W. Zhao, Z. Miao, J. Wang, Y. Ma, H. Wu, T. Sun, H. Qian, Z. Zha, *ACS Nano* **2020**, *14*, 2126.
- [145] S. Zada, W. Dai, Z. Kai, H. Lu, X. Meng, Y. Zhang, Y. Cheng, F. Yan, P. Fu, X. Zhang, H. Dong, *Angew. Chem.* **2020**, *132*, 6663.
- [146] a) Z. Wang, T. Jia, Q. Sun, Y. Kuang, B. Liu, M. Xu, H. Zhu, F. He, S. Gai, P. Yang, *Biomaterials* **2020**, *228*, 119569; b) N. Yu, Z. Wang, J. Zhang, Z. Liu, B. Zhu, J. Yu, M. Zhu, C. Peng, Z. Chen, *Biomaterials* **2018**, *161*, 279.
- [147] H. Sun, R. Chang, Q. Zou, R. Xing, W. Qi, X. Yan, *Small* **2019**, *15*, 1905326.
- [148] X. Zheng, L. Wang, M. Liu, P. Lei, F. Liu, Z. Xie, *Chem. Mater.* **2018**, *30*, 6867.
- [149] M. Qiu, D. Wang, W. Liang, L. Liu, Y. Zhang, X. Chen, D. K. Sang, C. Xing, Z. Li, B. Dong, F. Xing, D. Fan, S. Bao, H. Zhang, Y. Cao, *Proc. Natl. Acad. Sci. USA* **2018**, *115*, 501.
- [150] A. Favron, E. Gauffrès, F. Fossard, A.-L. Phaneuf-L'Heureux, N. Y. W. Tang, P. L. Lévesque, A. Loiseau, R. Leonelli, S. Francoeur, R. Martel, *Nat. Mater.* **2015**, *14*, 826.
- [151] J. Shao, H. Xie, H. Huang, Z. Li, Z. Sun, Y. Xu, Q. Xiao, X.-F. Yu, Y. Zhao, H. Zhang, H. Wang, P. K. Chu, *Nat. Commun.* **2016**, *7*, 12967.
- [152] W. Chen, J. Ouyang, H. Liu, M. Chen, K. Zeng, J. Sheng, Z. Liu, Y. Han, L. Wang, J. Li, L. Deng, Y.-N. Liu, S. Guo, *Adv. Mater.* **2017**, *29*, 1603864.
- [153] L. Kyllönen, M. D'Este, M. Alini, D. Eglin, *Acta Biomater.* **2015**, *11*, 412.
- [154] X. Wang, J. Shao, M. Abd El Raouf, H. Xie, H. Huang, H. Wang, P. K. Chu, X.-F. Yu, Y. Yang, A. M. AbdEl-Aal, N. H. M. Mekkawy, R. J. Miron, Y. Zhang, *Biomaterials* **2018**, *179*, 164.
- [155] L. Zhao, Y. Liu, R. Chang, R. Xing, X. Yan, *Adv. Funct. Mater.* **2019**, *29*, 1806877.
- [156] a) Z. Tan, Y. Jiang, M. S. Ganewatta, R. Kumar, A. Keith, K. Twaroski, T. Pengo, J. Tolar, T. P. Lodge, T. M. Reineke, *Macromolecules* **2019**, *52*, 8197; b) D. Chen, Y. Tang, J. Zhu, J. Zhang, X. Song, W. Wang, J. Shao, W. Huang, P. Chen, X. Dong, *Biomaterials* **2019**, *221*, 119422.
- [157] Y. Lyu, C. Xie, S. A. Chechetka, E. Miyako, K. Pu, *J. Am. Chem. Soc.* **2016**, *138*, 9049.
- [158] Y. Yang, X. Fan, L. Li, Y. Yang, A. Nuernisha, D. Xue, C. He, J. Qian, Q. Hu, H. Chen, J. Liu, W. Huang, *ACS Nano* **2020**, *14*, 2509.
- [159] Y. Jiang, J. Li, X. Zhen, C. Xie, K. Pu, *Adv. Mater.* **2018**, *30*, 1705980.
- [160] Y. Lai, Y. Zhu, Z. Xu, X. Hu, M. Saeed, H. Yu, X. Chen, J. Liu, W. Zhang, *Adv. Funct. Mater.* **2020**, *30*, 1908473.
- [161] B. Guo, Z. Sheng, D. Hu, C. Liu, H. Zheng, B. Liu, *Adv. Mater.* **2018**, *30*, 1802591.
- [162] D. Wang, Z. Zhang, L. Lin, F. Liu, Y. Wang, Z. Guo, Y. Li, H. Tian, X. Chen, *Biomaterials* **2019**, *223*, 119459.
- [163] D. Wu, X. Duan, Q. Guan, J. Liu, X. Yang, F. Zhang, P. Huang, J. Shen, X. Shuai, Z. Cao, *Adv. Funct. Mater.* **2019**, *29*, 1900095.
- [164] Y. Wang, Q. Huang, X. He, H. Chen, Y. Zou, Y. Li, K. Lin, X. Cai, J. Xiao, Q. Zhang, Y. Cheng, *Biomaterials* **2018**, *183*, 10.
- [165] D.-Y. Zhang, Y. Zheng, H. Zhang, J.-H. Sun, C.-P. Tan, L. He, W. Zhang, L.-N. Ji, Z.-W. Mao, *Adv. Sci.* **2018**, *5*, 1800581.
- [166] Z. Jin, K. T. Nguyen, G. Go, B. Kang, H.-K. Min, S.-J. Kim, Y. Kim, H. Li, C.-S. Kim, S. Lee, S. Park, K.-P. Kim, K. M. Huh, J. Song, J.-O. Park, E. Choi, *Nano Lett.* **2019**, *19*, 8550.
- [167] F. Liu, L. Lin, Y. Zhang, S. Sheng, Y. Wang, C. Xu, H. Tian, X. Chen, *Biomaterials* **2019**, *223*, 119470.
- [168] Z. Yuan, B. Tao, Y. He, C. Mu, G. Liu, J. Zhang, Q. Liao, P. Liu, K. Cai, *Biomaterials* **2019**, *223*, 119479.
- [169] Z. Yuan, C. Lin, Y. He, B. Tao, M. Chen, J. Zhang, P. Liu, K. Cai, *ACS Nano* **2020**, *14*, 3546.
- [170] a) Y.-N. Zhang, W. Poon, A. J. Tavares, I. D. McGilvray, W. C. W. Chan, *J. Controlled Release* **2016**, *240*, 332; b) S. Wang, F. Li, X. Hu, M. Lv, C. Fan, D. Ling, *Adv. Ther.* **2018**, *1*, 1800059; c) Q. Guan, L.-L. Zhou, Y.-A. Li, W.-Y. Li, S. Wang, C. Song, Y.-B. Dong, *ACS Nano* **2019**, *13*, 13304.
- [171] a) H. Li, H. Liu, T. Nie, Y. Chen, Z. Wang, H. Huang, L. Liu, Y. Chen, *Biomaterials* **2018**, *178*, 620; b) Y. Deng, F. Käfer, T. Chen, Q. Jin, J. Ji, S. Agarwal, *Small* **2018**, *14*, 1802420; c) C. Zhu, D. Huo, Q. Chen, J. Xue, S. Shen, Y. Xia, *Adv. Mater.* **2017**, *29*, 1703702.
- [172] L. Huang, Y. Li, Y. Du, Y. Zhang, X. Wang, Y. Ding, X. Yang, F. Meng, J. Tu, L. Luo, C. Sun, *Nat. Commun.* **2019**, *10*, 4871.
- [173] H. He, J. Zhou, Y. Liu, S. Liu, Z. Xie, M. Yu, Y. Wang, X. Shuai, *ACS Appl. Mater. Interfaces* **2018**, *10*, 7413.
- [174] X. Mu, Y. Lu, F. Wu, Y. Wei, H. Ma, Y. Zhao, J. Sun, S. Liu, X. Zhou, Z. Li, *Adv. Mater.* **2020**, *32*, 1906711.
- [175] Q. Chen, G. Huang, W. Wu, J. Wang, J. Hu, J. Mao, P. K. Chu, H. Bai, G. Tang, *Adv. Mater.* **2020**, *32*, 1908185.
- [176] Y. Liu, G. Shu, X. Li, H. Chen, B. Zhang, H. Pan, T. Li, X. Gong, H. Wang, X. Wu, Y. Dou, J. Chang, *Adv. Funct. Mater.* **2018**, *28*, 1802026.
- [177] D. Xi, M. Xiao, J. Cao, L. Zhao, N. Xu, S. Long, J. Fan, K. Shao, W. Sun, X. Yan, X. Peng, *Adv. Mater.* **2020**, *32*, 1907855.
- [178] R. Xing, Q. Zou, C. Yuan, L. Zhao, R. Chang, X. Yan, *Adv. Mater.* **2019**, *31*, 1900822.
- [179] F. Wang, Z. Yuan, P. McMullen, R. Li, J. Zheng, Y. Xu, M. Xu, Q. He, B. Li, H. Chen, *Chem. Mater.* **2019**, *31*, 3948.
- [180] H. Zhang, Q. Li, R. Liu, X. Zhang, Z. Li, Y. Luan, *Adv. Funct. Mater.* **2018**, *28*, 1802830.
- [181] W. Lin, Y. Li, W. Zhang, S. Liu, Z. Xie, X. Jing, *ACS Appl. Mater. Interfaces* **2016**, *8*, 24426.
- [182] A. S. Braegelmann, M. J. Webber, *Theranostics* **2019**, *9*, 3017.
- [183] Y. Huang, S. He, W. Cao, K. Cai, X.-J. Liang, *Nanoscale* **2012**, *4*, 6135.
- [184] J.-L. Li, B. Tang, B. Yuan, L. Sun, X.-G. Wang, *Biomaterials* **2013**, *34*, 9519.
- [185] a) J. Zhang, Z. Qiao, P. Yang, J. Pan, L. Wang, H. Wang, *Chin. J. Chem.* **2015**, *33*, 35; b) R. Vankayala, K. C. Hwang, *Adv. Mater.* **2018**, *30*, 1706320.
- [186] T. Curry, R. Kopelman, M. Shilo, R. Popovtzer, *Contrast Media Mol. Imaging* **2014**, *9*, 53.
- [187] R. Fernando, J. Downs, D. Maples, A. Ranjan, *Pharm. Res.* **2013**, *30*, 2709.
- [188] X. Wei, S. Sebastian, *Rep. Prog. Phys.* **2014**, *77*, 116502.
- [189] C. Guo, Y. Jin, Z. Dai, *Bioconjugate Chem.* **2014**, *25*, 840.
- [190] P. Tuersun, X. e. Han, *Optik* **2014**, *125*, 3702.
- [191] W. Li, W. Hou, X. Guo, L. Luo, Q. Li, C. Zhu, J. Yang, J. Zhu, Y. Du, J. You, *Theranostics* **2018**, *8*, 3059.
- [192] A. Albanese, P. S. Tang, W. C. W. Chan, *Annu. Rev. Biomed. Eng.* **2012**, *14*, 1.
- [193] H. Vihola, A. Laukkanen, L. Valtola, H. Tenhu, J. Hirvonen, *Biomaterials* **2005**, *26*, 3055.
- [194] a) V. I. Minkin, *Chem. Rev.* **2004**, *104*, 2751; b) Y. Li, Y. Duan, J. Li, J. Zheng, H. Yu, R. Yang, *Anal. Chem.* **2012**, *84*, 4732.
- [195] a) S. K. Nalluri, J. Voskuhl, J. B. Bultema, E. J. Boekema, B. J. Ravoo, *Angew. Chem., Int. Ed.* **2011**, *50*, 9747; b) H. M. D. Bandara, S. C. Burdette, *Chem. Soc. Rev.* **2012**, *41*, 1809.
- [196] S. Angelos, Y.-W. Yang, N. M. Khashab, J. F. Stoddart, J. I. Zink, *J. Am. Chem. Soc.* **2009**, *131*, 11344.
- [197] S. Jia, W.-K. Fong, B. Graham, B. J. Boyd, *Chem. Mater.* **2018**, *30*, 2873.
- [198] Q. Yuan, Y. Zhang, T. Chen, D. Lu, Z. Zhao, X. Zhang, Z. Li, C.-H. Yan, W. Tan, *ACS Nano* **2012**, *6*, 6337.
- [199] a) J. Lu, E. Choi, F. Tamanoi, J. I. Zink, *Small* **2008**, *4*, 421; b) Y. Zhu, M. Fujiwara, *Angew. Chem., Int. Ed.* **2007**, *46*, 2241.
- [200] L. Chen, W. Wang, B. Su, Y. Wen, C. Li, Y. Zhou, M. Li, X. Shi, H. Du, Y. Song, L. Jiang, *ACS Nano* **2014**, *8*, 744.

- [201] E. Aznar, R. Casasús, B. García-Acosta, M. D. Marcos, R. Martínez-Máñez, F. Sancenón, J. Soto, P. Amorós, *Adv. Mater.* **2007**, *19*, 2228.
- [202] H. Yan, C. Teh, S. Sreejith, L. Zhu, A. Kwok, W. Fang, X. Ma, K. T. Nguyen, V. Korzh, Y. Zhao, *Angew. Chem., Int. Ed.* **2012**, *51*, 8373.
- [203] J. W. Brown, B. L. Henderson, M. D. Kiesz, A. C. Whalley, W. Morris, S. Grunder, H. Deng, H. Furukawa, J. I. Zink, J. F. Stoddart, O. M. Yaghi, *Chem. Sci.* **2013**, *4*, 2858.
- [204] A. Presa, R. F. Brissos, A. B. Caballero, I. Borilovic, L. Korrodi-Gregório, R. Pérez-Tomás, O. Roubeau, P. Gamez, *Angew. Chem., Int. Ed.* **2015**, *54*, 4561.
- [205] G. Das, T. Prakasam, M. A. Addicoat, S. K. Sharma, F. Ravoux, R. Mathew, M. Baias, R. Jagannathan, M. A. Olson, A. Trabolsi, *J. Am. Chem. Soc.* **2019**, *141*, 19078.
- [206] a) D. Liu, S. Wang, S. Xu, H. Liu, *Langmuir* **2017**, *33*, 1004; b) H. Zhang, X. Fan, R. Suo, H. Li, Z. Yang, W. Zhang, Y. Bai, H. Yao, W. Tian, *Chem. Commun.* **2015**, *51*, 15366.
- [207] Z.-K. Cui, T. Phoeung, P.-A. Rousseau, G. Rydzek, Q. Zhang, C. G. Bazuin, M. Lafleur, *Langmuir* **2014**, *30*, 10818.
- [208] J. W. Hindley, Y. Elani, C. M. McGilvery, S. Ali, C. L. Bevan, R. V. Law, O. Ces, *Nat. Commun.* **2018**, *9*, 1093.
- [209] H. Shen, M. Zhou, Q. Zhang, A. Keller, Y. Shen, *Colloid Polym. Sci.* **2015**, *293*, 1685.
- [210] a) S. J. Leung, M. Romanowski, *Theranostics* **2012**, *2*, 1020; b) J. E. Sheldon, M. M. Dcona, C. E. Lyons, J. C. Hackett, M. C. T. Hartman, *Org. Biomol. Chem.* **2016**, *14*, 40.
- [211] D. K. Prusty, V. Adam, R. M. Zadegan, S. Irsen, M. Famulok, *Nat. Commun.* **2018**, *9*, 535.
- [212] S. Sun, S. Liang, W.-C. Xu, G. Xu, S. Wu, *Polym. Chem.* **2019**, *10*, 4389.
- [213] a) R. Tong, H. H. Chiang, D. S. Kohane, *Proc. Natl. Acad. Sci. USA* **2013**, *110*, 19048; b) R. Tong, H. D. Hemmati, R. Langer, D. S. Kohane, *J. Am. Chem. Soc.* **2012**, *134*, 8848; c) Y. Zhang, C. Yan, C. Wang, Z. Guo, X. Liu, W. H. Zhu, *Angew. Chem., Int. Ed.* **2020**, *132*, 2.
- [214] X. Wang, J. Hu, G. Liu, J. Tian, H. Wang, M. Gong, S. Liu, *J. Am. Chem. Soc.* **2015**, *137*, 15262.
- [215] Q. Xing, N. Li, D. Chen, W. Sha, Y. Jiao, X. Qi, Q. Xu, J. Lu, *J. Mater. Chem. B* **2014**, *2*, 1182.
- [216] J. Ji, X. Li, T. Wu, F. Feng, *Chem. Sci.* **2018**, *9*, 5816.
- [217] X. Wang, Y. Yang, P. Gao, F. Yang, H. Shen, H. Guo, D. Wu, *ACS Macro Lett.* **2015**, *4*, 1321.
- [218] a) Y. Tang, X. Lu, C. Yin, H. Zhao, W. Hu, X. Hu, Y. Li, Z. Yang, F. Lu, Q. Fan, W. Huang, *Chem. Sci.* **2019**, *10*, 1401; b) Y.-M. Zhang, Y.-H. Liu, Y. Liu, *Adv. Mater.* **2020**, *32*, 1806158.
- [219] A. Khayyami, A. Philip, M. Karppinen, *Angew. Chem.* **2019**, *131*, 13534.
- [220] D. Hu, Y. Deng, F. Jia, Q. Jin, J. Ji, *ACS Nano* **2020**, *14*, 347.
- [221] P. Li, G. Xie, P. Liu, X.-Y. Kong, Y. Song, L. Wen, L. Jiang, *J. Am. Chem. Soc.* **2018**, *140*, 16048.
- [222] C. Matera, A. M. J. Gomila, N. Camarero, M. Libergoli, C. Soler, P. Gorostiza, *J. Am. Chem. Soc.* **2018**, *140*, 15764.
- [223] J. Moratz, A. Samanta, J. Voskuhl, S. K. Mohan Nalluri, B. J. Ravoo, *Chem. - Eur. J.* **2015**, *21*, 3271.
- [224] Z. L. Pianowski, J. Karcher, K. Schneider, *Chem. Commun.* **2016**, *52*, 3143.
- [225] J. Ji, T. Wu, Y. Zhang, F. Feng, *ACS Appl. Mater. Interfaces* **2019**, *11*, 15222.
- [226] O. Rifaie-Graham, S. Ulrich, N. F. B. Galensowske, S. Balog, M. Chami, D. Rentsch, J. R. Hemmer, J. Read de Alaniz, L. F. Boesel, N. Bruns, *J. Am. Chem. Soc.* **2018**, *140*, 8027.
- [227] Y. Chen, G. Ke, Y. Ma, Z. Zhu, M. Liu, Y. Liu, H. Yan, C. J. Yang, *J. Am. Chem. Soc.* **2018**, *140*, 8990.
- [228] D. Moldenhauer, J. P. Fuenzalida Werner, C. A. Strassert, F. Gröhn, *Biomacromolecules* **2019**, *20*, 979.
- [229] M. Wegener, M. J. Hansen, A. J. M. Driessen, W. Szymanski, B. L. Feringa, *J. Am. Chem. Soc.* **2017**, *139*, 17979.
- [230] a) J. Croissant, A. Chaix, O. Mongin, M. Wang, S. Clément, L. Raehm, J.-O. Durand, V. Hugues, M. Blanchard-Desce, M. Maynadier, A. Gallud, M. Gary-Bobo, M. Garcia, J. Lu, F. Tamanoi, D. P. Ferris, D. Tarn, J. I. Zink, *Small* **2014**, *10*, 1752; b) J. Croissant, M. Maynadier, A. Gallud, H. Peindy N'Dongo, J. L. Nylosaso, G. Derrien, C. Charnay, J.-O. Durand, L. Raehm, F. Serein-Spirau, N. Cheminet, T. Jarrosson, O. Mongin, M. Blanchard-Desce, M. Gary-Bobo, M. Garcia, J. Lu, F. Tamanoi, D. Tarn, T. M. Guardado-Alvarez, J. I. Zink, *Angew. Chem., Int. Ed.* **2013**, *52*, 13813.
- [231] M. Li, H. Yan, C. Teh, V. Korzh, Y. Zhao, *Chem. Commun.* **2014**, *50*, 9745.
- [232] a) M. Dong, A. Babalhavaeji, S. Samanta, A. A. Beharry, G. A. Woolley, *Acc. Chem. Res.* **2015**, *48*, 2662; b) D. Bléger, J. Schwarz, A. M. Brouwer, S. Hecht, *J. Am. Chem. Soc.* **2012**, *134*, 20597; c) C. Knie, M. Utecht, F. Zhao, H. Kulla, S. Kovalenko, A. M. Brouwer, P. Saalfrank, S. Hecht, D. Bléger, *Chem. - Eur. J.* **2014**, *20*, 16492; d) D. B. Konrad, J. A. Frank, D. Trauner, *Chem. - Eur. J.* **2016**, *22*, 4364; e) K. Higashiguchi, G. Taira, J.-i. Kitai, T. Hirose, K. Matsuda, *J. Am. Chem. Soc.* **2015**, *137*, 2722.
- [233] J. A. Frank, M. Moroni, R. Moshourab, M. Sumser, G. R. Lewin, D. Trauner, *Nat. Commun.* **2015**, *6*, 7118.
- [234] J. Broichhagen, J. A. Frank, D. Trauner, *Acc. Chem. Res.* **2015**, *48*, 1947.
- [235] D. Wang, S. Wu, *Langmuir* **2016**, *32*, 632.
- [236] a) S. Chen, Y. Gao, Z. Cao, B. Wu, L. Wang, H. Wang, Z. Dang, G. Wang, *Macromolecules* **2016**, *49*, 7490; b) C. Yao, P. Wang, X. Li, X. Hu, J. Hou, L. Wang, F. Zhang, *Adv. Mater.* **2016**, *28*, 9341; c) J. Dong, J. I. Zink, *Small* **2015**, *11*, 4165.
- [237] N. M. Idris, M. K. Gnanasammandhan, J. Zhang, P. C. Ho, R. Mahendran, Y. Zhang, *Nat. Med.* **2012**, *18*, 1580.
- [238] J. Liu, W. Bu, L. Pan, J. Shi, *Angew. Chem., Int. Ed.* **2013**, *52*, 4375.
- [239] Y. Zhang, Y. Zhang, G. Song, Y. He, X. Zhang, Y. Liu, H. Ju, *Angew. Chem., Int. Ed.* **2019**, *58*, 18207.
- [240] T. Zhao, P. Wang, Q. Li, A. A. Al-Khalaf, W. N. Hozzein, F. Zhang, X. Li, D. Zhao, *Angew. Chem., Int. Ed.* **2018**, *57*, 2611.
- [241] Y. Dai, H. Xiao, J. Liu, Q. Yuan, P. a. Ma, D. Yang, C. Li, Z. Cheng, Z. Hou, P. Yang, J. Lin, *J. Am. Chem. Soc.* **2013**, *135*, 18920.
- [242] W. Li, K. Dong, H. Wang, P. Zhang, Y. Sang, J. Ren, X. Qu, *Biomaterials* **2019**, *217*, 119310.
- [243] L. Zhou, Z. Chen, K. Dong, M. Yin, J. Ren, X. Qu, *Adv. Mater.* **2014**, *26*, 2424.
- [244] C. Liu, Y. Zhang, M. Liu, Z. Chen, Y. Lin, W. Li, F. Cao, Z. Liu, J. Ren, X. Qu, *Biomaterials* **2017**, *139*, 151.
- [245] Y. Mi, H.-B. Cheng, H. Chu, J. Zhao, M. Yu, Z. Gu, Y. Zhao, L. Li, *Chem. Sci.* **2019**, *10*, 10231.
- [246] A. Galvan-Gonzalez, M. Canva, G. I. Stegeman, L. Sukhomlinova, R. J. Twieg, K. P. Chan, T. C. Kowalczyk, H. S. Lackritz, *J. Opt. Soc. Am. B* **2000**, *17*, 1992.
- [247] J. Rao, A. Khan, *J. Am. Chem. Soc.* **2013**, *135*, 14056.
- [248] a) N. T. Program, *Natl. Cancer Inst. Carcinog. Tech. Rep. Ser.* **1979**, *154*, 1; b) J. M. Joseph, H. Destailats, H.-M. Hung, M. R. Hoffmann, *J. Phys. Chem. A* **2000**, *104*, 301; c) C. Alvarez-Lorenzo, L. Bromberg, A. Concheiro, *Photochem. Photobiol.* **2009**, *85*, 848.
- [249] a) O. Babii, S. Afonin, M. Berditsch, S. Reißer, P. K. Mykhailiuk, V. S. Kubyshkin, T. Steinbrecher, A. S. Ulrich, I. V. Komarov, *Angew. Chem., Int. Ed.* **2014**, *53*, 3392; b) A. Gautier, C. Gauron, M. Volovitch, D. Bensimon, L. Jullien, S. Vriza, *Nat. Chem. Biol.* **2014**, *10*, 533; c) R. H. Kramer, D. L. Fortin, D. Trauner, *Curr. Opin. Neurobiol.* **2009**, *19*, 544.
- [250] a) M. C. Chen, Z. W. Lin, M. H. Ling, *ACS Nano* **2016**, *10*, 93; b) Z. Zhang, J. Wang, C. Chen, *Adv. Mater.* **2013**, *25*, 3869;

- c) K. Zhu, G. Liu, J. Hu, S. Liu, *Biomacromolecules* **2017**, *18*, 2571; d) Z. Meng, F. Wei, R. Wang, M. Xia, Z. Chen, H. Wang, M. Zhu, *Adv. Mater.* **2016**, *28*, 245.
- [251] a) L. Tan, A. Wan, H. Li, *Langmuir* **2013**, *29*, 15032; b) D. Amitava, M. Priyabrata, K. S. Sumit, G. Praveen, C. F. Megan, M. Debabrata, H. S. Vijay, P. Chitta Ranjan, *Nanotechnology* **2010**, *21*, 305102; c) I. Chakraborty, S. J. Carrington, J. Hauser, S. R. J. Oliver, P. K. Mascharak, *Chem. Mater.* **2015**, *27*, 8387.
- [252] a) R. Vankayala, C. L. Kuo, K. Nuthalapati, C. S. Chiang, K. C. Hwang, *Adv. Funct. Mater.* **2015**, *25*, 5934; b) L. Yin, H. Tang, K. H. Kim, N. Zheng, Z. Song, N. P. Gabrielson, H. Lu, J. Cheng, *Angew. Chem., Int. Ed.* **2013**, *52*, 9182; c) A. Kala, P. K. Jain, D. Karunakaran, S. Shah, S. H. Friedman, *Nat. Protoc.* **2014**, *9*, 11.
- [253] a) Q. Pei, X. Hu, X. Zheng, S. Liu, Y. Li, X. Jing, Z. Xie, *ACS Nano* **2018**, *12*, 1630; b) H. Zhao, W. Hu, H. Ma, R. Jiang, Y. Tang, Y. Ji, X. Lu, B. Hou, W. Deng, W. Huang, Q. Fan, *Adv. Funct. Mater.* **2017**, *27*, 1702592.
- [254] C. Xing, Q. Xu, H. Tang, L. Liu, S. Wang, *J. Am. Chem. Soc.* **2009**, *131*, 13117.
- [255] C. Zhang, J. Zhang, G. Shi, H. Song, S. Shi, X. Zhang, P. Huang, Z. Wang, W. Wang, C. Wang, D. Kong, C. Li, *Mol. Pharmaceutics* **2017**, *14*, 1760.
- [256] a) W. Li, J. Wang, J. Ren, X. Qu, *Adv. Mater.* **2013**, *25*, 6737; b) W. Li, J. Wang, J. Ren, X. Qu, *Angew. Chem., Int. Ed.* **2013**, *52*, 6726; c) W. Li, J. Wang, J. Ren, X. Qu, *J. Am. Chem. Soc.* **2014**, *136*, 2248; d) W. Li, Z. Chen, L. Zhou, Z. Li, J. Ren, X. Qu, *J. Am. Chem. Soc.* **2015**, *137*, 8199; e) Z. Ming, X. Ruan, C. Bao, Q. Lin, Y. Yang, L. Zhu, *Adv. Funct. Mater.* **2017**, *27*, 1606258; f) G. Chen, Y. Cao, Y. Tang, X. Yang, Y. Liu, D. Huang, Y. Zhang, C. Li, Q. Wang, *Adv. Sci.* **2020**, *7*, 1903783.
- [257] a) Y.-L. Zhao, J. F. Stoddart, *Langmuir* **2009**, *25*, 8442; b) D. Wang, M. Wagner, H.-J. Butt, S. Wu, *Soft Matter* **2015**, *11*, 7656.
- [258] V. San Miguel, C. G. Bochet, A. del Campo, *J. Am. Chem. Soc.* **2011**, *133*, 5380.



Yu Tao is a Professor at Sun Yat-sen University. She obtained her BSc degree from Nanjing Normal University in 2009, and received her Ph.D. degree in Inorganic Chemistry and Chemical Biology from the Chinese Academy of Sciences in 2015. She then did her postdoctoral training at the City College of New York and Columbia University from 2015 to 2018. Her research interests are in biomaterials, nanotechnology, and tissue engineering.



Mingqiang Li is a Professor of Molecular Medicine at Sun Yat-sen University. He received his BSc degree from University of Science and Technology of China in 2009 and obtained his Ph.D. degree under the supervision of Prof. Xuesi Chen from Changchun Institute of Applied Chemistry, Chinese Academy of Sciences, in 2015. From 2015 to 2018, he carried out postdoctoral research with Prof. Kam W. Leong at Columbia University. His current research is mainly focused on bio-materials, microfluidics, and nanomedicines.



Kam W. Leong is the Samuel Y. Sheng Professor of Biomedical Engineering at Columbia University, with a joint appointment in the Department of Systems Biology at Columbia University Medical Center. His research focuses on nanoparticle-mediated drug-, gene-, and immunotherapy, from the design and synthesis of new carriers to applications for cancer, hemophilia, infectious diseases, and cellular reprogramming.